

**WATER DESALINATION THROUGH THERMAL  
SYSTEMS - MED TECHNOLOGY**

BY

**Khalid Abdelbasit Khalid**

A Thesis Presented to the  
DEANSHIP OF GRADUATE STUDIES

**KING FAHD UNIVERSITY OF PETROLEUM & MINERALS**

DHAHRAN, SAUDI ARABIA

In Partial Fulfillment of the  
Requirements for the Degree of

**MASTER OF SCIENCE**

In

**MECHANICAL ENGINEERING**

December 2015

KING FAHD UNIVERSITY OF PETROLEUM & MINERALS

DHAHRAN- 31261, SAUDI ARABIA

**DEANSHIP OF GRADUATE STUDIES**

This thesis, written by **KHALID ABDELBASIT KHALID ABDELBASIT** under the direction of his thesis advisor and approved by his thesis committee, has been presented and accepted by the Dean of Graduate Studies, in partial fulfillment of the requirements for the degree of **MASTER OF SCIENCE IN MECHANICAL ENGINEERING**

Thesis Committee



Dr. Zuhair Gasem

Department Chairman



Dr. Salam A. Zummo  
Dean of Graduate Studies

Date

2/4/16



Dr. Mohammed A. Antar (Advisor)



Dr. Osman A. Hamed (Member)



Dr. Atia E. Khalifa (Member)

© Khalid Abdelbasit Khalid

2015

## Dedication

To my mother and my father, for the early alphabet that they taught me

## **ACKNOWLEDGMENTS**

I would like to express my thanks to Allah for giving me power and health to complete this work. I am also grateful to King Fahd University of petroleum & minerals and Mechanical Engineering Department for giving me this opportunity to pursue my Ms Program. I take this opportunity to express my sincere thank to my adviser Dr. Mohammed Abdelkarim Antar for his patience and motivation. His guidance helped me in all the time of research. Special thanks to the committee members Dr. Osman Ahmed Hamed and Dr. Atia Esmail Khalifa for their Assistance and their useful comments throughout the research. Last but not the least I thank my Mother, Father, Brothers , Sister and all my friends for supporting and encouraging me in this work.

# TABLE OF CONTENTS

ACKNOWLEDGMENTS.....	III
TABLE OF CONTENTS .....	IV
LIST OF TABLES.....	VI
LIST OF FIGURES.....	VII
ABSTRACT .....	X
ملخص الرسالة.....	XII
<b>1 INTRODUCTION.....</b>	<b>1</b>
<b>1.1. Water Resources.....</b>	<b>1</b>
<b>1.2. Water classifications.....</b>	<b>1</b>
<b>1.3. World population .....</b>	<b>2</b>
<b>1.4. Desalination processes .....</b>	<b>2</b>
1.4.1. Thermal distillation classifications .....	3
1.4.2. Membrane desalination classifications .....	6
<b>1.5. Multi stage flash distillation (MSF D) .....</b>	<b>6</b>
1.5.1. Developments in MSF .....	7
1.5.2. Types of multi stage flashing system.....	7
<b>1.6. Single effect evaporation .....</b>	<b>9</b>
<b>1.7. Multi effect desalination system (MED).....</b>	<b>10</b>
<b>1.8. Vapor Compression Distillation (VCD).....</b>	<b>14</b>
1.8.1. Working principle of vapor compression desalination system .....	14
1.8.2. Performance of multi effect evaporation system .....	15
<b>1.9. Objectives.....</b>	<b>15</b>
<b>1.10. Methodology .....</b>	<b>16</b>
<b>2 LITERATURE REVIEW .....</b>	<b>17</b>
<b>2.1. Thermal Desalination.....</b>	<b>17</b>
<b>2.2. Thermo-economic analysis .....</b>	<b>26</b>
<b>3 FORWARD FEED MULTI EFFECT EVAPORATION DESALINATION SYSTEMS.....</b>	<b>28</b>
<b>3.1. Working Principle .....</b>	<b>29</b>
<b>3.2. Modeling the multi effect evaporation forward feed system.....</b>	<b>31</b>
3.2.1. Model interpretation and Validation .....	36
<b>3.3. Elaborated model of Forward Feed Multi Effect Desalination system .....</b>	<b>39</b>
3.3.1. Elaborated model validation and interpretation .....	43
<b>3.4. MEE/FF/Thermal Vapor Compression (TVC) .....</b>	<b>44</b>
3.4.1. System Configuration .....	44
<b>3.5. MEE/FF/Thermal Vapor Compression (TVC) Modeling.....</b>	<b>44</b>
<b>3.6. MEE/FF/Thermal Vapor Compression Model interpretation and Validation .....</b>	<b>50</b>
3.6.1. Model Interpretation .....	50
3.6.2. Model Validation.....	52
<b>3.7. MEE/FF/TVC different Ejector Positions.....</b>	<b>53</b>
3.7.1. System Configuration .....	53
<b>3.8. MEE/FF/TVC different Ejector Positions Model.....</b>	<b>54</b>
<b>3.9. MEE/FF/TVC different Ejector Positions Model interpretation .....</b>	<b>55</b>

<b>3.10.</b>	<b>Exergetic and Economic Analysis .....</b>	<b>64</b>
3.10.1.	Exegetic and Economic Calculations.....	64
<b>4</b>	<b>PARALLEL FEED MULTI EFFECT EVAPORATION DESALINATION SYSTEMS .....</b>	<b>71</b>
<b>4.1.</b>	<b>Working Principle .....</b>	<b>72</b>
<b>4.2.</b>	<b>MEE/PF Desalination System Modeling .....</b>	<b>73</b>
4.2.1.	System Configuration .....	74
<b>4.3.</b>	<b>MEE/PF/Thermal Vapor Compression (TVC) .....</b>	<b>78</b>
4.3.1.	System Configuration .....	78
<b>4.4.</b>	<b>MEE/PF/Thermal Vapor Compression (TVC) Modeling .....</b>	<b>79</b>
<b>4.5.</b>	<b>MEE/PF(with and without TVC) Model interpretation and validation.....</b>	<b>82</b>
<b>4.6.</b>	<b>MEE/PF/TVC different Ejector Positions .....</b>	<b>87</b>
4.6.1.	System Configuration .....	87
4.6.2.	MEE/PF/TVC different Ejector Positions Model .....	88
<b>4.7.</b>	<b>MEE/PF/TVC different Ejector Positions Model interpretation .....</b>	<b>89</b>
<b>4.8.</b>	<b>MED/PF Exergy Analysis .....</b>	<b>98</b>
<b>5</b>	<b>PARALLEL CROSS MULTI EFFECT EVAPORATION DESALINATION SYSTEM.....</b>	<b>105</b>
<b>5.1.</b>	<b>Working Principle .....</b>	<b>105</b>
<b>5.2.</b>	<b>Multi Effect Evaporation Parallel Cross Feed Desalination System Modeling.....</b>	<b>107</b>
5.2.1.	System Configuration .....	108
<b>5.3.</b>	<b>Multi Effect Evaporation Parallel Cross Feed Thermal Vapor Compression (TVC).....</b>	<b>113</b>
5.3.1.	System Configuration .....	113
<b>5.4.</b>	<b>Multi Effect Evaporation Parallel Cross Feed Thermal Vapor Compression (TVC) Modeling ....</b>	<b>114</b>
<b>5.5.</b>	<b>Multi Effect Evaporation Parallel Cross Feed (with and without TVC) Model interpretation and validation .....</b>	<b>116</b>
<b>5.6.</b>	<b>Multi Effect Evaporation Parallel Cross Thermal Vapor Compression different Ejector Positions Model.....</b>	<b>121</b>
<b>5.7.</b>	<b>Multi Effect Evaporation Parallel Cross Feed Thermal Vapor Compression different Ejector Positions Model interpretation.....</b>	<b>123</b>
<b>5.8.</b>	<b>Exergy Analysis .....</b>	<b>135</b>
5.8.1.	Exergy Analysis Calculations.....	135
<b>5.9.</b>	<b>Economic Analysis .....</b>	<b>144</b>
5.9.1.	Unit cost of water calculations.....	144
<b>6</b>	<b>CONCLUSIONS.....</b>	<b>150</b>
<b>6.1.</b>	<b>Conclusion .....</b>	<b>150</b>
	<b>REFERENCES.....</b>	<b>152</b>
	<b>VITAE .....</b>	<b>156</b>

## LIST OF TABLES

Table 3.1: Validation of MEE/FF model with El-Dessouky model .....	38
Table 3.2: Comparison of MEE/FF/TVC Model with El-Dessouky Model.....	52
Table 3.3: Exergy analysis calculation for four effects MED/FF/TVC with ejector located after the last effect .....	68
Table 4.1: Exergy Analysis Calculations for PF/TVC system when the ejector is located after effect 4.....	101
Table 5.1: Exergy analysis for PCF/TVC system when the ejector is located after effect 4.....	138
Table 5.2: Cost Parametric analysis for MED PCF system for fuel energy cost of 4 <b>\$Gj</b> .....	148

## LIST OF FIGURES

Figure 1.1: World population in recent years [1].....	2
Figure 1.2: Desalination process.....	3
Figure 1.3 Classification of Desalination Process .....	4
Figure 1.4: Desalination process based on energy.....	5
Figure 1.5: Brine circulation MSF Process [1] .....	8
Figure 1.6: Single effect evaporation.....	10
Figure 1.7: Forward feed MED distillation system .....	12
Figure 1.8: Backward feed MED distillation system.....	13
Figure 1.9: Parallel feed MED distillation system.....	13
Figure 3.1: Forward Feed Multi Effect Evaporation System.....	29
Figure 3.2: Effect of stem temperature on the system performance ratio.....	36
Figure 3.3: Effect of steam temperature on the specific cooling water flow rate .....	37
Figure 3.4: Forward Feed Multi Effect Desalination System .....	39
Figure 3.5: The system performance ratio as a function of effects number .....	43
Figure 3.6: MEE/FF/Thermal Vapor Compression .....	44
Figure 3.7: Effect of steam temperature on Performance ratio MEE/FF/TVC System.....	50
Figure 3.8: Effect of steam temperature on Specific cooling water flow rate MEE/FF/TVC System.....	51
Figure 3.9: Different ejector positions in a MED-FF desalination system .....	53
Figure 3.10: Effect of steam temperature on Performance ratio different thermal vapor ejector positions 4 effects.....	55
Figure 3.11: Effect of steam temperature on Performance ratio different thermal vapor ejector positions 8 effects.....	56
Figure 3.12: Effect of steam temperature on Performance ratio different thermal vapor ejector positions 12 effects.....	57
Figure 3.13: Effect of steam temperature on specific heat transfer surface area different thermal vapor ejector positions 4 effects.....	58
Figure 3.14: Effect of steam temperature on specific heat transfer surface area different thermal vapor ejector positions 8 effects.....	59
Figure 3.15: Effect of steam temperature on specific heat transfer surface area different thermal vapor ejector positions 12 effects.....	60
Figure 3.16: Effect of steam temperature on specific cooling water flow rate different thermal vapor ejector positions 4 effects.....	61
Figure 3.17: Effect of steam temperature on specific cooling water flow rate different thermal vapor ejector positions 8 effects.....	62
Figure 3.18: Effect of steam temperature on specific cooling water flow rate different thermal vapor ejector positions 12 effects.....	63

Figure 3.19: MED/FF/TVC System.....	67
Figure 3.20: Second Law efficiency MEE/FF system TVC after last effect .....	69
Figure 3.21: Exergy analysis break down for forward feed system .....	70
Figure 4.1: Parallel Feed Multi Effect Desalination System .....	72
Figure 4.2: MEE/PF/Thermal Vapor Compression .....	78
Figure 4.3: Effect of number of effects on the Performance ratio PF/MEE .....	82
Figure 4.4: Effect of number of effects on the specific heat transfer surface area PF/MEE.....	83
Figure 4.5: Effect of Steam Temperature on Performance Ratio .....	84
Figure 4.6: Effect of Steam Temperature on Specific heat transfer surface area .....	85
Figure 4.7: Effect of Steam Temperature on Specific cooling water flow rate .....	86
Figure 4.8: MEE/PF/TVC desalination system .....	87
Figure 4.9: Effect of steam temperature on Performance ratio for different ejector positions 4 effects .....	89
Figure 4.10: Effect of steam temperature on Performance ratio for different ejector positions 8 effects. ....	90
Figure 4.11: Effect of steam temperature on Performance ratio for different ejector positions 12 effects .....	91
Figure 4.12: Effect of steam temperature on specific heat transfer surface area for different ejector positions 4 effects .....	92
Figure 4.13: Effect of steam temperature on specific heat transfer surface area for different ejector positions 8 effects .....	93
Figure 4.14: Effect of steam temperature on specific heat transfer surface area for different ejector positions 12 effects .....	94
Figure 4.15: Effect of steam temperature on specific cooling water flow rate for different ejector positions 4 effects .....	95
Figure 4.16: Effect of steam temperature on specific cooling water flow rate for different ejector positions 8 effects .....	96
Figure 4.17: Effect of steam temperature on specific cooling water flow rate for different ejector positions 12 effects .....	97
Figure 4.18: Total input and output exergy for parallel feed system.....	98
Figure 4.19: Exergy analysis breaks down Parallel Feed System .....	102
Figure 4.20: Exergy analysis break down for parallel feed system .....	103
Figure 4.21 Total exergatic efficiency for parallel feed system .....	104
Figure 5.1: Parallel Cross Multi Effect Desalination System .....	105
Figure 5.2: MEE/PCF/Thermal Vapor Compression.....	113
Figure 5.3: Effect of steam temperature on performance ratio .....	116
Figure 5.4: Effect of steam temperature on specific heat transfer surface area.....	117
Figure 5.5: Effect of steam temperature on performance ratio .....	118
Figure 5.6: Effect of steam temperature on specific heat transfer surface area.....	119

Figure 5.7: Effect of steam temperature on specific cooling water flow rate.....	120
Figure 5.8: Effect of steam temperature on Performance ratio 4 effects .....	123
Figure 5.9: Effect of steam temperature on Performance ratio 6 effects .....	124
Figure 5.10: Effect of steam temperature on Performance ratio 8 effects .....	125
Figure 5.11: Effect of steam temperature on Performance ratio 12 effects .....	126
Figure 5.12: Effect of steam temperature on specific heat transfer surface area 4 effects.....	127
Figure 5.13: Effect of steam temperature on specific heat transfer surface area 6 effects.....	128
Figure 5.14: Effect of steam temperature on specific heat transfer surface area 8 effects.....	129
Figure 5.15: Effect of steam temperature on specific heat transfer surface area 12 effects.....	130
Figure 5.16: Effect of steam temperature on specific cooling water flow rate 4 effects.....	131
Figure 5.17: Effect of steam temperature on specific cooling water flow rate 6 effects.....	132
Figure 5.18: Effect of steam temperature on specific cooling water flow rate 8 effects.....	133
Figure 5.19 Effect of steam temperature on specific cooling water flow rate 12 effects.....	134
Figure 5.20: Exergy analysis for PCF/TVC system 4 effects .....	139
Figure 5.21: Exergy analysis for PCF/TVC system 6 effects .....	140
Figure 5.22: Exergy analysis for PCF/TVC system 8 effects .....	140
Figure 5.23: Exergy analysis for PCF/TVC system 10 effects .....	141
Figure 5.24: Exergy analysis for PCF/TVC system 12 effects .....	142
Figure 5.25: Exergy analysis breaks down for parallel cross feed system .....	142
Figure 5.26:Cost Parametric analysis for MED system for different fuel energy costs .....	149

## **ABSTRACT**

Full Name : [KHALID ABDELBASIT KHALID]

Thesis Title : [WATER DESALINATION THROUGH THERMAL SYSTEMS -  
MED TECHNOLOGY]

Major Field : [MECHANICAL ENGINEERING]

Date of Degree : [December 2015]

Desalination is a process that takes a place in order to eliminate the salt and other minerals from seawater, the cost of desalinating saline water is generally high due to high energy consumption. In this research mathematical models based on mass and energy balances have been developed and validated with available models in the literature for three types of Multi Effect Desalination systems: forward Feed, parallel feed and parallel cross feed type of systems, The performance of the system is evaluated through evaluating the surface area of the evaporators and condenser, the system performance ratio or GOR and the flow rate of the cooling water needed for the system. Thermal vapor compression has been added to the system and different positions of the ejector have been studied. In addition, exergetic and economic analysis have been performed.

The study showed that adding thermal vapor compression increases the performance ratio and decreases the specific cooling water flow rate, in addition the best position

achieved for the thermal vapor compression located in the middle of the plant, the second law analysis also showed that the maximum efficiency achieved when the thermal vapor compression is located in the middle of the plant.

## ملخص الرسالة

الاسم الكامل: خالد عبد الباسط خالد عبد الباسط

عنوان الرسالة: تحلية المياه عن طريق الانظمة الحرارية, نظام تحلية المياه متعددة المبخرات.

التخصص: الهندسة الميكانيكية

تاريخ الدرجة العلمية: ديسمبر 2015

عملية تحلية المياه هي عملية ازالة الملح وبعض المعادن الاخرى من مياه البحر. غالبا تكون تكلفة المياه التي تتم تحليتها عالية وذلك لاستهلاك الطاقة العالي. في هذا البحث تم عمل نموذج رياضي مبني على ائزان الكتلة والطاقة لتقييم اداء انظمة التحلية متعددة المبخرات من خلال تقييم المساحة السطحية النوعية لانتقال الحرارة للمبخرات ونسبة الاداء للنظام ككل ومعدل السريان النوعي لمياه التبريد المطلوبة للنظام وتم التاكيد من صحة هذا النموذج بمقارنتها بالنماذج السابقة لثلاثة انواع من انظمة التبخير متعدد المراحل: التغذية الامامية, التغذية المتوازية, التغذية المتوازية العكسية, تم تقييم اداء النظام عن طريق حساب المساحة السطحية لانتقال الحرارة للمبخرات والمكثف, معدل الاداء ومعدل انسياب مياه البريد المطلوبة للنظام. تم اضافة نظام ضغط البخار الحراري وتم اختبار مواقع مختلفة في النظام الكلي. بالاضافة الي ذلك تم عمل تحليل القانون الثاني للديناميكا الحرارية وعمل تحليل اقتصادي للنظام. وضحت الدراسة ان اضافة نظام ضغط البخار الحراري يزيد من معدل الاداء كما انه يعمل علي تقليل معدل سريان كمية مياه التبريد المطلوبة للنظام, بالاضافة الي ذلك افضل موقع تم الحصول عليه لنظام ضغط البخار الحراري هو في منتصف المحطة, كما ان القانون الثاني للديناميكا الحرارية وضع ان اعلي كفاءة للنظام تكون عندما يوضع نظام ضغط البخار الحراري في منتصف المحطة.

# Introduction

## 1.1. Water Resources

Our planet contains huge amount of water. About 70% of the earth surface area is covered with water but the problem is that 97.5% of this water is saline water and the rest is fresh water. However, 80% of it is not accessible since it is found in the form of moisture in the soil or frozen in the icecaps. The remaining part is about 5% of the total quantity is fresh and accessible but it is not evenly distributed all over the earth [1].

## 1.2. Water classifications

Water classifications depend on the purpose of using it. For instance, drinking water and water used for industry have different values of salinity that range from 5 to 1000 part per million. It is of the same quality of water that can be found in rivers and lakes. The consumption of water for drinking is 2 liter per day per person. However, the quantity of water used for other house purposes which may have higher salinity is about 200-400 liter per person per day. In addition, the type of water used for industry has a maximum salinity of 5 part per million and it is used for feeding boilers. In the industry of electronics, iron heat exchangers are used to provide this kind of high purified water.

### 1.3. World population

The fresh drinking water decreases as population increases as depicted in Figure 1. So the demand for the fresh water increases. In order to fulfill this demand the desalination processes takes place. The feed water for desalination is seawater or brackish water, which has less salt than sea water and it is generally found in estuaries.

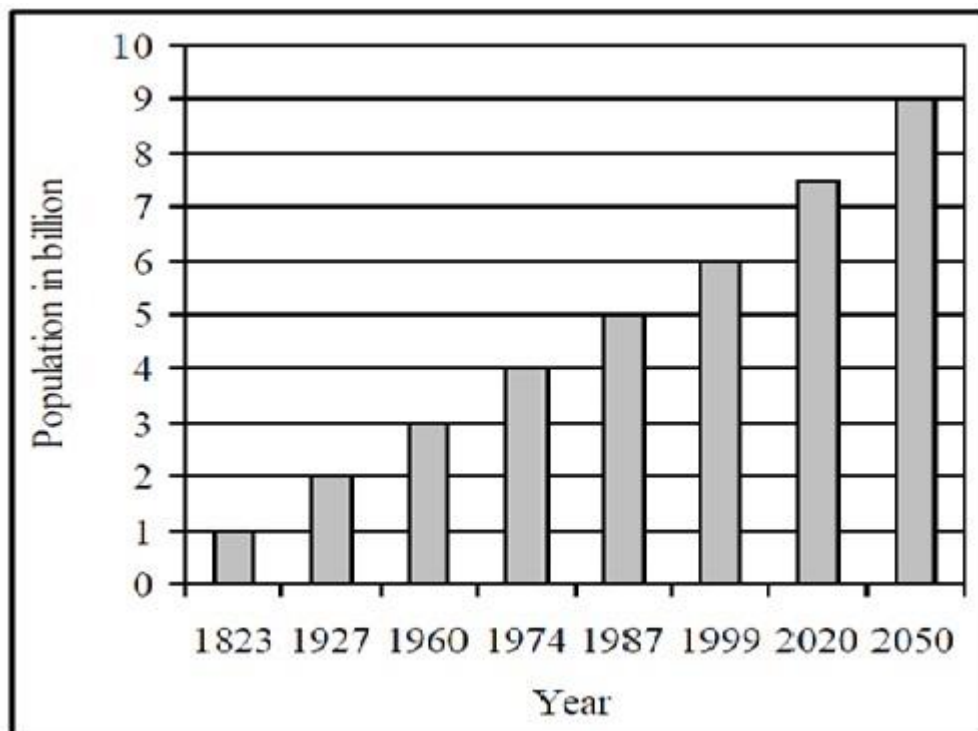


Figure 1.1: World population in recent years [1]

### 1.4. Desalination processes

Desalination includes a number of processes that take place in order to eliminate the salt and other minerals from sea- or brackish water, the cost of desalinating saline water is generally high due to high energy consumption. Basically, there two ways used to

desalinate the water around the world: thermal distillation and membrane based methods.

In the two cases, energy is needed to produce fresh water as shown in Figure 1.2.

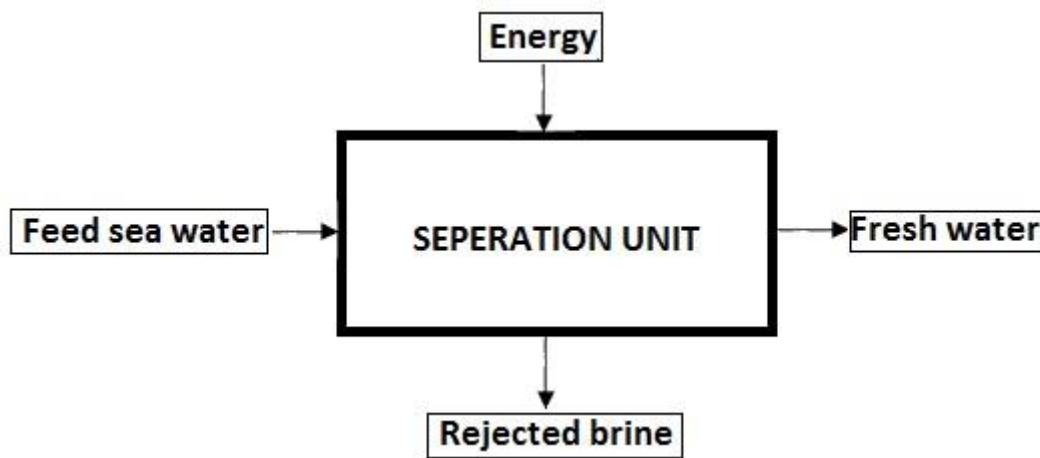


Figure 1.2: Desalination process

#### 1.4.1. Thermal distillation classifications

Thermal distillation technologies are commonly used in Middle East, because it is fitted with steam power plants. Low energy costs are another reason why these technologies are dominant. Basically, thermal distillation is a process in which saline or brackish water converts into vapor due to evaporation and then obtain fresh water upon condensation of this vapor. Figure 1.3 shows various desalination methods using either thermal or membrane technologies.

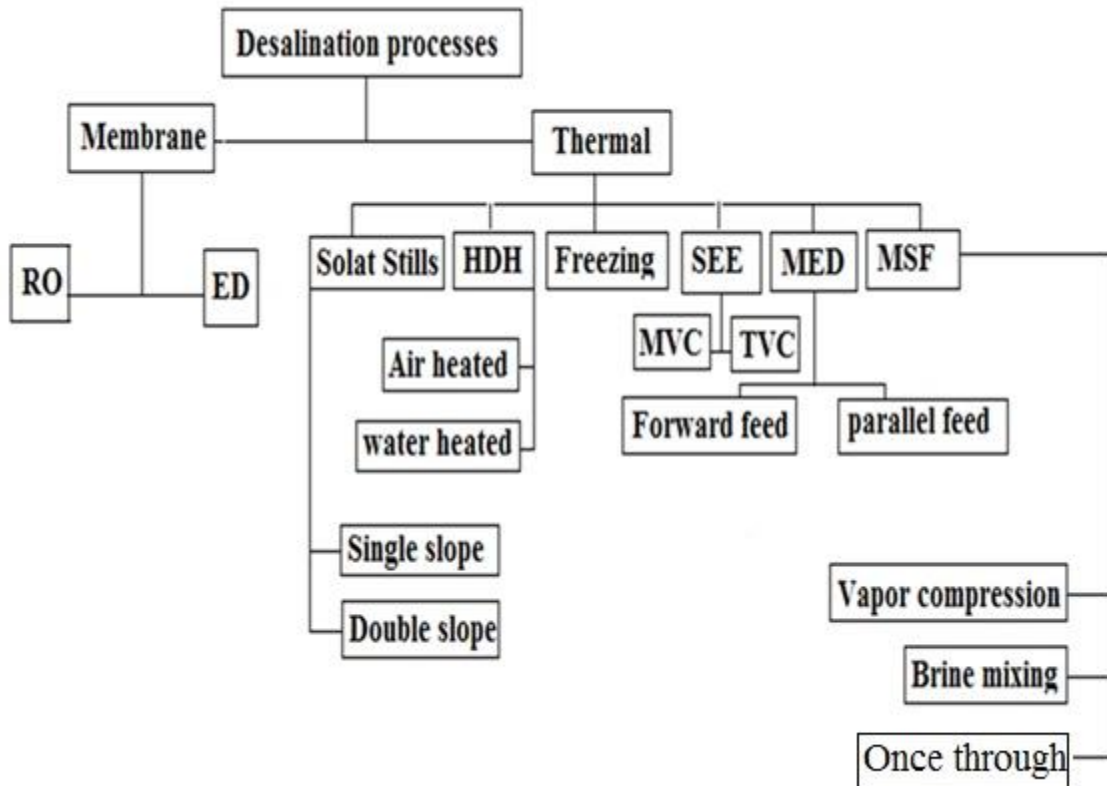


Figure 1.3 Classification of Desalination Process

**There are two ways of thermal desalination**

- Evaporation then condensation
- Freezing then melting

**There are two ways of membrane desalination**

- Reverse osmosis (Ro)
- Electro dialysis (ED)

Another classification can be made based on the type of energy used for desalinating water as shown in Figure 1.4. They are Electrical energy, thermal energy as well as mechanical energy

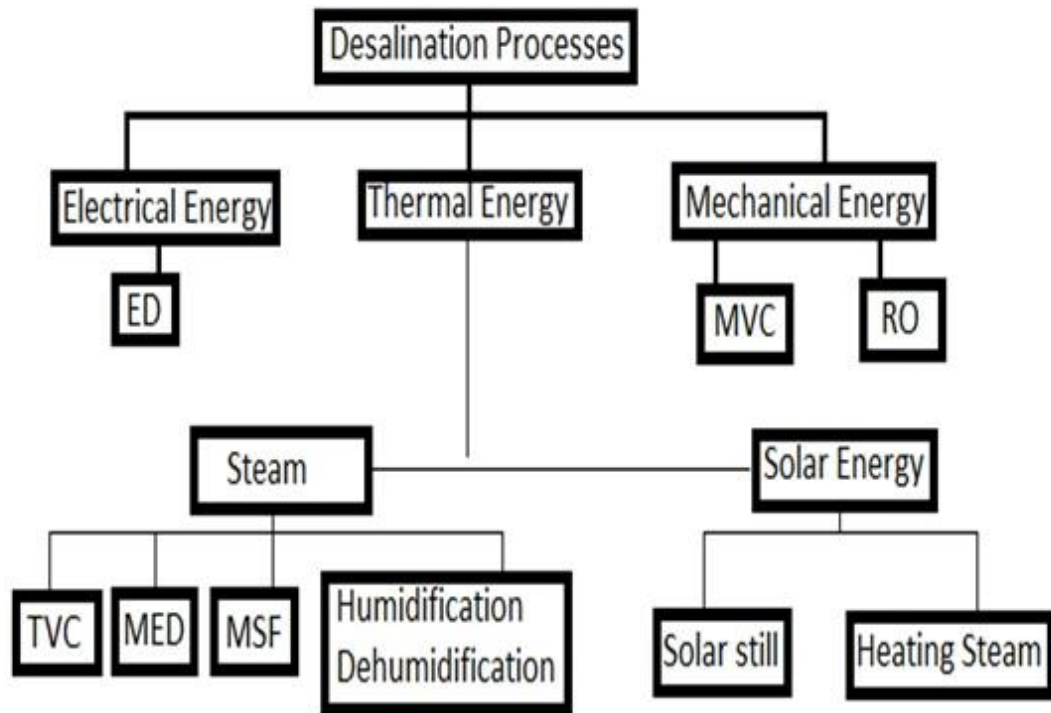


Figure 1.4: Desalination process based on energy

In the term of thermal distillation there are three major categories:

- Multi stage flash distillation
- Multi effect distillation vapor compression (VCD)
- Solar distillation that is used for small production rates

### **1.4.2. Membrane desalination classifications**

Reverse osmosis (RO) is the essential type of the membrane desalination, in this type of desalination, sea or brackish water passes through the membrane under high pressure that exceeds the osmotic pressure; however the other process is an electro dialysis (ED) which has a very narrow applications.

### **1.5. Multi stage flash distillation (MSF D)**

Seawater passes through several chambers in this process (multistage). Each stage in the multi stage flashing system operates at a pressure less than the previous one. First, feed sea water or brackish water is heated by steam to top brine temperature. Then, admitting the hot brine into the first chamber that has lower pressure such that vapor flashing occurs. This evaporation or flashing makes the operation continuous because in each stage the pressure is going to be less than the previous stage. The vapor generated is condensed into distilled water on the tubes of the heat exchanger in each stage. The numbers of stages in several MSF plants are between (15- 25). This type of plants has been in service since 1950s. There are two types of MSF plants either once through or brine recycled process. The feed seawater is passed through the brine heater and the flash chambers and then disposed to the sea as rejected brine in the once-through (OT) design. On the other hand, the feed sea water is recycled after disposing a part of it and replacing it with fresh seawater that has already passed through the condenser of the heat rejection stages.

MSF plants extensively utilize Stainless steel to prevent corrosion. Distillation processes produce approximately 50% of the world wide desalination capacity, but MSF units produce almost 84% of this capability.

### **1.5.1. Developments in MSF**

In MSF process, the formation of the vapor occurs within the liquid bulk temperature as the hot brine temperature flows and flashes in a number of chambers. The performance of this configuration is not satisfactory due to accumulation of the salt progressively around the outside surface of the tubes; this formation of the salt may act as an insulation result in reducing the evaporation rate dramatically. Therefore, to restore the efficiency cleaning becomes very important, in the earlier designs which has such a problem the system operates for/less than 14 days and blackout for 28 days or more[1].

### **1.5.2. Types of multi stage flashing system**

- Brine circulation MSF process
- Once through Multi stage flashing stage

#### **Brine circulation in MSF**

In the brine circulation process, the flashing stages are separated into two parts, heat rejection section and heat recovery section. Heated steam is used as a motivated flow, the recycle or raw water temperature increases by steam to the required top brine temperature in the brine heater. The recycled brine or feed water flows inside the tubes of the condenser to recover energy from the latent heat of condensation of the formed vapor.

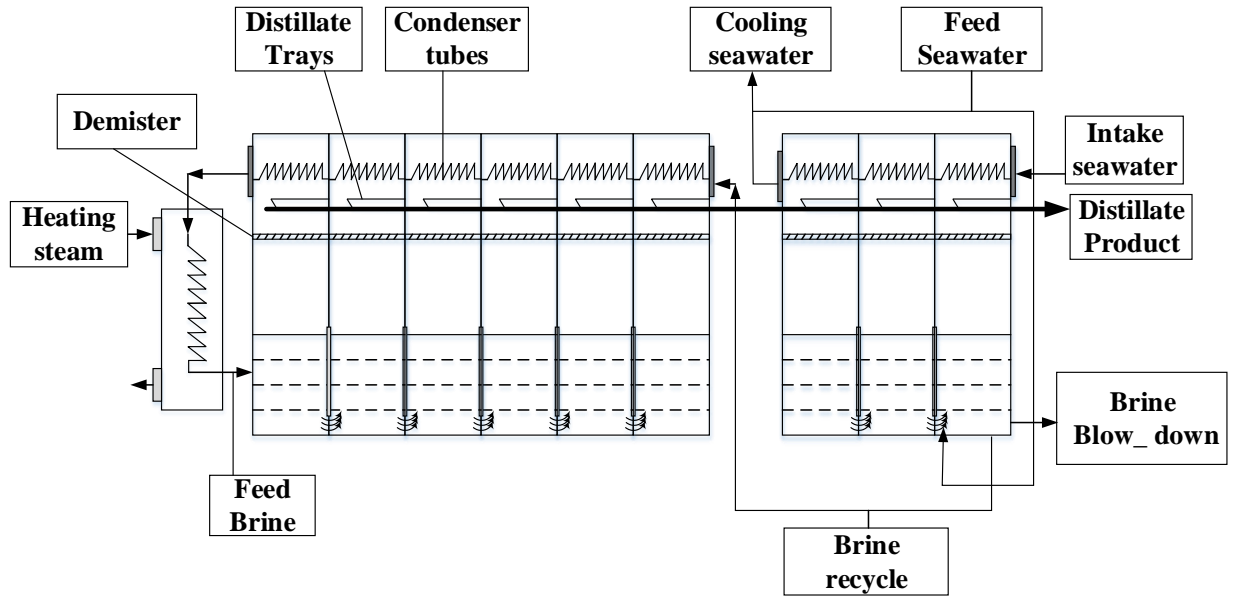


Figure1.5: Brine circulation MSF Process [1]

The MSF system is the dominant system in the Middle East. The reasons for that are:

- The product is an important element in people live. It is needed in huge qualities.
- Wide knowledge in operation, maintenance and installation.
- Process reliability.
- The needs to develop skills, unfamiliar problem types associated with new technologies [2].

Although there are several developments in the system that have been attained such as:

- Raising the ability of producing desalinated water from 454.6 to 27276 - 32731  $m^3$  per day.
- Consumption of the power has been reduced from 25-70  $KW/m^3$  in 1995 to 4-10 $KW/m^3$ .

The operation of the plant is significantly developed by introducing corrosion control chemicals. In the beginning, there was a problem of cleaning the system which cause long down times for the plants. In 1995, an achievement of operating MSF unit for 2 years without stopping has been realized through the use of the sponge ball cleaning.

**The MSF flashing stage includes the following:**

- Large pool for brine water
- Transfer device for the brine water between the stages. It is used to seal the spaces between the stages to prevent vapor escapes and to enhance mixing and turbulence for the inlet brine steam.
- The demister which is formed of wire meshes layers. It is used to entrain the brine droplets from the flashes of vapor.
- Condenser (preheater) tubes used to condense the vapor on its outer surface.
- Distillate tray in which the distillate product is collected.
- Removal of the non-condensable gases ( $O_2$ ,  $N_2$ , and  $CO_2$ ) using venting system.
- Other instruments like thermocouples, sensors and conductivity meters.

The MSF process operates at a top brine temperature between  $110^{\circ}\text{C}$  -  $130^{\circ}\text{C}$ , it is designed to withstand vacuum as well as a 2 bar maximum pressure.

## **1.6. Single effect evaporation**

A single effect evaporation system consists of two main elements as shown in Figure 1.6, the condenser and the evaporator. Seawater enters the condenser where it is preheated by the condensed distilled vapor. Then, part of it flows into the evaporator whereas the rest is rejected to the sea. The feed water that enters to the evaporator is sprayed over the

horizontal tube bundle. After it is heated to its saturation temperature, part of it evaporates and the rest is collected in a brine pool before it is rejected to the sea. The vapor flows into the condenser to condense into distilled water [1].

### Main features of single effect evaporation system:

- It has very limited applications in the industry
- Its performance ratio does not reaches one
- On the other hand it is an essential step to understand the multi effect evaporation system

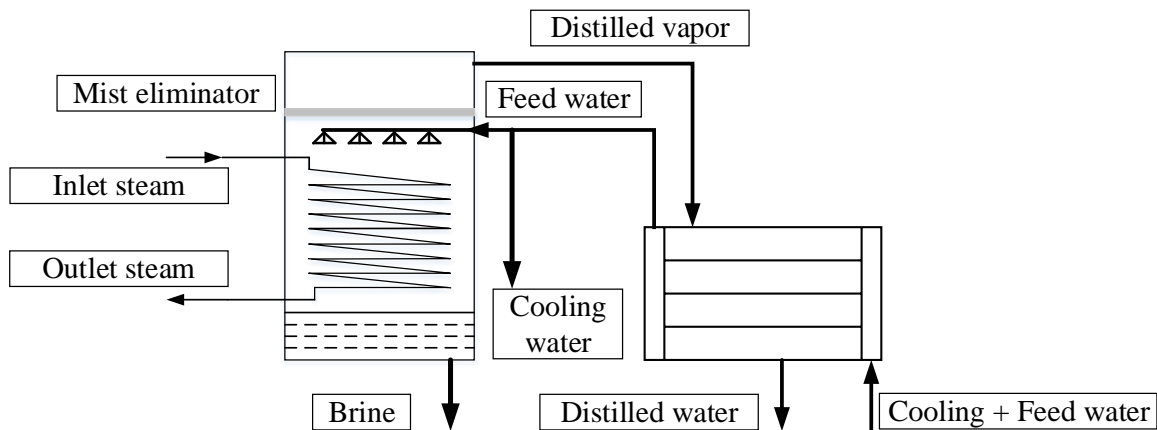


Figure1.6: Single effect evaporation

### 1.7. Multi effect desalination system (MED)

The multi effect desalination processes occur under the principle of condensation and evaporation at reduced ambient pressure through a series of effects. A number of evaporator effects generate water at progressively low pressure, as the pressure decrease water boils at lower temperature, then the vapor of an effect works as heating fluid for the

next effect, as the number of evaporators increases the performance ratio raises depending on the heat exchanger tubing arrangement. Fresh water is gained as the vapor condenses in each effect.

### **Main features of multi effect evaporation system (MED)**

- It is formed from a sequence of single effect evaporators
- The vapor formed in an evaporator is used as a source of heat in the next evaporator
- No rejection of large amount of energy to the surrounding, which is the main drawback of the single effect system

The advantages of MED system are that the specific consumption of the energy is low and the temperature of steam needed to run the system is low.

## Schemes of supplying feed water to the evaporators

- Forward feed MED distillation system

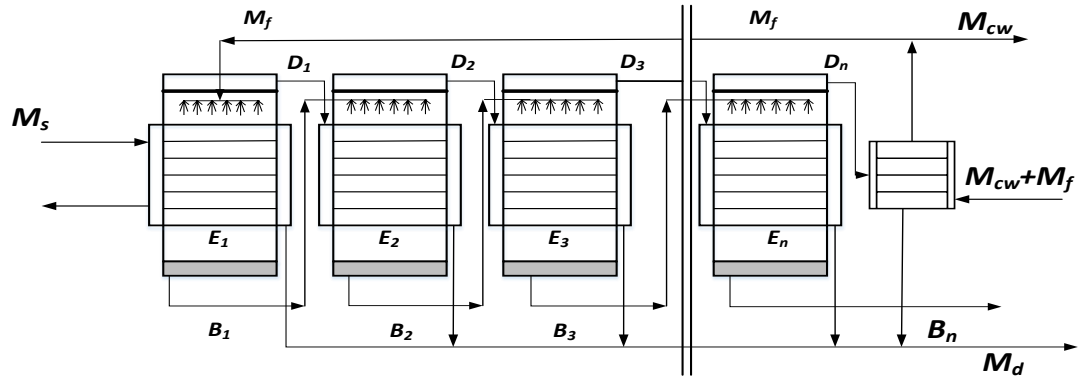


Figure1.7: Forward feed MED distillation system

Figure 1.7 shows the forward feed MED system where the feed water is directed to the first effect. The brine leaving an effect is sprayed in the next one. In this arrangement, both the feed stream and the vapor are flowing from the first effect to the last effect.

- Backward feed MED distillation system

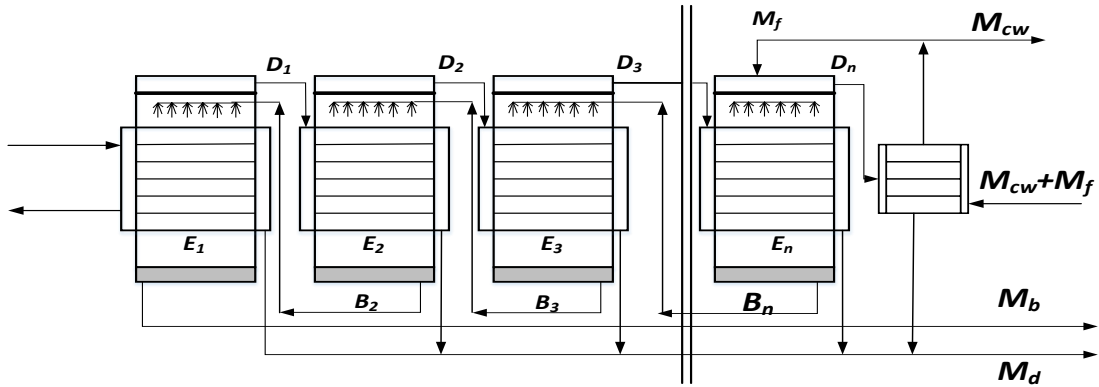


Figure 1.8: Backward feed MED distillation system

Figure 1.8 shows the backward MED arrangement where the feed stream is distributed in a reverse order from the last effect to the first effect. It is noted that, in this arrangement, both the salinity and temperature of the brine solution increase as they flow toward earlier effects till they reach their maximum values at the first effect.

- Parallel feed MED distillation system

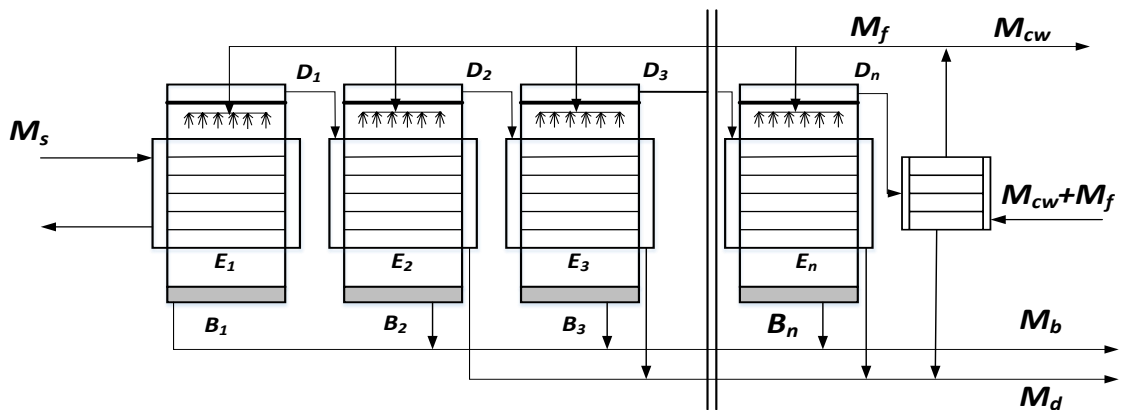


Figure 1.9: Parallel feed MED distillation system

Figure 1.9 shows the parallel feed arrangement where the feed stream leaving the condenser, after recovering the energy associated with vapor formed in the last effect, is

distributed evenly in all the effects at the same rate and thermal condition. The brine is collected from every stream and is rejected back to the sea in a common line.

## **1.8. Vapor Compression Distillation (VCD)**

VCD systems are either used separately or with multi effect desalination systems, the vapor is compressed to produce heat needed for water evaporation. There are different configurations, usually the heat of evaporation is generated by a mechanical compressor but generally it has small capacity.

As the received vapor from the evaporator is pressurized by the compressor its energy transferring to evaporate the feed stream and then the vapor condenses to formulate fresh water.

### **1.8.1. Working principle of vapor compression desalination system**

Generated vapor from the last effect is delivered to a compressor. After the vapor is compressed to high pressure and temperature, it is fed to inside the tubes of the first effect to condense and release its latent heat to heat the sprayed seawater and evaporate a portion of it. Then the condensed water is collected and the evaporated vapor goes to the next effect as a source of heat where it condenses to provide heat to the sprayed seawater in the next effect.

### 1.8.2. Performance of multi effect evaporation system

Performance ratio ( $PR$ ) is a term that is used to express the performance of multi effect evaporation system similar to thermal desalination systems. It is represented by the ratio of the produced water flow rate and the steam consumed flow rate of the system.

$$PR = \frac{\dot{m}_d}{\dot{m}_s} \quad (1.1)$$

$PR$ : Performance Ratio.

$\dot{m}_d$ : The amount of distillate produced in kg/s.

$\dot{m}_s$ : The amount of consumed steam in kg/s.

## 1.9. Objectives

- To develop mathematical models for design and operation of multi effect desalination system based on energy and mass balances.
- To estimate a multi effect evaporation desalination process performance through evaluating
  - The specific area of heat transfer for the evaporators.
  - The specific area of heat transfer for the condenser.
  - The performance ratio/GOR.
- To evaluate the specific cooling water flow rate needed.

- To test several layouts of MED in order to reach a preferred one in terms of energy consumption and performance characteristics.
- To study the effect of changing the position of thermal vapor compression.
- To perform second law analysis and economic analysis.

## **1.10. Methodology**

The models presented consist of mass and energy balance equations have been solved using Engineering equation solver software (EES). The solution starts with inserting the values of the input parameters for instance: feed water salinity and temperature, rejected brine salinity, last effect temperature. In the case of thermal vapor compression, two separate codes have been developed, one for the multi effect evaporation system equations and the other for the thermal vapor compression.

The results generated by the models are used to calculate the system performance parameters: performance ratio, specific heat transfer surface area and the specific cooling water flow rate. In addition, the results consist of Brine flow rate, Distillate flow rate and Effect temperatures.

# Literature Review

## 2.1. Thermal Desalination

The need for improvements of the thermal desalination units is important especially when we are dealing with high salinity or contamination of feed water. In general, the MSF is the most used type of thermal desalination systems for large scale production in the gulf region but the multiple effect distillation is thermodynamically superior since it consumes lower energy compared to multi stage flashing system. The ability to run at low temperature and using the output heat from the power station turbines as a heat source for MED system result in low specific energy costs for water desalination Ophir and Lokiec [3]. In order to reduce the cost and increase the availability of clean water, further research is needed. However, to achieve this, it is needed to merge thermal desalination systems with power plants, such as MED with power plants in a combined water power cogeneration system. The advantage of two functioning technology is the ability to generate both water and power at lower costs Mistry et al. [4]. El-Dessouky et al. [5] reported that the best performance is gained for both the parallel/cross flow and the parallel flow system. Furthermore, it has a simple operation, construction and design. Running of two systems is preferential when the temperature is higher as a result of the extreme decrease in the specific heat transfer area. El-Dessouky and Ettouney [1] developed a simplified model to simulate the system performance. Darwish et al. [6] reported that, the normal Multi Effect Boiling system has the benefit of exploit a heat source with low-temperature when it works at low TBT, which results in much lower

work and consumed energy than Multi Stage Flash units. The heat transfer areas increase considerably due to decreases of  $\Delta T$  to less than  $2^{\circ}\text{C}$ . The Gain Output Ratio increases due to using feed heaters, although the feed heaters make the system more complex, increase the initial cost, and also increase the energy used by pumps. The Multi Effect Boiling system consumes almost half of the pumping power of the Multi Stage Flash system. The MED can be coordinated to produce more product if required, but at lower Gain Output Ratio. Darwish and Abdulrahim [7] also developed a simple MED model and analyzed different arrangements. They examined the relation between performance ratio and the heat transfer area. They [7] analyzed three feed layouts (forward feed FF, backward feed BF, and parallel feed PF). They reported that for all arrangements, increasing the number of effects raises the gain output ratio (GOR), and the specific heat transfer area. The backward feed BF has lower specific heat transfer area and a promising higher gain ratio than the forward feed. On the other hand, the backward feed BF is rarely used in desalination since the highest salinity in the system takes place at the highest temperature in the first effect. This in turn results in an increased risk of accumulating scales of salts like  $\text{CaSO}_4$ ,  $\text{CaCO}_3$ , and  $\text{Mg}(\text{OH})_2$  in the backward feed BF system than in the FF system. One more drawback for the backward feed BF system is the need for pumping the feed between effects to the previous effect pressure (at higher pressure).

Aly and El-Figi [8] studied the performance of multiple effect distillation forward feed MED-FF process via a mathematical model and pointed that the performance ratio notably depends on the number of evaporators rather than the top brine temperature TBT. It is concluded that for the MSF system, increasing the number of effects will decrease the specific area of heat transfer. This would decrease the capital cost to a particular

limit. On the other hand, the specific heat transfer area reduces by reducing the number of evaporators in the MED system, but, this will result in a decrease in the performance ratio. The MSF unit that has a higher performance ratio uses lower steam and lower operating cost; but in contrast, it is a higher capital cost due to a higher specific area of heat transfer. The fouling factor increases during the operation of the MSF unit. The fouling causes system degradation with time, in the study of Tahir et al.[9] the fouling is considered for design and rating aspects, they reported that estimating the fouling resistance into the model avoids the over sizing of the plant and then the time intervals between the shutdowns is calculated. Another work conducted by Mistry et al. [10] developed a flexible model of MED system that is suitable for use in optimization of cogeneration systems to produce water and power. It is found that the developed model in a very good agreement compares with the models available in literature, the results showed that the model allows for studying forward feed and parallel feed arrangement without need for new code.

The effects of various parameters on multi effect desalination system performance are studied by Ameri et al. [11]. The parameters they considered include the number of effects, pressure of inlet steam to the first effect, the difference in temperature between the effects, and inlet saline water temperature. They analyzed the effect of these parameters on the performance ratio, required heat transfer area and the cooling sea water needed for the system, the findings of this study illustrated that for the number of effects, there is a best possible value for the system at constant production rate. It is a function of salinity of the seawater, the temperature difference between the stages and the temperature of the sea water, it is also reported that the performance ratio and the heat

transfer area increase as the steam pressure increases while the cooling water flow rate reduces.

The multi-effect (ME) system can generate fresh water at a cost lower than the MSF system when both of them are provided with steam from turbines. Thermal or mechanical vapor compression desalination systems are more cost-effective than MSF systems that operates directly by a boiler [12].

Alasfour et al. [13] studied different arrangements of thermal vapor compression multi effect desalination system, the three different arrangements are a conventional multi effect thermal vapor compression, multi effect thermal vapor compression using feed heaters and multi effect thermal vapor compression fitted with a conventional multi effect evaporation system, the effect of motive steam pressure, feed seawater temperature, top brine temperature and temperature difference between effects was carried out, it is reported that the main source of exergy destruction is the irreversibility in the evaporators and the ejector, the results illustrated that 50% of the exergy destruction occurs in the first effect. Reducing the temperature difference increases the evaporator surface area but decreases the specific heat consumption.

El-Dessouky et al. [14] examined different MED arrangements taking into account parallel flow, parallel cross flow, and combined systems with (MVC) mechanical vapor compressor or a thermal vapor compressor (TVC). They concluded that the thermal performance ratio of MEE/P/TVC system is lower than that of the MEE/PC/TVC system. In addition, the specific power consumption for the two systems reduces when the

temperature is higher. The specific power consumption of MEE/P/MVC system is higher than that of the MEE/PC/MVC system.

In 2004, another study conducted by Darwish et al. [15] showed a comparison between the multi stage flashing system (MSF) with thermal vapor compression combined with multi effect evaporation system. They showed that the advantages of TVC/MED system compared with the MSF for instance: it has better sensitivity to the inlet steam variation, the pumping energy is less, and it has the ability to run at various modes.

The performance ratio of the plant is almost independent of the top brine temperature and powerfully associated to the number of stages, while raising the number of stages and decreasing the top brine temperature result in increasing the specific heat transfer area, which was also reported by ElDessouky et al. [16]

In 2007 a computer code has been developed by Kamali and Mohebinia [17] for multi effect desalination system, thermal vapor compression MED/TVC, in this work the influence of many factors have been considered to increase the gain output ratio, it is concluded that the system temperature and pressure depend on the condenser temperature and pressure. Raising the condenser surface area results in decreasing the top brine temperature. Accordingly, the gain output ratio increases and the system lifetime increases.

Further development have taken place in the MED system with TVC which allowed the production capacity to increase, which represent actual competition to the MSF systems. Bin Amer et al. [18] developed a mathematical model to examine multi effect thermal

vapor compression system. Results illustrated that the highest gain ratio changes from 8.5 for four effects to 18.5 for 12 effects at best top brine temperature from 55.8°C to 67.5°C while the optimal compression ratio between 1.81 to 3.68 and the optimal entrainment ratio varies from 0.73 to 1.65.

Recently in 2014 AlMutaz and Wazeer [19] performed a study to build up a mathematical model of MEE/TVC system and compared the results of the mathematical model with the available existing plants. The program has been developed by MATLAB. The model outcomes showed a good agreement with some commercial MEE-TVC systems, it is concluded that the GOR for each plant is close to the GOR for the actual plant.

Al-Sahali and Ettouney [20] conducted a study on thermal desalination processes taking into account the point of design, cost and energy aspects. They reported that over the years the attractive processes of multi effect desalination and mechanical vapor compression have been improved and in the future there will be continuous growth in its share in the market. But this development would be focus on additional raise in the capacity of the unit, utilization of economical construction materials. This improvement should also lead to significant cost drop, which makes this system competitive to others like multi stage flashing system (MSF) and reverse osmosis systems (RO).

Kouhikamali and Sharifi [21] conducted a numerical analysis to investigate the performance of a system with a thermo-compressor. Then, the improvement was performed on the model and the system analyzed and verified. It is concluded that when the entrainment ratio increases, it leads to better performance for the thermo compressor. Another conclusion is that the entrainment ratio is affected by the geometry of the

thermo-compressor. Combining the system of absorption heat pump multi effect evaporation with a vapor compression refrigeration cycle is proposed by Esfahani et al.[22], to generate fresh water and cooling in the same time. The condenser in the combined system of the vapor compression cycle system is changed by the absorption heat pump-multi-effect evaporation system, where a part of the distilled water formed in the final effect of the MEE system is used for the vapor-compression refrigeration cycle system as the refrigerant. The results illustrated that the improved system can save 57.12% in electric power, 5.61% in heat energy, and 25.6% in the annual cost compared to the vapor compression refrigeration cycle and absorption heat pump multi-effect evaporation systems when it works separately.

Combination of an absorption heat pump with a multi effect desalination system has merits stated by Padillaa and Rodriguezb [23]. They showed that the importance of study for optimizing and evaluating such a desalination system. The earlier work on such system has been reviewed in this work. It is pointed out that for the process of multi effect desalination system the absorption heat pump is able to reduce the cooling water mass flow rate needed in the MED system, consequently, it decreases the pumping energy which reduces the capital costs. Moreover, the heat rejected to the environment from the MED unit reduces since a part of it is recovered in the absorption heat pump.

In addition, the combination of a solar power plant with the multi effect desalination system is a promising technique M.Al-Shammari [24].

Yilmaz and Soylemez [25] presented a mathematical model for a forward feed multi effect desalination system using solar and wind as a source of energy in Turkey. In this

work, MED system is designed and a computer-code for 18 plants positioned at on-shore areas of Turkey. It is concluded that solar energy is steadier than wind energy.

A mathematical model has been developed recently [26] to assess the optimal heat transfer area and the optimal operating conditions that assure a fixed production of freshwater at minimum total cost. The problem targeted maximization of the water production. One of the results obtained reveals that the increase of the water produced by 20%, results in increasing in the total operating cost by 0.6 million US/yr. However, the flow rate of the seawater and the temperature of the steam are also increasing about 23 and 5%, respectively.

Diego et al in 2010 [27] reported the first experimental design proposal for multi effect desalination system using solar energy and double effect absorption heat pump MED-DEAHP system, the achieved improvement results in 50% reduction in the total solar area required comparing with solar multi effect desalination system. The results of the study of Joo and Kwak [28] showed that for multi-step evaporative distiller in which heating calories of 40 kW were used to generate fresh water of  $3 \text{ m}^3/\text{day}$  at a PR of the developed system of 2.0191.

Zhao and Liu [29] investigated multi effect solar desalination unit using tidal and solar energy, the system can use the tidal energy without transferring it to electricity, tidal energy used to provide the power instead of pumps which operated by electricity. So there is a great reduction in the cost.

Obtaining the pure water can be done by using wastewater energy of power plant using desalination [30], the returned water will be utilized as a make-up water. This multi effect desalination unit can provide the power plant by 83% of that water needed. As an outcome of this study as temperature difference in the evaporators decreases the quantity of water condensate increases.

HAMED et al. [31] performed a study to examine the exergy losses caused by irreversibility in various arrangements, thermal vapor compression (TVC) system, mechanical vapor compression (MVC) systems and conventional multi effect desalination system (MED). It is concluded that the least exergy losses are related to the thermal vapor compression among the three arrangements. Most of these losses occur in the thermo-compressor and in the first effect. However, the exergy destruction can be decreased by reducing the top brine temperature, increasing the number of stages, and increasing entrainment ratio of the thermo compressor.

There are two possibilities to increase the gain output ratio either by increasing the number of effects to specific limit or by connecting the system to a heat pump; there are three kinds of heat pumps that can be fitted to the MED systems, LIBR heat pump, thermal vapor compression and adsorption pumps [24].

Choi et al. [32] conducted another study to evaluate the exergy balance of MEE/TVC system as well as the exergy losses. They reported that the main source of the exergy losses is the thermal vapor compression and the effects that contribute to about 70 percent of the whole quantity, in the modified design the entrainment ratio of 120% lead to 12% reduction in the surface area of the heat transfer.

Piacentino and Cardona [33] conducted a study of multi effect desalination system, It is revealed that the exergy destruction and the flash at the inlet of the brine at the pre-heaters, both of them do not mainly affect the heat transfer at the evaporators, main factor of exergy losses is the increase of the temperature difference between two evaporators.

## **2.2. Thermo-economic analysis**

There are many studies that have been reported in the literature talking about the thermo economic analysis of the desalination systems, the main purpose of the second law analysis is to find the source of irreversibility, Second Law efficiency is a helpful parameter for representing the energy requirements. On the other hand, in view of the fact that the costs of energy characterize less than 50% of the total cost of product desalination systems [4]. The unit cost of the distillate product depends on the configuration of the system itself, either it is a single purpose desalination system or it works as a cogeneration with power plant. In 1993 Morin [34] conducted a study that compares MSF with MED in operating and design aspects. It is reported that MED is lower in operating cost than that in the case of MSF. Ophir and Lokiec [35] reported that the Lower Temperature Multi Effect Desalination plants are extremely economical in terms of operational and capital costs.

In 2005, a study have been reported by Nafey et al. [36] for Multi effect desalination system that have been compared with a hybrid system of Multi effect desalination and Multi stage flash system using exergy and thermo economic analysis. The comparison between MEE/FF and MEE/PC shows that the unit of distillate cost of Forward Feed

desalination system is 25% less than that in the Parallel Cross arrangement. However, for the hybrid system of MEE/MSF the results concluded that the unit of distillate cost for the One-Through MEE/MSF is 5% less than that of the Brine mixing configuration. Another study shows a methodology of thermo-economic and exergy analysis of Multi Stage Flash (MSF) plant through a developed computerized package presented by Nafey et al. [37]. The major goal of this analysis is to analyze the MSF unit and to calculate the unit cost of the product of the water distilled. The analysis results show that for MSF plant in the operation of the partial load, the unit cost of the product rises to 21% when the load reduces to 50%.

In addition another study in 2006 reported by Abdunnasser et al. [38] where thermo-economic analysis have been presented for the most used desalination processes as multi effect evaporation (MEE), mechanical vapor compression (MEE-MVC), thermal vapor compression (MEE-TVC), Multi stage flash (MSF), and reverse osmosis RO. They were compared with each others. The results demonstrate that both Reverse Osmosis (RO) and Mechanical Vapor Compression (MEE-MVC) systems offer lower unit cost of the product. The irreversibility in the flash at brine inlet and the pre-heaters, both in fact are important factors after the heat transfer in the evaporators. However, the main source of exergy destruction is the temperature difference between two effects. As it increases, the exergy destruction increases as reported by Piacentino and Cardona [33].

# **Forward Feed Multi Effect Evaporation Desalination**

## **Systems**

A number of single effect evaporators form a multi effect evaporation unit, the first effect is heated by an external source, for instance, steam from a power plant. The rest of effects are heated by the vapor formed in the previous effect. This process prevents rejection of heated brine, consequently reduces energy loss.

There are different arrangements of the multi effect desalination systems; namely, forward, backward and parallel feed arrangements. The difference between these arrangements is mainly the flow directions of brine and heating steam/vapor. The forward feed multiple effect evaporation system is widely used in sugar industry as well as paper industry. It is more complex than parallel feed desalination systems. The horizontal evaporators are mostly used type in multi effect evaporation systems.

### 3.1. Working Principle

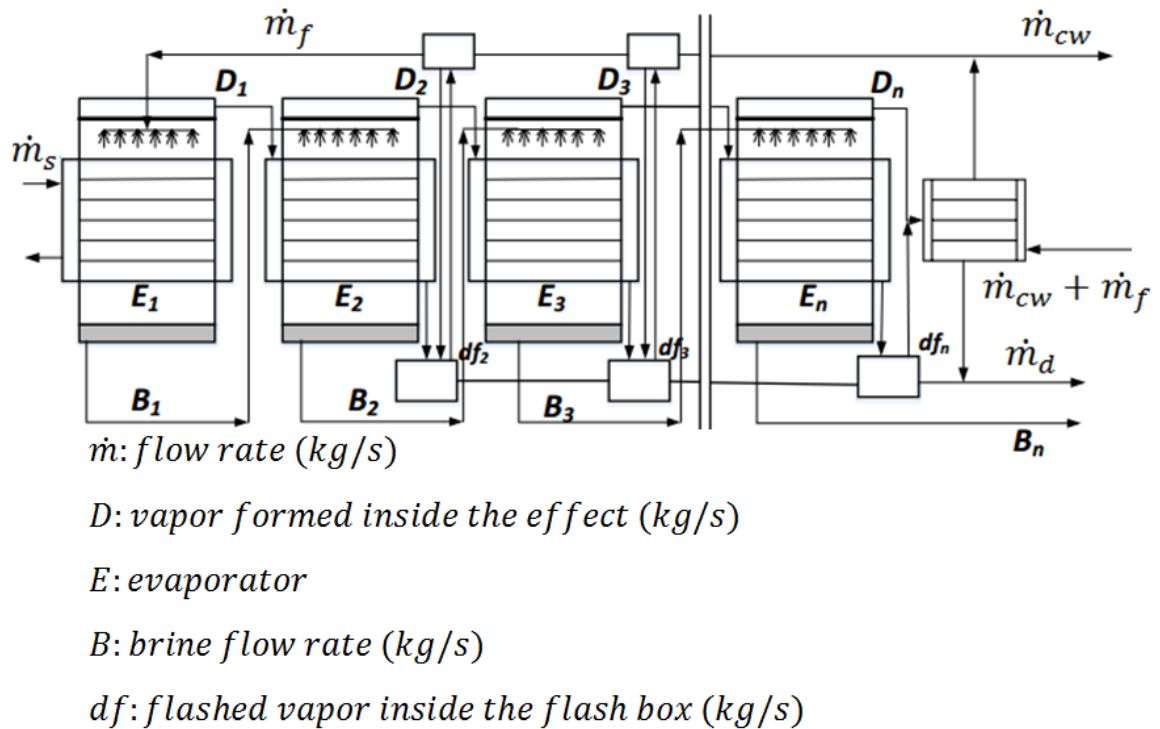


Figure 3.1: Forward Feed Multi Effect Evaporation System

Figure 3.1 shows a schematic of the forward feed MED system combined of (n) number of evaporators, (n-1) flash boxes, (n-2) preheaters and a down condenser. The directions of vapor and brine flows are from first effect in the left to the last effect in the right and the feed water flows in the reverse direction.

The main components of multi effect desalination systems are: a down condenser, evaporators (effects), feed water preheaters and flash boxes. Intake water enters the condenser with flow rate of  $(\dot{m}_f + \dot{m}_{cw})$  feed water and cooling water, the cooling water is rejected back to the sea and the feed water is chemically treated before it enters to the evaporators. The feed water absorbs the latent heat of the vapor generated in the last

effect, ( $D_n$ ). Accordingly, the temperature of the feed water rises from ( $T_{cw}$ ) to ( $T_f$ ), the cooling water is used to take away the additional amount of heat added in the last effect and return back to the sea ( $m_{cw}$ ), However, the feed water enters the first effect after passing through the preheaters with a flow rate of ( $m_f$ ) such that its temperature increases from ( $T_f$ ) to ( $t_2$ ). Then, it enters the first effect. In the first effect, part of the feed water transfers into vapor ( $D_1$ ) and the remaining brine is fed to the second effect ( $B_1$ ). The vapor formed in the first effect is the source of heat for the second effect ( $D_1$ ), the temperature of the brine in the first effect increases from ( $t_2$ ) to ( $T_1$ ) and the first effect formed vapor temperature ( $T_{v1}$ ) is less than the first effect brine temperature by boiling point elevation ( $BPE_1$ ). Brine ( $B_1$ ) is the feed to the second effect and the brine in the second effect is the feed to the third effect until effect number ( $n$ ). The vapor formed in the first effect is due to boiling only but for other effects the vapor is formed due boiling and flashing.

The vapor formed in the last effect enters the condenser to increase the temperature of inlet feed water stream from ( $T_{cw}$ ) to ( $T_f$ ). This result in condensing the vapor and producing the distillate water from the condenser and the water formed in all effects. At the first effect, an external source of heat is introduced to raise the temperature of the feed at the first effect from ( $t_2$ ) to ( $T_1$ ), as vapor and brine pass from the first effect to the last effect, the salinity of the brine increases while the temperature and pressure of the vapor and brine decrease, the plant is in vacuum pressure and without this vacuum no vapor will be formed.

### 3.2. Modeling the multi effect evaporation forward feed system

In this section, a mathematical model of forward feed multi effect evaporation system is presented to provide an effective way to evaluate and design such a system. The mathematical model is solved using Engineering Equation Solver software (EES).

The mathematical model is based on energy and mass balances for the system components, the down condenser governing equations are included in the model.

The calculated properties in the model (for a given effect,  $i$ ) include:

- The vapor flow rate  $D_i$
- The brine flow rate  $B_i$
- The brine salinity  $X_i$
- The brine temperature  $T_i$
- The heat transfer surface area  $A_i$
- The steam flow rate entering the first effect  $\dot{m}_s$
- The cooling water flow rate  $\dot{m}_{cw}$
- The heat transfer surface area of the condenser  $A_c$

To develop mathematical model for the forward feed multi effect desalination system a number of assumptions are made:

- The vapor salinity is zero (does not contain salt)
- No energy loss between the effects and the surroundings

- The thermal load is equal for all effects except for the first effect
- The specific heat capacity,  $c_p$ , is constant
- The thermal losses like boiling point elevation, thermal losses due to pressure drop as the vapor passes through the mist eliminator, condensation process and non equilibrium allowance are constants.

Overall mass balance

$$\dot{m}_f = \dot{m}_d + \dot{m}_b \quad (3.1)$$

Where,  $f$ : feed,  $d$ : distillate,  $b$ : brine

$$\dot{m}_f * X_f = \dot{m}_b * X_b \quad (3.2)$$

The overall heat transfer coefficient for the effect is ( $U_i$ ) and the total temperature difference is

$$\Delta T_t = T_s - T_n \quad (3.3)$$

Where,  $\Delta T_t$  is the total temperature difference,  $T_s$  is the steam temperature,  $T_n$  is the last effect temperature

To determine the difference in temperature in each effect, it is important to calculate the overall heat transfer coefficient El-Dessouky et al.[1]

$$\sum_{i=1}^n \frac{1}{U_i A_i} = \frac{1}{U_1 A_1} + \frac{1}{U_2 A_2} + \frac{1}{U_3 A_3} + \dots + \frac{1}{U_n A_n} \quad (3.4)$$

The temperature difference in the first effect El-Dessouky et al.[1]

$$\Delta T_1 = \frac{\Delta T_1}{U_1 \sum_{i=1}^n \frac{1}{U_i}} \quad (3.5)$$

The temperature difference of the rest of the effects, for  $i$  from 2 to  $n$  is given by

$$\Delta T_i = \frac{\Delta T_1 * U_1}{U_i} \quad (3.6)$$

The temperature in the first effect is

$$T_1 = T_s - \Delta T_1 \quad (3.7)$$

The temperature of the rest of effects, for  $i = 2$  to  $n$ , is calculated using the following relation

$$T_i = T_{i-1} - \Delta T_i \quad (3.8)$$

The latent heat value ( $L_j$ ) is given in a correlation as function of steam and effect temperature ( $T_s$ ) and ( $T_j$ ). It may also be calculated from stored function in the Engineering Equation Solver (EES).

The flow rate of the vapor formed is the sum of formed vapor in all effects

$$\dot{m}_d = \sum_{i=1}^n D_i \quad (3.9)$$

Substituting,  $Q_i = D_1 * L_{v1}$ , constant heat load for  $i$  from 2 to  $n$ .

$$D_1 = \frac{\dot{m}_d}{1 + (L_1 * \sum_{i=2}^n \frac{1}{L_i})} \quad (3.10)$$

The flow rate of the vapor formed in the rest of effect, for  $i$  from 2 to  $n$

$$D_i = \frac{D_{i-1} * Lv_{i-1}}{Lv_i} \quad (3.11)$$

The flow rate of the first effect brine

$$B_1 = \dot{m}_f - D_1 \quad (3.12)$$

The brine flow rate of the rest of effects, for  $i = 2$  to  $n$

$$B_i = B_{i-1} - D_i \quad (3.13)$$

The salinity of the first effect

$$X_1 = \frac{\dot{m}_f * X_f}{B_1} \quad (3.14)$$

The salinity of the rest of the effects, for  $i = 2$  to  $n$  is

$$X_i = \frac{B_{i-1} * X_{i-1}}{B_i} \quad (3.15)$$

The heat transfer surface area of the first effect is given by the following expression

$$A_1 = \frac{D_1 * Lv_1 + \dot{m}_f * c_p * (T_1 - t_{f2})}{U_1 * (T_s - T_1)} \quad (3.16)$$

The heat transfer surface area of the first effect, for  $i = 2$  to  $n$

$$A_i = \frac{D_i * Lv_i}{U_1 * (\Delta T_i - \Delta T_{loss})} \quad (3.17)$$

It is important to calculate the steam flow rate in order to determine the system performance ratio

$$\dot{m}_s = \frac{D_1 * Lv_1 + \dot{m}_f * c_p * (T_1 - t_{f2})}{L_s} \quad (3.18)$$

The heat load in the condenser is

$$Q_c = D_n * L_{vn} \quad (3.19)$$

Condenser energy balance is also yields:

$$D_n * L_{vn} = (\dot{m}_f + \dot{m}_{cw}) * c_p * (T_f - T_{cw}) \quad (3.20)$$

The condenser Log Mean Temperature Difference is needed to calculate the condenser heat transfer surface area

$$LMTD_c = \frac{T_f - T_{cw}}{\ln \frac{T_n - \Delta T_{loss} - T_{cw}}{T_n - \Delta T_{loss} - T_f}} \quad (3.21)$$

The heat transfer surface area of the condenser

$$A_c = \frac{Q_c}{U_c * LMTD_c} \quad (3.22)$$

The main output parameters are

- The System Performance Ratio

$$PR = \frac{\dot{m}_d}{\dot{m}_s} \quad (3.23)$$

- The Specific Cooling water flow rate

$$s\dot{m}_{cw} = \frac{\dot{m}_{cw}}{\dot{m}_d} \quad (3.24)$$

- The Specific Heat Transfer Surface Area

$$sA = \frac{\sum_{i=1}^n A_i + A_c}{\dot{m}_d} \quad (3.25)$$

### 3.2.1. Model interpretation and Validation

The developed model of forward feed multi effect evaporation system is analyzed through studying the effects of the steam temperatures on the performance ratio, specific heat transfer surface area and the specific cooling water flow rate.

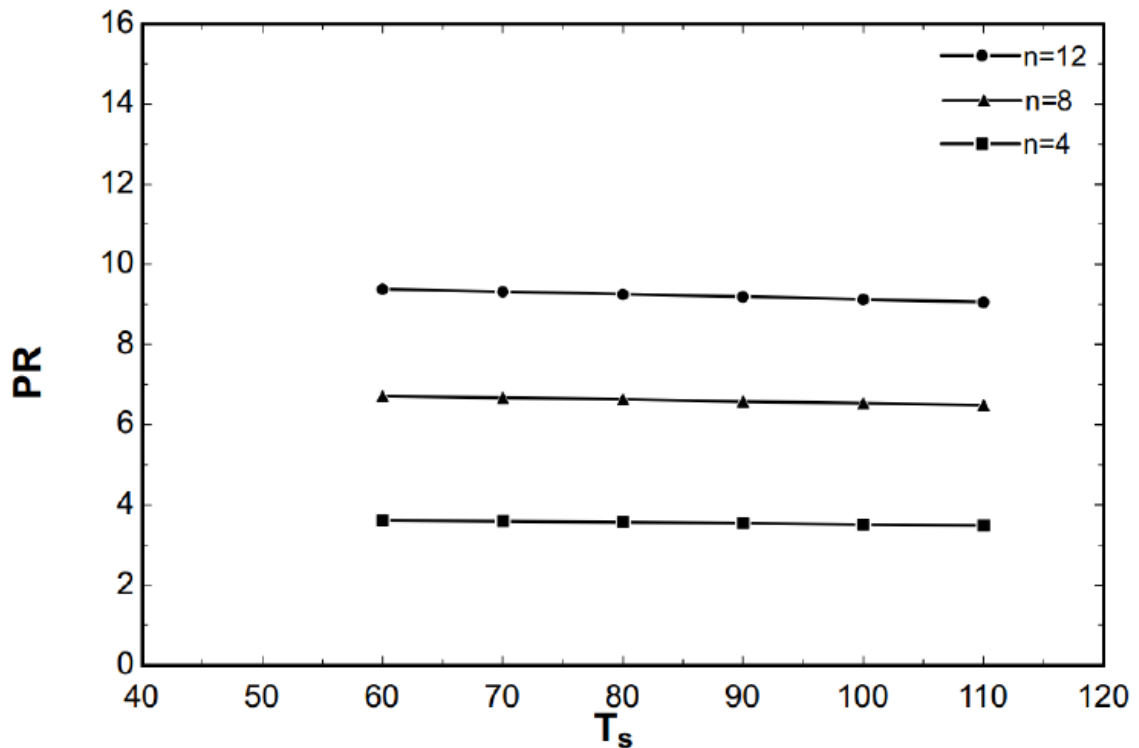


Figure 3.2: Effect of stem temperature on the system performance ratio

Figure 3.2 shows the effect of steam temperature on the system performance ratio, the figure shows that the steam temperature does not have a significant effect on the system performance ratio because increasing steam temperature reduce the latent heat insignificantly, however it can be clearly seen that increasing the number of effects

increases the performance ratio and that is due to the better use of energy such that additional vapor occurs in every effect due to the release of latent heat of condensation.

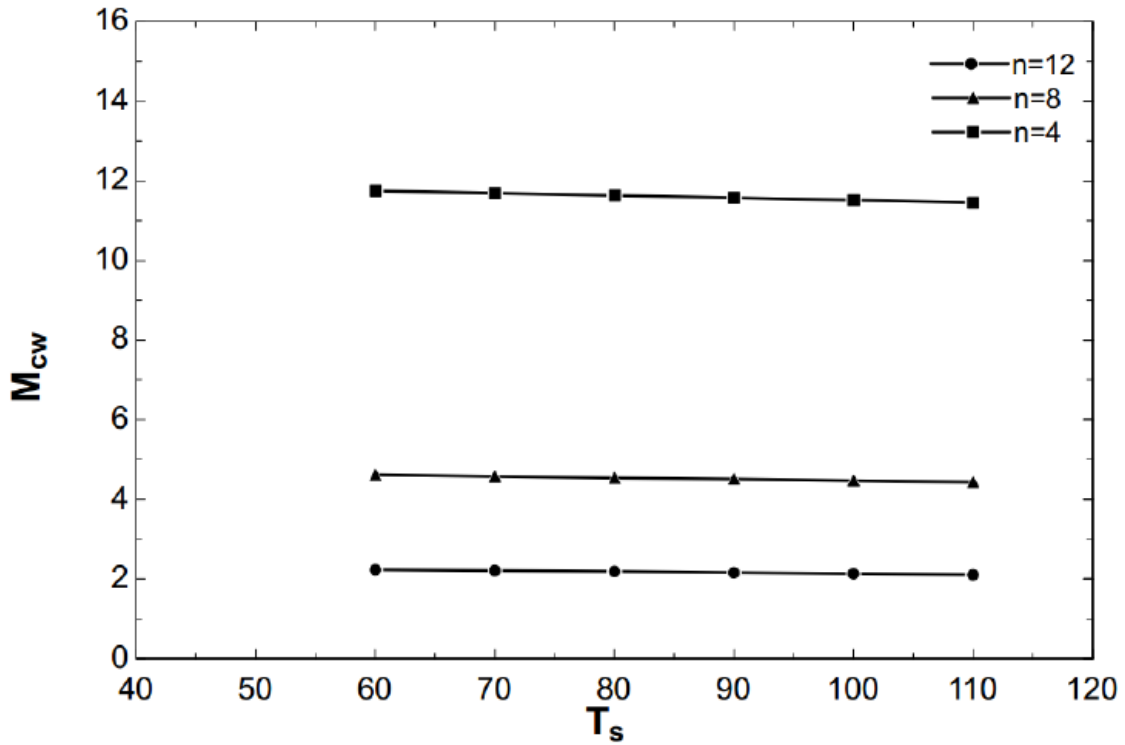


Figure 3.3: Effect of steam temperature on the specific cooling water flow rate

Figure 3.3 shows that increasing the steam temperature do not affect significantly the specific cooling water flow rate because the cooling water flow rate depends on the thermal load entering the condenser from the last effect, while steam temperature changes the last effect temperature remains constant. On the other hand, the specific cooling water flow rate is affected by the number of effects, and that is because when the number of effects is low the vapor formed in the last effect will be higher so it needs higher water flow rate to condense it.

Table 3.1 shows model validity by comparing it with El-Dessouky model [1]. The results are in a good agreement with El-Dessouky model, the performance ratio and condenser heat load have error percentages of 0.34%, the specific heat transfer surface area has an error percentage of 0.42%, however the maximum error percentage is reported in the specific cooling water flow rate; 0.51%.

**Table 3.1: Validation of MEE/FF model with El-Dessouky model**

Parameter	Present Model	El-Dessouky model	Error percentage
	MEE/ FF	MEE/FF	
$T_s$	100	100	-
$T_n$	40	40	-
$T_{cw}$	25	25	-
$T_f$	35	35	-
$n$	6	6	-
$s\dot{m}_{cw}$	6.805	6.77	0.51%
$A_c$	32.75	32.628	0.37%
$sA$	166.1	165.49	0.42%
$PR$	5.77	5.79	0.34%
$Q_c$	390.8	389.44	0.34%

### 3.3. Elaborated model of Forward Feed Multi Effect Desalination system

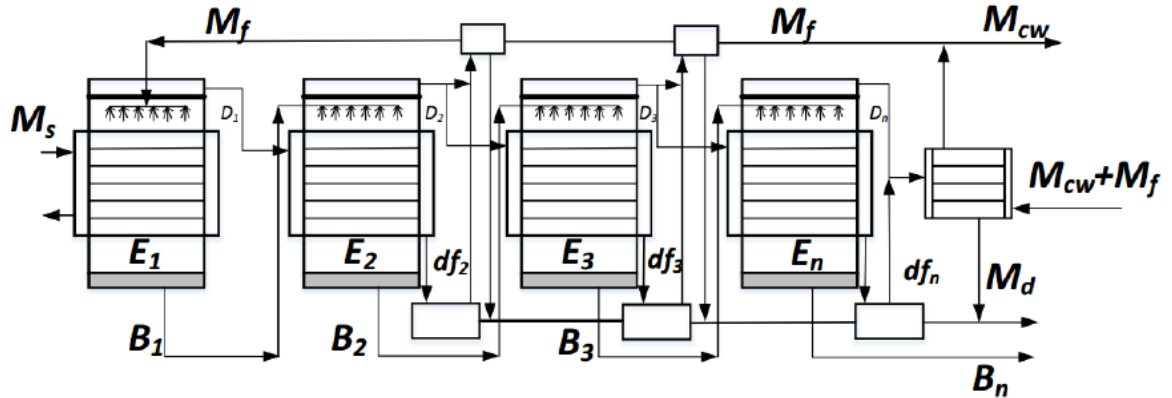


Figure 3.4: Forward Feed Multi Effect Desalination System

In this model, we take into account all the elements of the system, for instance flash boxes and preheaters.

Overall mass balance

$$\dot{m}_f = \dot{m}_d + \dot{m}_b \quad (3.26)$$

$$\dot{m}_f * X_f = \dot{m}_b * X_b \quad (3.27)$$

Where,  $\dot{m}_f$  is the feed mass flow rate,  $\dot{m}_d$  is the total distillate flow rate while  $\dot{m}_b$  is the total brine flow rate

$$\dot{m}_f = B_1 + D_1 \quad (3.28)$$

$$\dot{m}_d = \sum_{i=1}^n D_i + \sum_{i=1}^n d_i \quad (3.29)$$

Where,  $d_i$  is the flashed vapor in the flash box

The flow rate of the vapor formed in the rest of the effects, for  $i$  varies from 2 to  $n$

$$D_j = \frac{D_{j-1} * Lv_{j-1}}{Lv_j} \quad (3.30)$$

The brine flow rate of the first effect is given by

$$B_1 = \dot{m}_f - D_1 \quad (3.31)$$

The brine flow rate for the rest of the effects, for  $i$  from 2 to  $n$  is

$$B_j = \dot{m}_f - \sum_{i=1}^n D_i - \sum_{i=1}^n d_i \quad (3.32)$$

The salinity of the first effect is expressed as

$$X_1 = \frac{\dot{m}_f * X_f}{B_1} \quad (3.33)$$

The salinity of the rest of effects, for  $i$  from 2 to  $n$

$$X_j = \frac{\dot{m}_f * X_f}{B_j} \quad (3.34)$$

The thermal load of the first effect can be expressed by the following equation

$$Q_1 = D_1 * Lv_1 + \dot{m}_f * C_p * (T_1 - t_{f2}) = \dot{m}_s * L_s \quad (3.35)$$

The flashed vapor formed in the effect is then given by

$$d_2 = \frac{(\dot{m}_f - D_1) * C_p * (T_1 - T_2)}{Lv_2} \quad (3.36)$$

$$d_j = \frac{B_j * C_p * (T_{j-1} - T_j)}{L_{vj}} \quad (3.37)$$

The temperature in the flash box differs from the vapor temperature by non equilibrium allowance

$$\ddot{T}_j = \ddot{T}_{vj} + N\ddot{E}A_j \quad (3.38)$$

The flashed vapor in the first flash box is expressed as

$$\bar{d}_2 = \frac{D_1 * c_p * (T_{v1} - \ddot{T}_2)}{L_{v2}} \quad (3.39)$$

The flashed vapor in the rest of the flash boxes is:

$$d_j = \frac{(\sum_{i=1}^j D_i + \sum_{i=2}^{j-2} d_i) * c_p * (T_{vj-1} - T_j)}{L_{vj}} \quad (3.40)$$

The energy balance in the condenser is expressed in term of the following energy balance

$$d_n * L_{vn} + \bar{d}_n * \ddot{L}_{vn} + D_n * L_{vn} = (\dot{m}_{cw} + \dot{m}_f) * c_p * (T_f - T_{cw}) \quad (3.41)$$

The energy balance in the preheater is

$$d_j * L_{vj} + \bar{d}_j * \ddot{L}_{vj} = \dot{m}_f * c_p * (t_j - t_{j+1}) \quad (3.42)$$

Area of the first effect

$$A_1 = \frac{m_s * L_s}{U_{e1} * (T_s - T_1)} \quad (3.43)$$

The preheaters heat transfer surface area

$$A_{hj} = \frac{\dot{m}_f * c_p * (t_j - t_{j+1})}{U_{hj} * (LMTD_j)} \quad (3.44)$$

$$LMTD_j = \frac{t_j - t_{j+1}}{\ln \frac{\dot{T}_{vj} - t_{j+1}}{\dot{T}_{vj} - t_j}} \quad (3.45)$$

The heat load in the condenser

$$Q_c = D_n * Lv_n \quad (3.46)$$

$$Q_c = (\dot{m}_{cw} + \dot{m}_f) * c_p * (T_f - T_{cw}) \quad (3.47)$$

The condenser Log Mean Temperature Difference is needed to calculate the condenser heat transfer surface area. It is given by:

$$LMTD_c = \frac{T_f - T_{cw}}{\ln \left( \frac{\dot{T}_{vn} - T_{cw}}{\dot{T}_{vn} - T_f} \right)} \quad (3.48)$$

The heat transfer surface area of the condenser ( $A_c$ ) is:

$$A_c = \frac{Q_c}{U_c * LMTD_c} \quad (3.49)$$

The main output parameters are

- The System Performance Ratio

$$PR = \frac{\dot{m}_d}{\dot{m}_s} \quad (3.50)$$

- The Specific Cooling water flow rate

$$s\dot{m}_{cw} = \frac{\dot{m}_{cw}}{\dot{m}_d} \quad (3.51)$$

- The Specific Heat Transfer Surface Area

$$sA = \frac{\sum_{i=1}^n A_i + A_c + \sum_{i=2}^{n-1} A_{hi}}{\dot{m}_d} \quad (3.52)$$

### 3.3.1. Elaborated model validation and interpretation

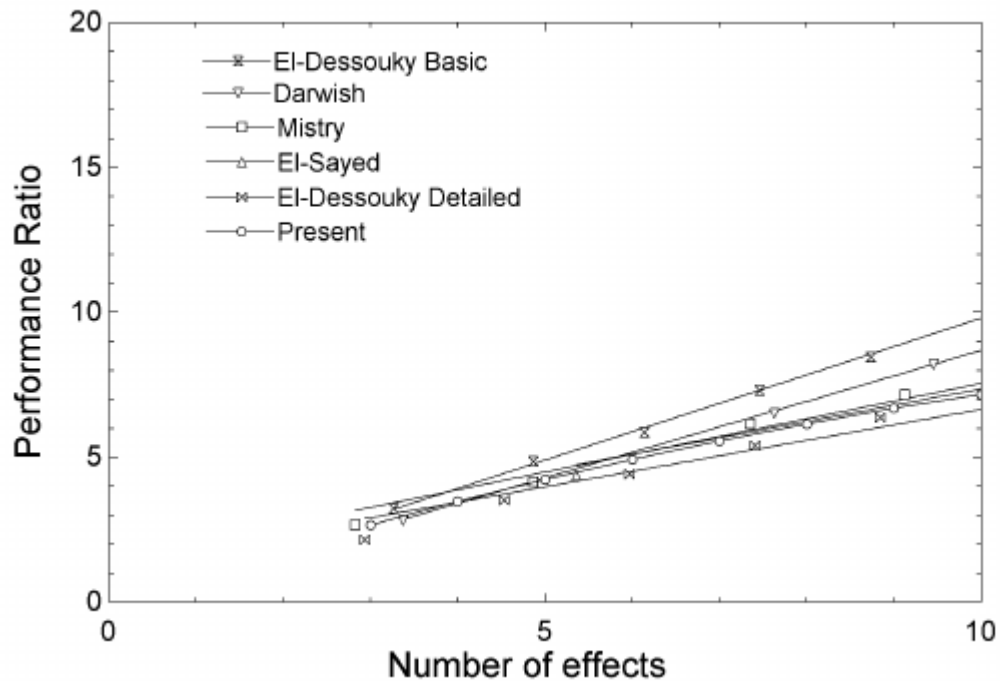


Figure 3.5: The system performance ratio as a function of effects number

Figure 3.5 shows that the system performance ratio increases by increasing the number of effects due to the reuse of the vapor formed in the effect which in turn increases the vapor formed and the performance ratio. The elaborated model results show a good agreement with the models found in the literature. The elaborated model has a different configuration from the first model as illustrated in figures 3.1 and 3.4 although the results does not differ too much.

### 3.4. MEE/FF/Thermal Vapor Compression (TVC)

In the thermal vapor compression cycle, part of vapor formed in the last effect is entrained to the thermal vapor compression in which it combines with a motive steam that comes from turbine, boiler or another external heat source to compress vapor that leaves the ejector and enters into the first effect

#### 3.4.1. System Configuration

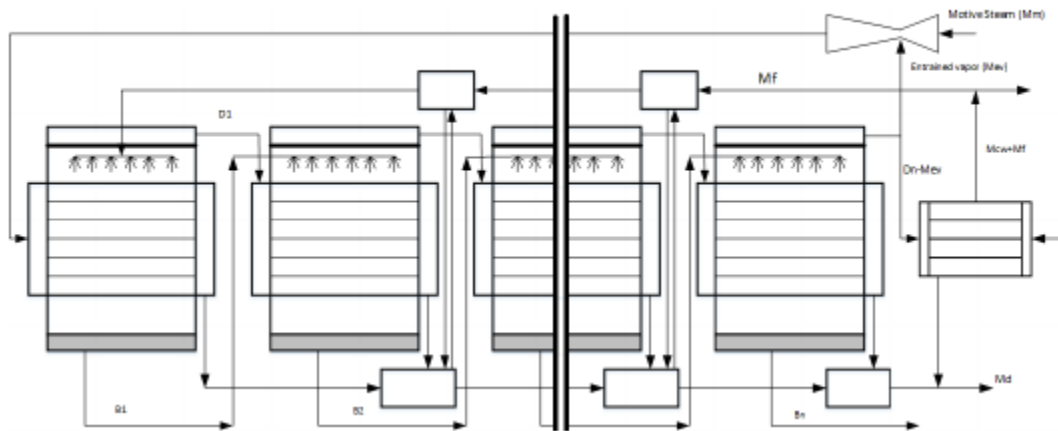


Figure 3.6: MEE/FF/Thermal Vapor Compression

### 3.5. MEE/FF/Thermal Vapor Compression (TVC) Modeling

Forward feed multi effect evaporation with thermal vapor compression is typical to forward feed multi effect evaporation except that for the first one, there is an additional element, which is the thermal vapor compression so that in the TVC model the equations of the thermal vapor compression have been added as shown in this section.

Overall mass balance

$$\dot{m}_f = \dot{m}_d + \dot{m}_b \quad (3.53)$$

$$\dot{m}_f * X_f = \dot{m}_b * X_b \quad (3.54)$$

The overall heat transfer coefficient for the effect is  $U_i$  and the total temperature difference is

$$\Delta T_t = T_s - T_n \quad (3.55)$$

To determine the difference in temperature in each effect, it is important to calculate the overall heat transfer coefficient

$$\sum_{i=1}^n \frac{1}{U_i} = \frac{1}{U_1} + \frac{1}{U_2} + \frac{1}{U_3} + \dots + \frac{1}{U_n} \quad (3.56)$$

The temperature difference in the first effect

$$\Delta T_1 = \frac{\Delta T_t}{U_1 \sum_{i=1}^n \frac{1}{U_i}} \quad (3.57)$$

The temperature difference for the rest of the effects, where  $i$  varies from 2 to  $n$

$$\Delta T_i = \frac{\Delta T_1 * U_1}{U_i} \quad (3.58)$$

The temperature in the first effect

$$T_1 = T_s - \Delta T_1 \quad (3.59)$$

The temperature for the rest of the effects, where  $i$  varies from 2 to  $n$

$$T_i = T_{i-1} - \Delta T_i \quad (3.60)$$

The latent heat value  $L_i$  is given in a correlation as a function of both steam and effect temperature  $T_s$  and  $T_i$ .

The total distillate flow rate is the sum of distillate flow from every effect

$$\dot{m}_d = \sum_{i=1}^n D_i \quad (3.61)$$

The distillate resulting from evaporation in the first effect  $D_1$  is given by:

$$D_1 = \frac{\dot{m}_d}{\left\{1 + L_1 * \sum_{i=1}^n \frac{1}{L_i}\right\}} \quad (3.62)$$

Substituting,  $Q_i = D_1 \times Lv_1$ , constant heat load for  $i$  from 2 to  $n$ .

The flow rate of the vapor formed in the rest of the effects, where  $i$  varies from 2 to  $n$

$$D_i = \frac{D_{i-1} * Lv_{i-1}}{Lv_i} \quad (3.63)$$

The flow rate of the first effect brine

$$B_1 = \dot{m}_f - D_1 \quad (3.64)$$

The brine flow rate of the rest of the effects, where  $i$  varies from 2 to  $n$

$$B_i = B_{i-1} - D_i \quad (3.65)$$

The salinity of the first effect,  $X_1$  is given by

$$X_1 = \frac{\dot{m}_f * X_f}{B_1} \quad (3.66)$$

The salinity of the rest of the effects, where  $i$  varies from 2 to  $n$

$$X_i = \frac{B_{i-1} * X_{i-1}}{B_i} \quad (3.67)$$

The heat transfer surface area of the first effect:

$$A_1 = \frac{D_1 * Lv_1 + \dot{m}_f * c_p * (T_1 - t_{f2})}{U_1 * (T_s - T_1)} \quad (3.68)$$

The heat transfer surface area of the first effect, for i from 2 to n

$$A_i = \frac{D_i * Lv_i}{U_1 * (\Delta T_i - \Delta T_{loss})} \quad (3.69)$$

It is important to calculate the steam flow rate in order to determine the system performance ratio

$$\dot{m}_s = \frac{D_1 * Lv_1 + \dot{m}_f * c_p * (t_{f2} - T_1)}{L_s} \quad (3.70)$$

The motive steam flow rate is the difference between the total steam entering the first effect and the entrained vapor

$$\dot{m}_m = \dot{m}_s - \dot{m}_{ev} \quad (3.71)$$

$$\dot{m}_{ev} = \frac{\dot{m}_m}{Ra} \quad (3.72)$$

The entrainment ratio, Ra, is given by [1]

$$Ra = 0.296 * \frac{P_s^{1.19}}{P_{ev}^{1.04}} * \frac{P_m^{0.015}}{P_{ev}^{0.015}} * \frac{PCF}{TCF} \quad (3.73)$$

Where,

$$PCF = 3 * 10^{-7} * P_m^2 - 0.0009 * P_m + 1.6101 \quad (3.74)$$

$$TCF = 2 * 10^{-8} * T_{ev}^2 - 0.0006 * T_{ev} + 1.0047 \quad (3.75)$$

The compression ratio of the ejector is given by:

$$C_r = \frac{P_s}{P_{ev}} \quad (3.76)$$

When the ejector is working in the limits of [1]:

- $Ra$  is less than or equal to 4
- $P_m$  is greater than or equal to 100 kpa and less than or equal to 3500 kpa
- $C_r$  is greater than or equal to 1.81 and less than or equal to 6

The heat load in the condenser is expressed as:

$$Q_c = (D_n - m_{ev}) * Lv_n \quad (3.77)$$

$$Q_c = (\dot{m}_{cw} + \dot{m}_f) * c_p * (T_f - T_{cw}) \quad (3.78)$$

The condenser Log Mean Temperature Difference is needed to calculate the condenser heat transfer surface area and is given by:

$$LMTD_c = \frac{T_f - T_{cw}}{\ln\left(\frac{\dot{T}v_n - T_{cw}}{\dot{T}v_n - T_f}\right)} \quad (3.79)$$

The heat transfer surface area of the condenser can be calculated

$$A_c = \frac{Q_c}{U_c * LMTD_c} \quad (3.80)$$

The main output parameters are

- The System Performance Ratio

$$PR = \frac{\dot{m}_d}{\dot{m}_s} \quad (3.81)$$

- The Specific Cooling water flow rate

$$s\dot{m}_{CW} = \frac{\dot{m}_{CW}}{\dot{m}_d} \quad (3.82)$$

- The Specific Heat Transfer Surface Area

$$sA = \frac{\sum_{i=1}^n A_i + A_c}{\dot{m}_d} \quad (3.83)$$

### 3.6. MEE/FF/Thermal Vapor Compression Model interpretation and Validation

#### 3.6.1. Model Interpretation

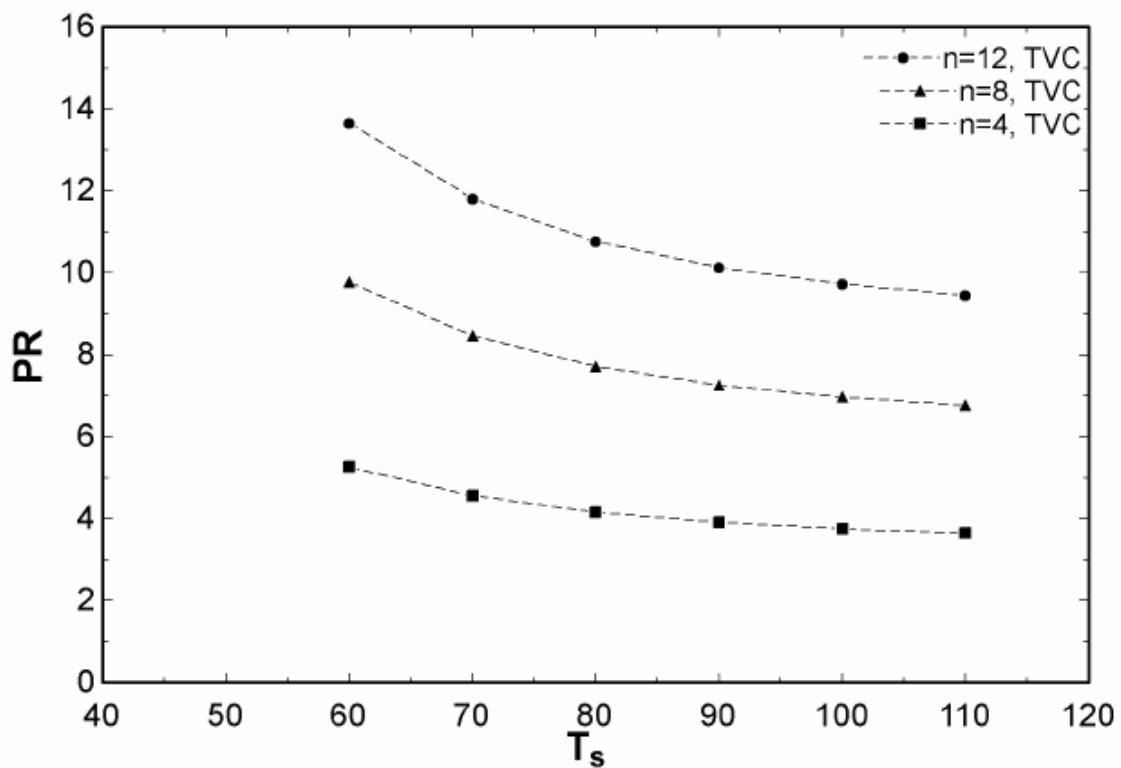


Figure 3.7: Effect of steam temperature on Performance ratio MEE/FF/TVC System

Figure 3.7 shows the effect of steam temperature on the performance ratio for MED FF system combined with thermal vapor compressor. At lower steam temperature the performance ratio is high, as the steam temperature increases the performance ratio decreases due to increasing of the motive steam flow rate in order to get higher compression ratio which in turn reduces the performance ratio. Increasing the number of

effects increases the performance ratio due to better use of energy and more vapors gained, however the number of effects is limited to the steam temperature.

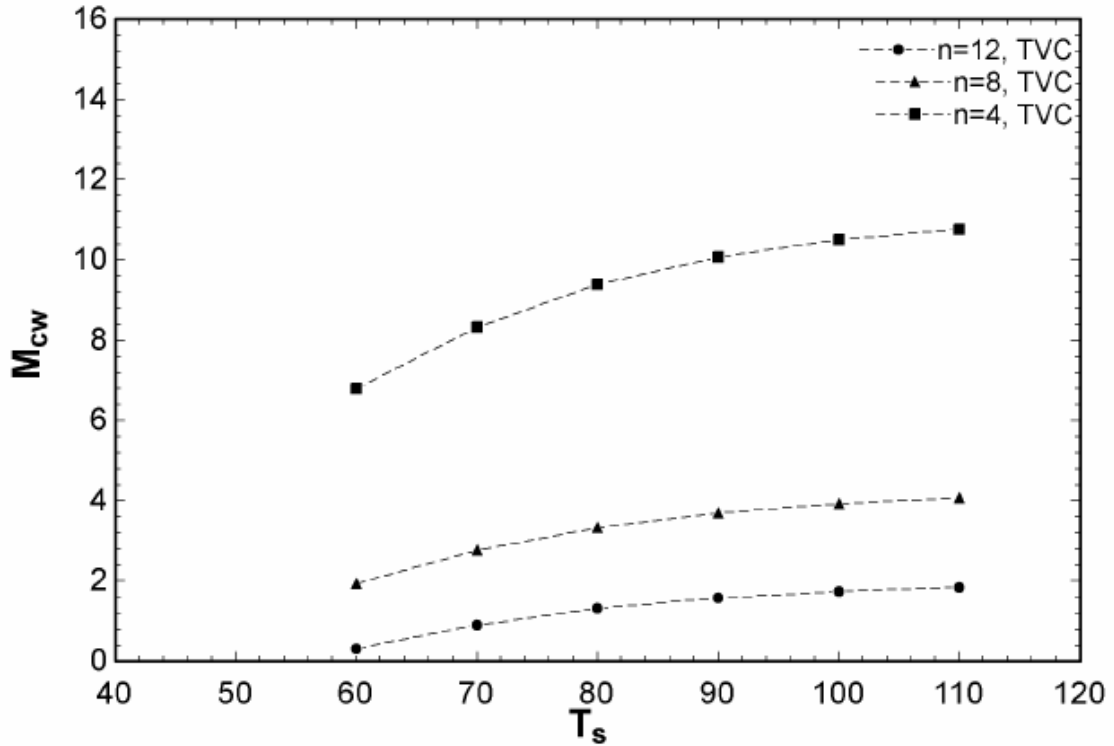


Figure 3.8: Effect of steam temperature on Specific cooling water flow rate MEE/FF/TVC System

Figure 3.8 shows the effect of steam temperature on the specific cooling water flow rate for MEE/FF/TVC System, it can be clearly seen that increasing the heating steam temperature increases the cooling water flow rate due to increase of the last effect thermal load as a result of increasing the compression ratio and the heat load of the first effect. In addition increasing the number of effect reduces the specific cooling water flow rate due to reducing the thermal heat load by increasing the number of effect.

### 3.6.2. Model Validation

Table 3.2: Comparison of MEE/FF/TVC Model with El-Dessouky Model

Parameter	Present Model	El-Dessouky model	Error percentage
	MEE/ FF/TVC	MEE/FF/TVC	
$T_s$	60	60	-
$T_n$	40	40	-
$T_{cw}$	25	25	-
$T_f$	35	35	-
$n$	4	4	-
$s\dot{m}_{cw}$	6.788	6.819	0.45%
$A_c$	32.92	32.79	0.39%
$sA$	346.3	345.76	0.15%
$PR$	5.275	5.26	0.28%
$C_r$	3.006	3.144	1.2%
$Ra$	2.199	2.228	1.3%

Table 3.2 include a comparison between the present model with a work of El- Dessouky [1] for a MEE/FF/TVC System. The maximum deviation did not exceed 1.3%. Therefore, it confirms the model validity.

### 3.7. MEE/FF/TVC different Ejector Positions

In this section, the MEE/FF/TVC is studied for different Thermal vapor ejector positions to examine the performance of the system at every different ejector position.

#### 3.7.1. System Configuration

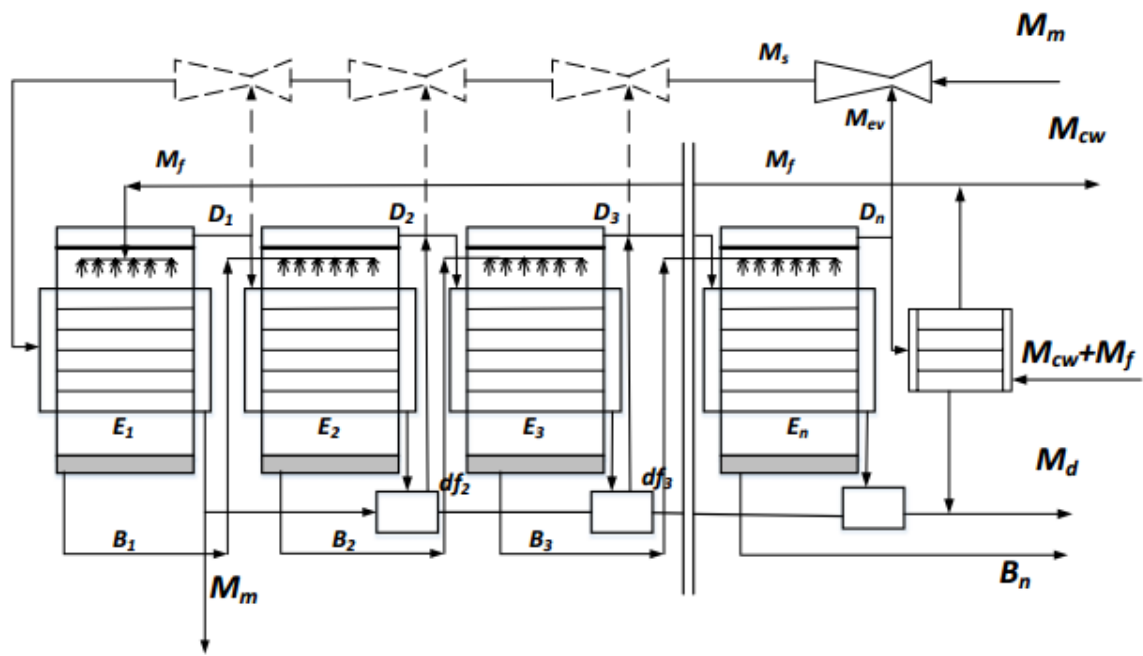


Figure 3.9: Different ejector positions in a MED-FF desalination system

Figure 3.9 shows different ejector positions for MEE/FF/TVC system when the ejector is located after the last, third, second and first effects.

### 3.8. MEE/FF/TVC different Ejector Positions Model

The model is carried out for MEE/FF/TVC system with 4 effects and the thermal ejector is located after effect number 3. The only difference between this model and the previous model is in the thermal heat load for the effect that has an inlet vapor of  $(D_{i-1} - \dot{m}_{ev})$ , it is given by the following formula:

$$D_i = \frac{(D_{i-1} - \dot{m}_{ev}) * Lv_{i-1}}{Lv_i} \quad (3.84)$$

The flow rate of the vapor formed of the rest of effects

$$D_i = \frac{D_{i-1} * Lv_{i-1}}{Lv_i} \quad (3.85)$$

In this example, the vapor formed in the last effect, effect number 4

$$D_4 = \frac{(D_3 - \dot{m}_{ev}) * Lv_3}{Lv_4} \quad (3.86)$$

### 3.9. MEE/FF/TVC different Ejector Positions Model interpretation

Figure 3.10 illustrates the effect of steam temperature on the performance ratio for MED/FF/TVC with different ejector positions for a system that consists of 4 effects, it can be clearly seen that changing ejector position affects the performance ratio, the best performance ratio occurs for a range of steam temperature between 70 to 100°C when the ejector is located in the middle of the plant. However the multi effect evaporation systems used to operate at temperature between 60°C to 80°C. Moreover the same results were obtained for the system with number of effects of 8 and 12 as shown in figures below.

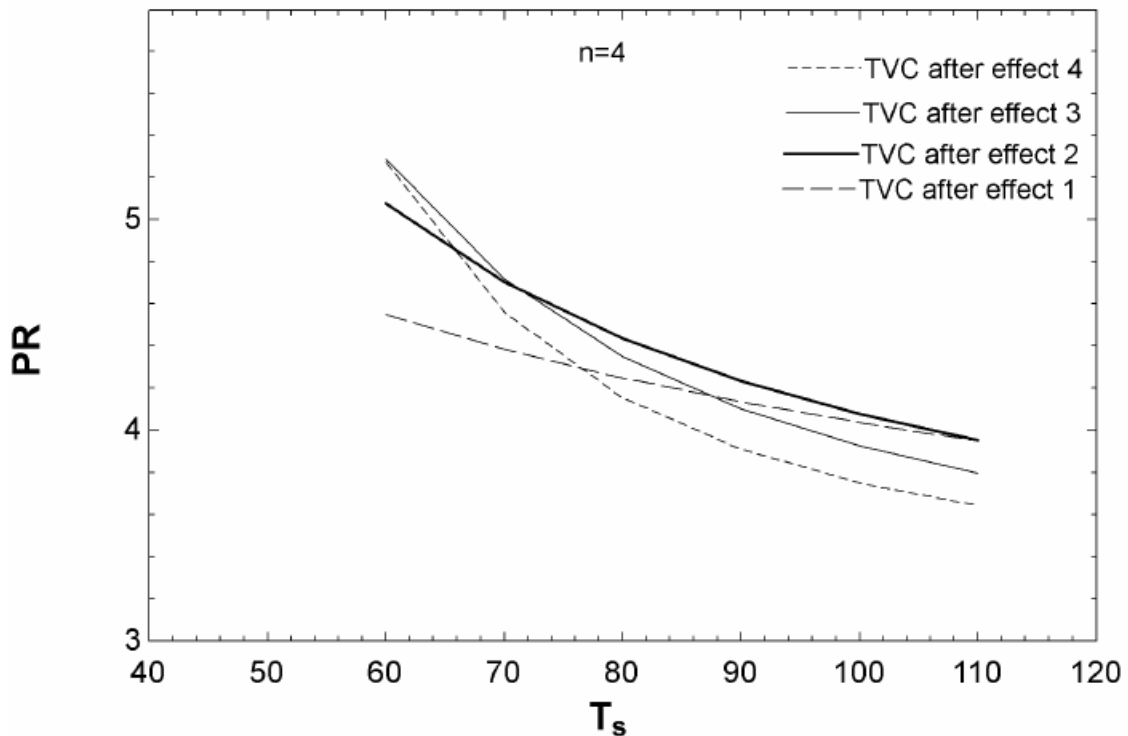
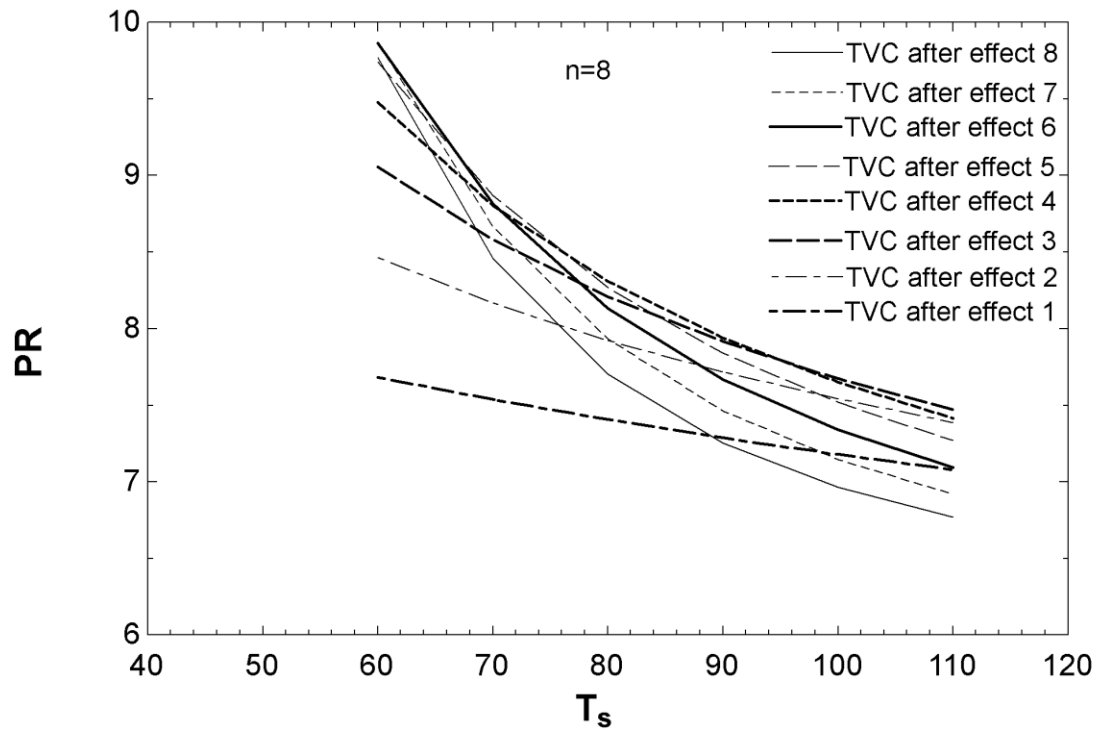


Figure 3.10: Effect of steam temperature on Performance ratio different thermal vapor ejector positions 4 effects



**Figure 3.11: Effect of steam temperature on Performance ratio different thermal vapor ejector positions 8 effects**

Figure 3.11 shows the effect of steam temperature on the performance ratio for MED/FF/TVC with different ejector positions for a system that consists of 8 effects.

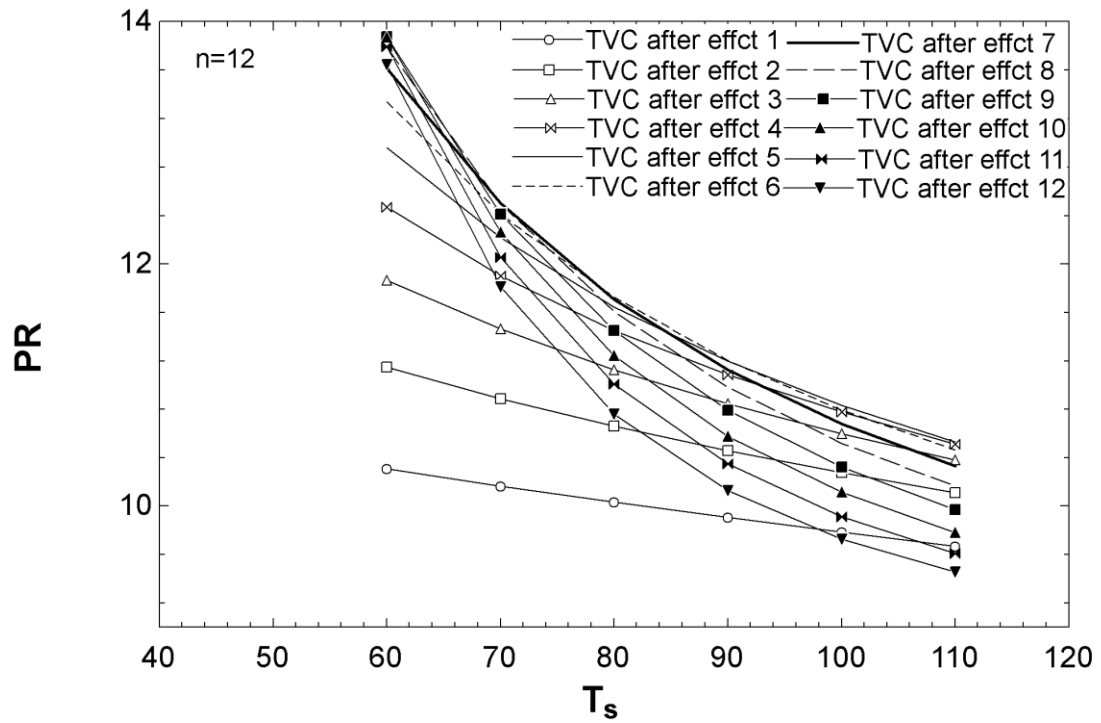
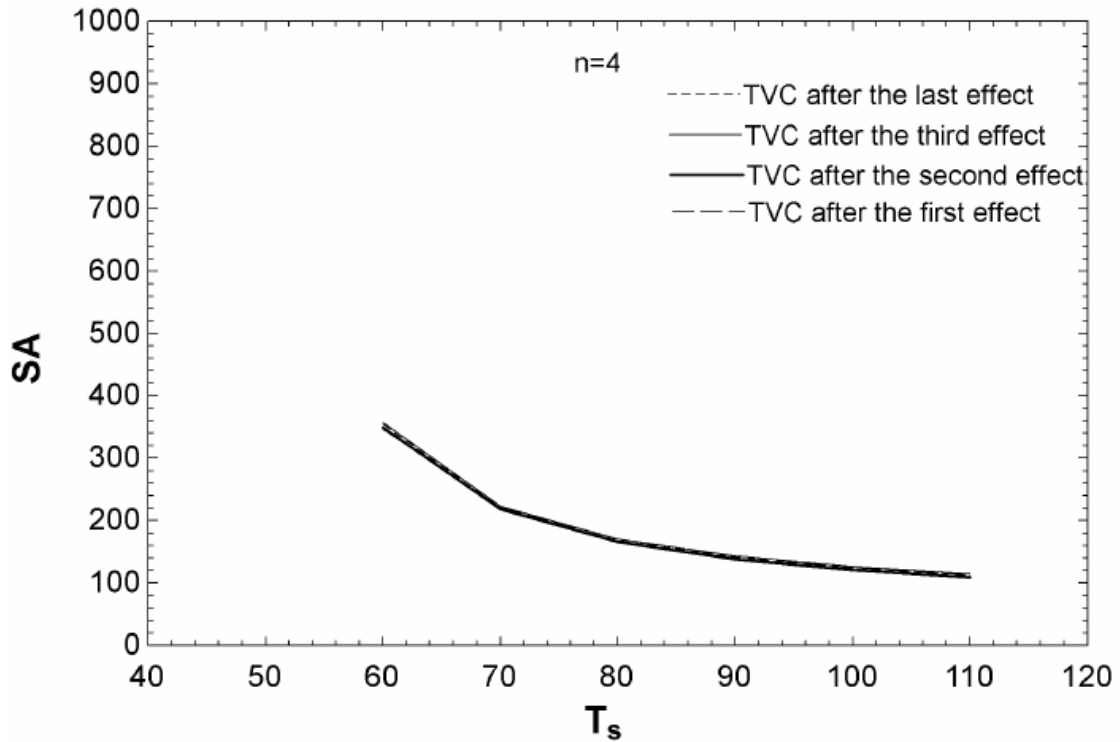


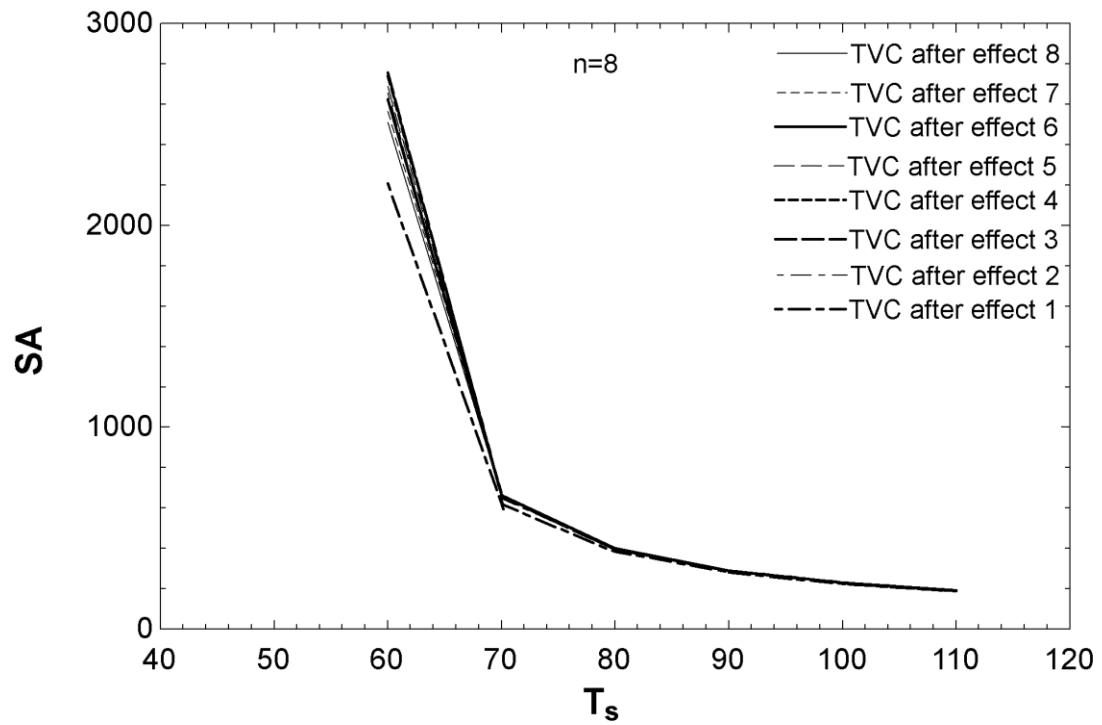
Figure 3.12: Effect of steam temperature on Performance ratio different thermal vapor ejector positions 12 effects

Figure 3.12 explains the effect of steam temperature on the performance ratio for MED/FF/TVC with different ejector positions for a system that consists of 12 effects.



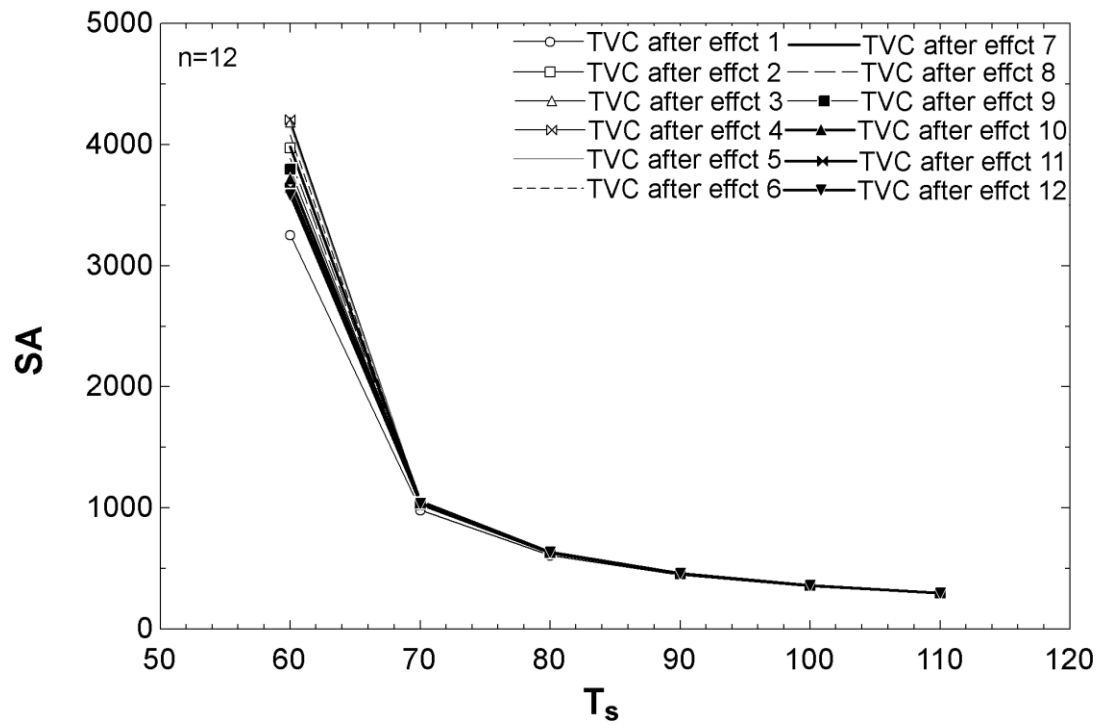
**Figure 3.13: Effect of steam temperature on specific heat transfer surface area different thermal vapor ejector positions 4 effects.**

Figure 3.13 shows the effect of the heating steam temperature on the specific heat transfer surface area for MEE/FF/TVC with 4 effect system, changing the position of the ejector does not affect the specific heat transfer surface area. In addition for other number of effects of 8 and 12 the same results has been found as shown in figures.



**Figure 3.14: Effect of steam temperature on specific heat transfer surface area different thermal vapor ejector positions 8 effects**

Figure 3.14 illustrates the effect of the heating steam temperature on the specific heat transfer surface area for MEE/FF/TVC with 8 effect system.



**Figure 3.15: Effect of steam temperature on specific heat transfer surface area different thermal vapor ejector positions 12 effects**

Figure 3.15 shows the effect of the heating steam temperature on the specific heat transfer surface area for MEE/FF/TVC with 12 effect system.

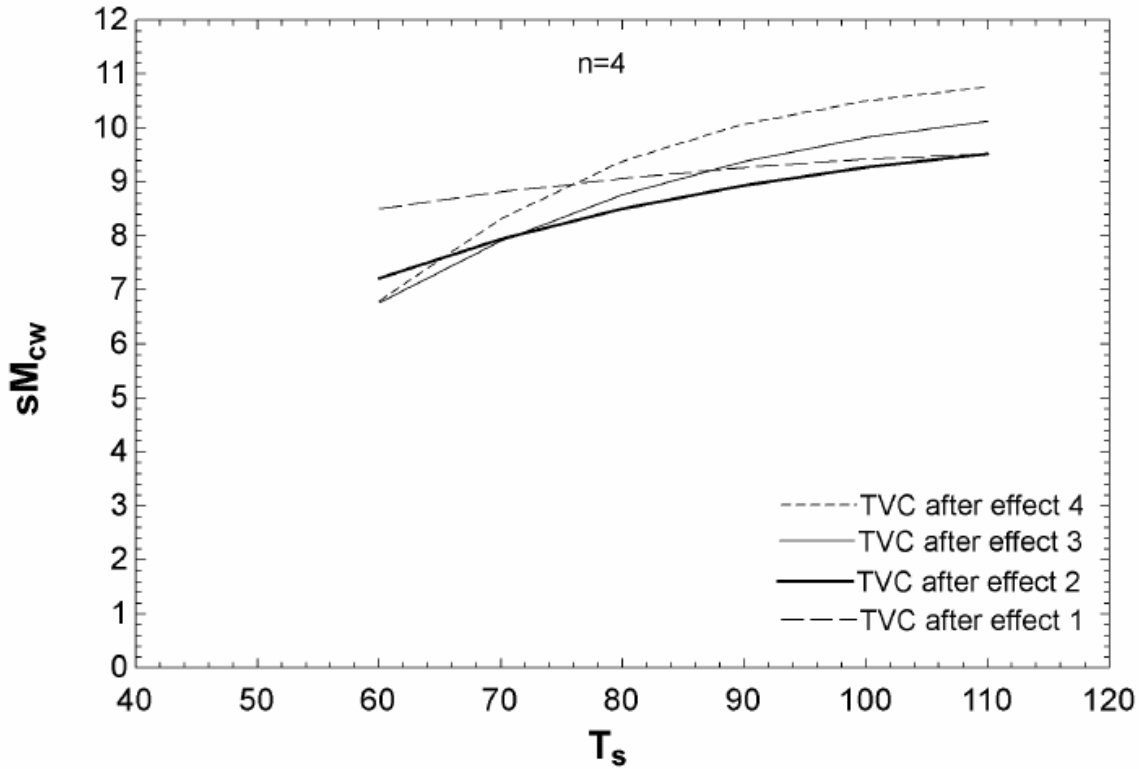


Figure 3.16: Effect of steam temperature on specific cooling water flow rate different thermal vapor ejector positions 4 effects.

Figure 3.16 shows the effect of steam temperature on the specific cooling water flow rate while the position of ejector has been changed for 4 effects system, the results shows that the lower specific cooling water flow rate gained when the thermal vapor ejector has been a located after the second effect for a range of temperature of 80°C to 100°C. The same trend found for systems with number of effects of 8 and 12.

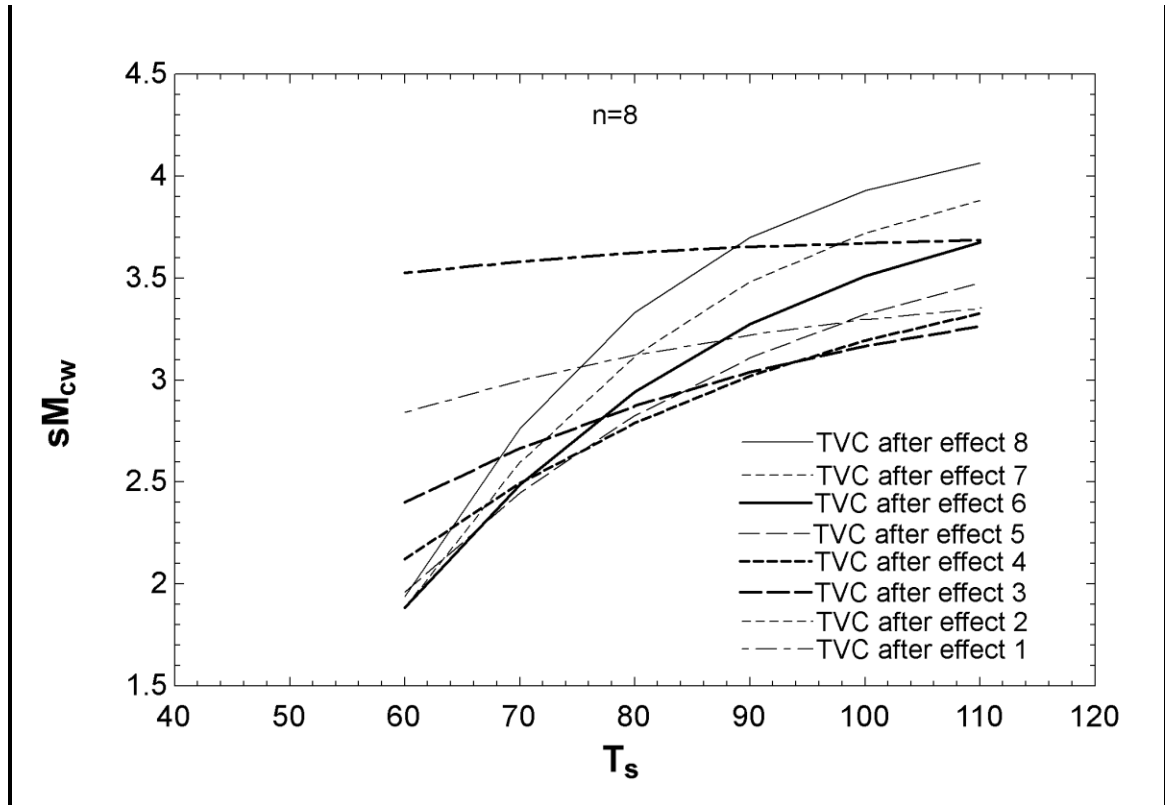


Figure 3.17: Effect of steam temperature on specific cooling water flow rate different thermal vapor ejector positions 8 effects.

Figure 3.17 explain the effect of steam temperature on the specific cooling water flow rate while the position of ejector has been changed for 8 effects system.

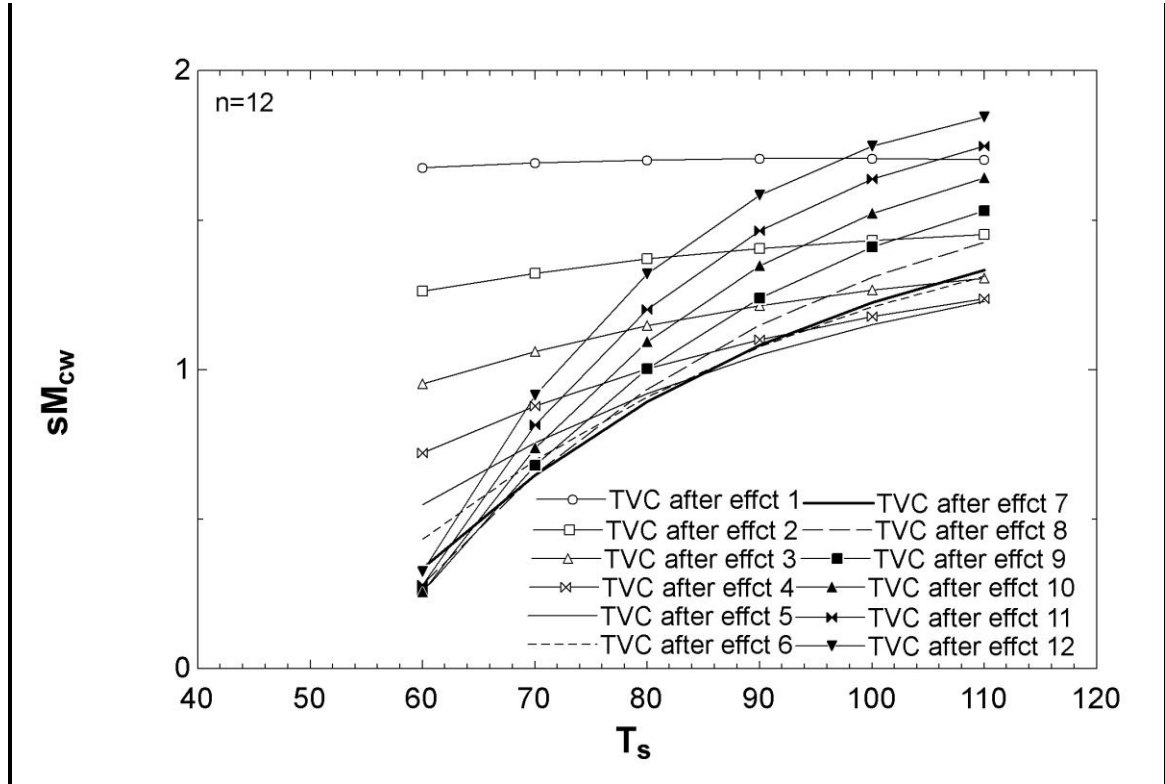


Figure 3.18: Effect of steam temperature on specific cooling water flow rate different thermal vapor ejector positions 12 effects.

Figure 3.18 shows the effect of steam temperature on the specific cooling water flow rate while the position of ejector has been changed for 12 effects system.

### 3.10. Exergetic and Economic Analysis

Exergy is the maximum useful work for a system in order to reach the equilibrium. The first law of thermodynamics can be used in order to evaluate the quantity of energy for a thermal process or cycle. However, it is also important to evaluate the quality of energy. Second law of thermodynamics shows that the heat cannot be totally converted into work. This loss of exergy is called exergy destruction.

This kind of analysis is the most logical technique in order to analyze system losses and the element that has significant loss. The exergy balance for the evaporators of the forward feed system is reported in this section

$$E_{fuel} = E_{product} + E_{distruction} + E_{loss} \quad (3.87)$$

The exergy of hot or cold fluid stream is

$$X = \dot{m} (h - h_o - T_o(s - s_o)) \quad (3.88)$$

Where  $T_o$  and  $s_o$  are the surrounding temperature and entropy, respectively.

#### 3.10.1.Exegetic and Economic Calculations

##### First Effect

For the hot stream

$$EX_{sin1} = \dot{m}_s * ((hs_{in1} - hs_o) - (T_o + 273) * (ss_{in1} - ss_o)) \quad (3.89)$$

$$EX_{sout1} = \dot{m}_s * ((hs_{out1} - hs_o) - (T_o + 273) * (ss_{out1} - ss_o)) \quad (3.90)$$

$$\Delta EX_{hot1} = EX_{sin1} - EX_{sout1} \quad (3.91)$$

$EX_{sin1}$  is the inlet steam exergy

$\dot{m}_s$  is the heating steam flow rate

$hs_{in1}$  is the first effect inlet steam enthalpy

$hs_o$  is the surrounding enthalpy

$T_o$  is the surrounding temperature in *kelvin*

$EX_{sout1}$  is the outlet steam exergy

$hs_{out1}$  is the first effect outlet steam enthalpy

$\Delta EX_{hot1}$  is the exergy difference of the hot stream

For the cold stream

(a) Feed Stream

$$EX_{fin1} = m_f * ((hf_{in1} - hf_o) - (T_o + 273) * (sf_{in1} - sf_o)) \quad (3.92)$$

$f$ : feed sea water

*in*: inlet

(b) Brine Stream

$$EX_{b_{out1}} = B_1 * ((hb_{out1} - hf_o) - (T_o + 273) * (sb_{out1} - sf_o)) \quad (3.93)$$

*b*: brine water

*out*: outlet

*cold*: cold stream

*hot*: hot stream

(c) Vapor Stream

$$EX_{v_{out1}} = D_1 * ((hv_{out1} - hs_o) - (T_o + 273) * (sv_{out1} - ss_o)) \quad (3.94)$$

Therefore;

$$\Delta EX_{cold1} = EX_{v_{out1}} + EX_{b_{out1}} - EX_{fin} \quad (3.95)$$

$$\Delta EX_1 = \Delta EX_{hot1} - \Delta EX_{cold1} \quad (3.96)$$

The exergetic efficiency is given by:

$$Efficiency_{EX1} = \frac{\Delta EX_{cold1}}{\Delta EX_{hot1}} \quad (3.97)$$



**Table 3.3: Exergy analysis calculation for four effects MED/FF/TVC with ejector located after the last effect**

Exergy Analysis Calculations FF/TVC after	Last Effect
Blow down Exergy (kw)	39.54
Distillate Exergy (kw)	3.568
Inlet Motive steam Exergy (kw)	117.5
Outlet Motive Exergy (kw)	1.529
Inlet Feed \& Cooling Sea water Exergy (kw)	0
Total Exegetic Efficiency (%)	3.1%
Compression Ratio CR (-)	3.006
Entrainment Ratio Ra (-)	2.199
Performance Ratio PR (-)	5.277
Cooling Water Flow Rate (kg/s)	6.794
Entrained Vapor Flow Rate (kg/s)	0.08624
Motive Steam Flow Rate (kg/s)	0.1897
Steam Flow Rate (kg/s)	0.2759
Condenser Exergetic Efficiency (%)	31.13
Ejector Exergetic Efficiency (%)	56.05
First Effect Exergetic Efficiency (%)	83.69
Second Effect Exergetic Efficiency (%)	79.01
Third Effect Exergetic Efficiency (%)	75.72
Fourth Effect Exergetic Efficiency (%)	70.10

Table 3.3 shows the exergy analysis calculation for four effects MED/FF/TVC with ejector located after the last effect. The total plant exergetic efficiency is 3.1%, increasing the number of effects increases the exergetic efficiency due to better use of energy.

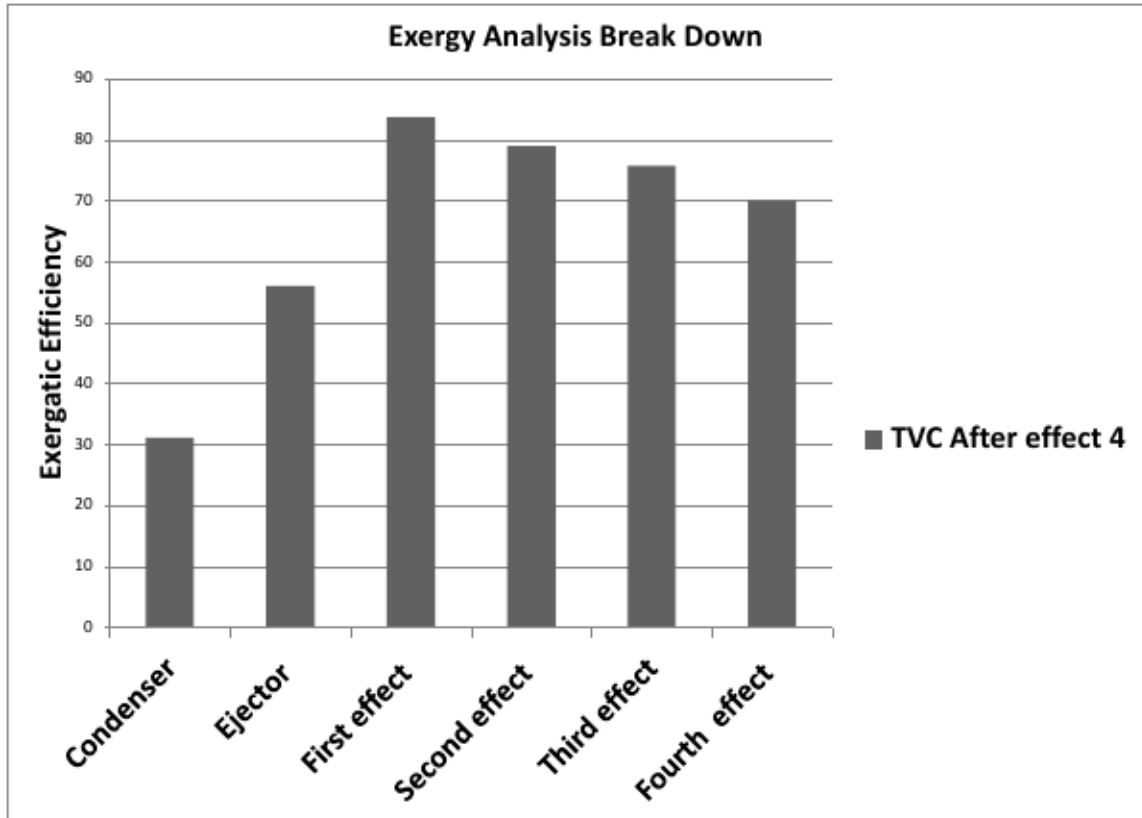
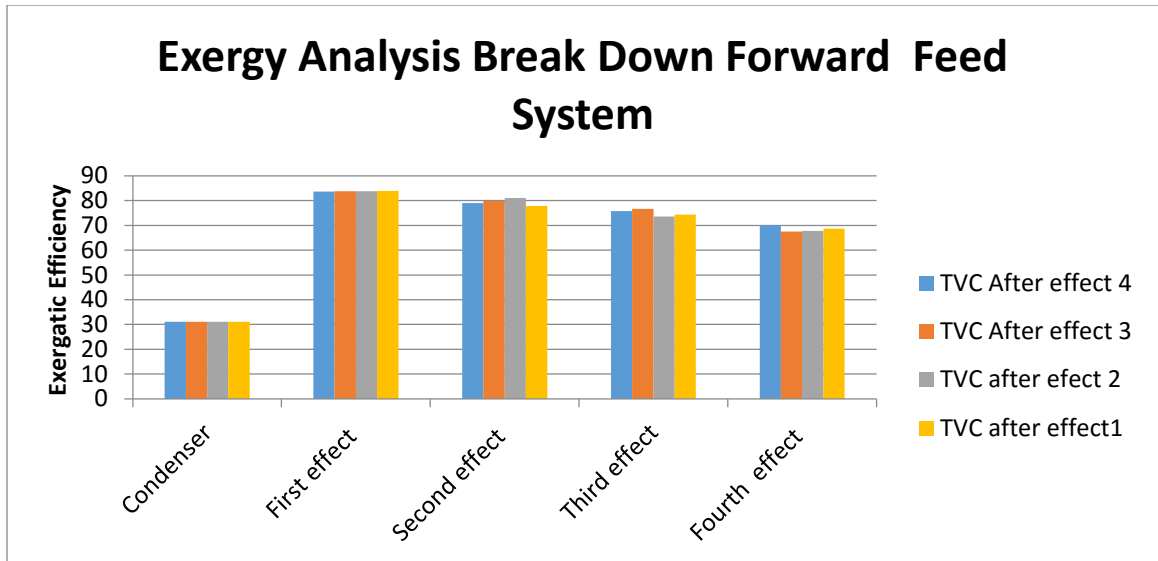


Figure 3.20: Second Law efficiency MEE/FF system TVC after last effect

Figure 3.14 shows the exergy analysis for 4 effects MEE/FF/TVC system when the ejector is located after the last effect. Results show that the second law efficiency for first effect is the highest and it reduces for the second, third until it reaches the lowest value for the condenser, however increases number of effects increases the second law efficiency due to better use of energy.



**Figure 3.21: Exergy analysis break down for forward feed system**

Figure 3.21 shows the exergy analysis break down for forward feed system, it can be clearly seen that the condenser exergatic efficiency does not changed with changing the ejector position and that because the temperature of the last effect is kept constant. However, the exergy destruction can be decreased by reducing the top brine temperature, increasing the number of stages, and increasing entrainment ratio of the thermo compressor.

# **Parallel Feed Multi Effect Evaporation Desalination**

## **Systems**

As explained before, a number of single effect evaporators form a multi effect evaporation unit, the first effect is heated by external source, for instance, steam from a power plant. The rest of effects are heated by the vapor formed in the previous effect, this process prevents a rejection of heated brine, consequently reduce energy loss. A parallel feed multi effect desalination systems is another arrangement of multi effect evaporation systems which is discussed in this chapter. A parallel feed multi effect desalination system is found in a huge number of plants in the desalination industry. The unit is found to be a stand alone or combined with thermal or mechanical vapor compression systems.

## 4.1. Working Principle

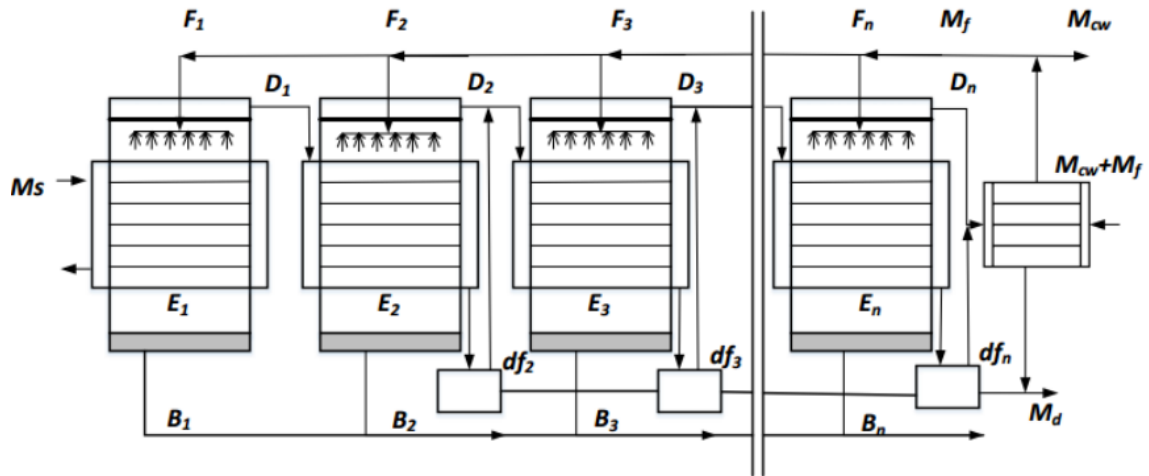


Figure 4.1: Parallel Feed Multi Effect Desalination System

Figure 4.1 shows the parallel feed multi effect evaporation system with  $n$  effects from the left hand side. The vapor flows from left to the right. Each effect has a heat transfer surface area, mist eliminator, brine pool. In this type of desalination systems, vapor flows in the direction of falling pressure and temperature whereas the feed sea water enters vertically. The system contains several evaporators and flash boxes in addition to a down condenser. The number of flash boxes in the parallel feed multi effect evaporation systems is  $(n-1)$ . Feed seawater enters the down condenser to absorb the latent heat of the condensing vapor from the last effect. Accordingly, its temperature increases to the feed seawater temperature. Part of this heated seawater is rejected to the sea as a cooling water, the function of this cooling water is to insure that all the vapor formed in the last effect is condensed. The feed seawater is chemically treated and then sprayed inside the evaporators such that it falls in the form of small droplets. In each evaporator, the feed seawater temperature increases to the boiling (saturation) temperature, then, a portion of

it evaporates. The heat required for preheating and evaporation in the first effect is provided by steam inside tubes. Steam is supplied to the system by an external source. The vapor saturation temperature is less than the boiling temperature of the brine in each effect by boiling point elevation (BPE). To dismiss the entrained brine droplets the vapor passes through demister or a mist eliminator. The amount of vapor formed in an effect is more than the vapor formed in the next one due to the increase in the specific latent heat of vaporization as temperature decreases.

## **4.2. MEE/PF Desalination System Modeling**

In this section, a mathematical model of parallel feed multi effect evaporation system is presented to provide an effective way to evaluate and design such a system, the mathematical model is solved using Engineering Equation Solver software (EES).

The mathematical model is based on mass and energy balances for the system components, the down condenser governing equations are included in the model.

The calculated parameters in the model include:

- Vapor flow rate,  $D_i$
- Brine flow rate,  $B_i$
- Brine salinity,  $X_i$
- Brine temperature,  $T_i$
- Heat transfer surface area,  $A_i$
- Steam flow rate entering the first effect,  $\dot{m}_s$

- Cooling water flow rate,  $\dot{m}_{cw}$
- Heat transfer surface area of the condenser,  $A_c$

To develop the Parallel Feed Multi Effect Desalination System mathematical model, a number of assumptions are made :

- The vapor salinity is zero (does not contain salt)
- No energy loss between the effects and the surrounding.
- The thermal load is equal for all effects except for the first effect.
- The specific heat capacity is constant,  $C_p$ .
- Thermal losses are constants.

#### **4.2.1. System Configuration**

A mathematical model of parallel feed arrangement is explained in this section, figure 4.1 shows parallel feed multi effect desalination system. The feed sea water  $\dot{m}_f$  with temperature  $T_f$  coming out from the condenser enters the evaporators in parallel. The steam supplied to the first effect S heats the feed seawater in the first effect,  $\dot{m}_{f1}$  from  $T_f$  to  $T_1$  and forms vapor  $D_1$  at temperature  $T_{v1}$  which in turn enters to the second effect representing the heat source that rises the temperature of  $\dot{m}_{f2}$  from  $T_f$  to  $T_2$  and forms vapor  $D_2$ . The vapor formed in the second effect is at a temperature  $T_{v2}$ . This process is repeated till the last effect. The vapor formed in the last effect enters the down condenser in which cooling water temperature rises from  $T_{cw}$  to  $T_f$ . As we monitor the flow direction, the brine temperature decreases from  $T_1$  to  $T_2$  and from  $T_2$  to  $T_3$  and so on.

Vapor flashed in the distilled flash boxes is added to the vapor formed in the same effect to enter to the next effect as a heat source.

The brine leaving any effect

$$B_i = F_i - D_i \quad (4.1)$$

The salinity in each effect

$$F_i * X_f = B_i * X_i \quad (4.2)$$

Energy balance equation in the first effect

$$m_s * L = F_1 * c_p * (T_1 - T_f) + D_1 * L_1 \quad (4.3)$$

Energy balance equation in each effect

$$D_{i-1} * L_{i-1} + df_{i-1} * L_{f_{i-1}} = F_i * c_p * (T_i - T_f) + D_i * L_i \quad (4.4)$$

The brine leaving the first and the second effect

$$B_2 = B_1 + (m_{f2} - D_2) \quad (4.5)$$

Using salt balance equations

$$\frac{\dot{m}_f}{\dot{m}_d} = \frac{X_b}{X_b - X_f} \quad (4.6)$$

$$\frac{\dot{m}_{f1}}{D_1} = \frac{X_1}{X_1 - X_f} \quad (4.7)$$

The temperature of the vapor formed in each effect

$$Tv_i = T_i - BPE_i \quad (4.8)$$

The Temperature of the condensing vapor in each effect is given by

$$Tc_i = T_i - BPE_i - \Delta T_{loss} \quad (4.9)$$

Where  $\Delta T_{loss} = \Delta T_p + \Delta T_t + \Delta T_c$

$\Delta T_p$  : a temperature loss as a result of pressure depression in the demister.

$\Delta T_t$  : a temperature loss as a result of friction in the transmission line

$\Delta T_c$  : a temperature loss as a result of condensation.

The temperature in the flash box differs from the vapor temperature by non equilibrium allowance, NEA such that:

$$\ddot{T}_j = \ddot{T}_{vj} + N\ddot{E}A_j \quad (4.10)$$

The flashed vapor in the first flash box

$$df_2 = D_1 * c_p * \frac{(Tv_1 - \ddot{T}_2)}{\ddot{L}_{v2}} \quad (4.11)$$

The flashed vapor in the rest of flash boxes

$$df_j = \left( \sum_{i=1}^j D_i \right) * c_p * \frac{(Tv_{j-1} - \ddot{T}_j)}{\ddot{L}_{vj}} \quad (4.12)$$

The energy balance in the condenser

$$df_n * Lf_{vn} + D_n * L_{vn} = (\dot{m}_{cw} + \dot{m}_f) * c_p * (T_f - T_{cw}) \quad (4.13)$$

Area of the first effect

$$A_1 = \frac{m_s * L_s}{U_{e1} * (T_s - T_1)} \quad (4.14)$$

The heat load in the condenser

$$Q_c = (D_n + df_n) * Lv_n \quad (4.15)$$

$$Q_c = (m_{cw} + m_f) * c_p * (T_f - T_{cw}) \quad (4.16)$$

The condenser Log Mean Temperature Difference is needed to calculate the condenser heat transfer surface area

$$LMTD_c = \frac{T_f - T_{cw}}{\ln\left(\frac{\dot{T}v_n - T_{cw}}{\dot{T}v_n - T_f}\right)} \quad (4.17)$$

The heat transfer surface area of the condenser

$$A_c = \frac{Q_c}{U_c * LMTD_c} \quad (4.18)$$

The main output parameters are

- The System Performance Ratio

$$PR = \frac{\dot{m}_d}{\dot{m}_s} \quad (4.19)$$

- The Specific Cooling water flow rate

$$s\dot{m}_{cw} = \frac{\dot{m}_{cw}}{\dot{m}_d} \quad (4.20)$$

- The Specific Heat Transfer Surface Area

$$sA = \frac{\sum_{i=1}^n A_i + A_c}{\dot{m}_d} \quad (4.21)$$

### 4.3. MEE/PF/Thermal Vapor Compression (TVC)

In the parallel feed thermal vapor compression, part of vapor formed in the last effect is entrained to the ejector in which it combines with motive steam that comes from turbine, boiler or other external heat source to form a compressed steam that is forwarded to the first effect as a source of heat.

#### 4.3.1. System Configuration

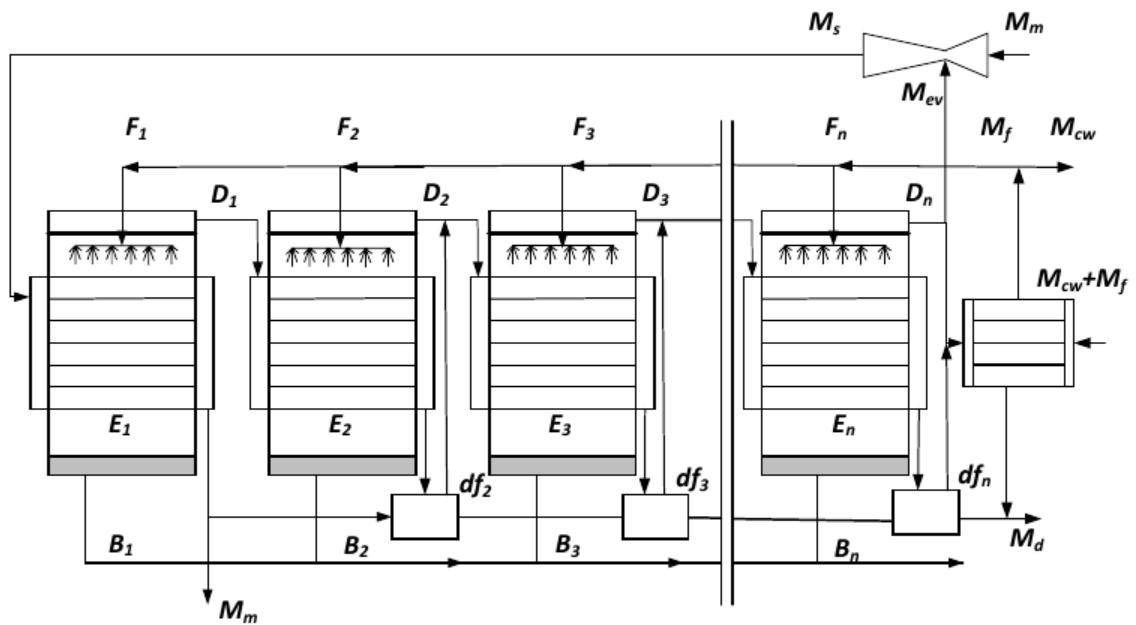


Figure 4.2: MEE/PF/Thermal Vapor Compression

Figure 4.2 shows a schematic layout of parallel feed multi effect evaporation system fitted with thermal vapor compressor. There are n effects from the left hand side and the vapor flows from left to the right. Each effect has a heat transfer surface area, mist eliminator, brine pool.

#### 4.4. MEE/PF/Thermal Vapor Compression (TVC) Modeling

Parallel Feed Multi Effect Evaporation Thermal Vapor Compression is similar to Parallel Feed Multi Effect Evaporation except that for the PF/TVC there is an additional element which is the ejector so that in modeling the system, there are two independent loops; the Parallel feed loop and the thermal ejector loop. The parallel feed loop has been explained earlier so in this part. Therefore, the thermal vapor compression loop will be only explained. It is important to calculate the steam flow rate in order to determine the system performance ratio

$$\dot{m}_s = \frac{D_1 * Lv_1 + \dot{m}_f * c_p * (t_{f2} - T_1)}{L_s} \quad (4.22)$$

The Motive steam is the difference between the steam leaving the ejector to the first effect and the entrained vapor

$$\dot{m}_m = \dot{m}_s - \dot{m}_{ev} \quad (4.23)$$

$$\dot{m}_{ev} = \frac{\dot{m}_m}{Ra} \quad (4.24)$$

The entrained Ratio, Ra, is given by El-Dessouky [1]

$$Ra = 0.296 * \frac{P_s^{1.19}}{P_{ev}^{1.04}} * \frac{P_m^{0.015}}{P_{ev}^{0.015}} * \frac{PCF}{TCF} \quad (4.25)$$

Where Pressure correction factor is;

$$PCF = 3 * 10^{-7} * P_m^2 - 0.0009 * P_m + 1.6101 \quad (4.26)$$

Temperature correction factor is;

$$TCF = 2 * 10^{-8} * T_{ev}^2 - 0.0006 * T_{ev} + 1.0047 \quad (4.27)$$

The compression ratio is;

$$C_r = \frac{P_s}{P_{ev}} \quad (4.28)$$

$P_m$  is in *kpa* , When the ejector is working for steam the limits are

- $Ra$  is less than or equal to 4
- $P_m$  is greater than or equal to 100 *kpa* and less than or equal to 3500 *kpa*
- $C_r$  is greater than or equal to 1.81 and less than or equal to 6

The heat load in the condenser becomes:

$$Q_c = (D_n - \dot{m}_{ev}) * Lv_n \quad (4.29)$$

And

$$Q_c = (\dot{m}_{cw} + \dot{m}_f) * c_p * (T_f - T_{cw}) \quad (4.30)$$

The condenser Log Mean Temperature Difference is needed to calculate the condenser heat transfer surface area is given by:

$$LMTD_c = \frac{T_f - T_{cw}}{\ln\left(\frac{\dot{T}v_n - T_{cw}}{\dot{T}v_n - T_f}\right)} \quad (4.31)$$

The heat transfer surface area of the condenser is

$$A_c = \frac{Q_c}{U_c * LMTD_c} \quad (4.32)$$

The main output parameters are:

- The System Performance Ratio

$$PR = \frac{\dot{m}_d}{\dot{m}_s} \quad (4.33)$$

- The Specific Cooling water flow rate

$$s\dot{m}_{CW} = \frac{\dot{m}_{CW}}{\dot{m}_d} \quad (4.34)$$

- The Specific Heat Transfer Surface Area

$$sA = \frac{\sum_{i=1}^n A_i + A_c}{\dot{m}_d} \quad (4.35)$$

#### 4.5. MEE/PF(with and without TVC) Model interpretation and validation

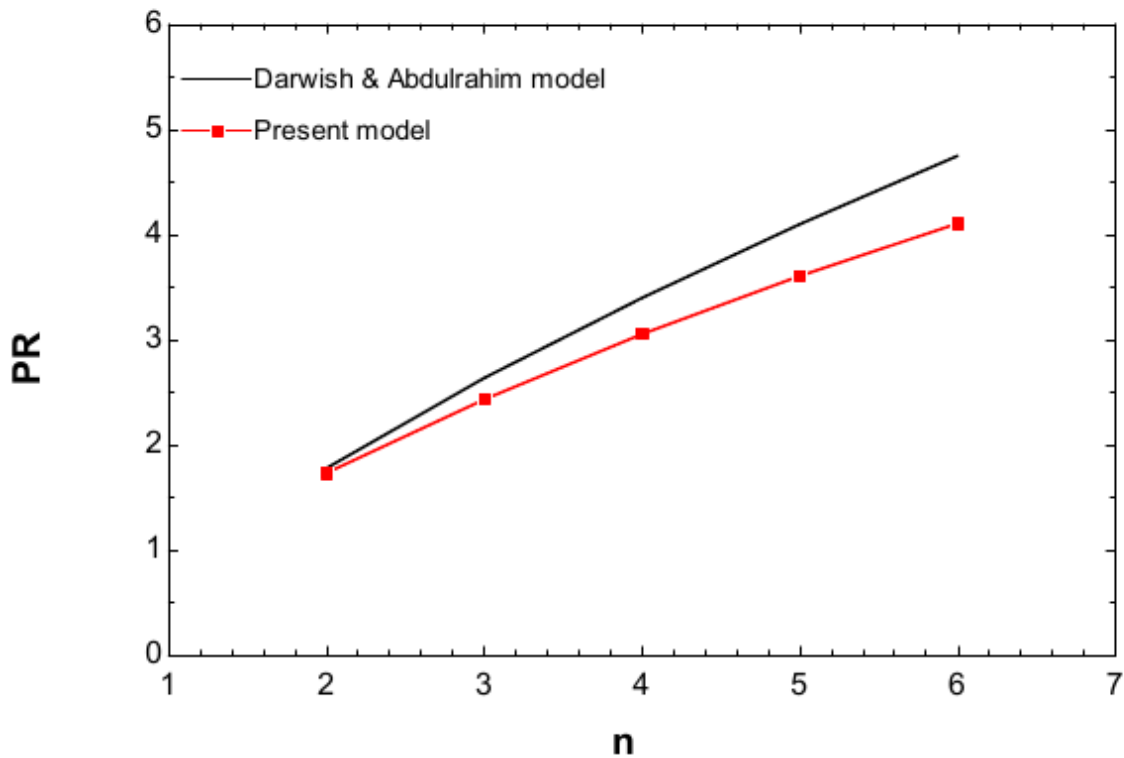
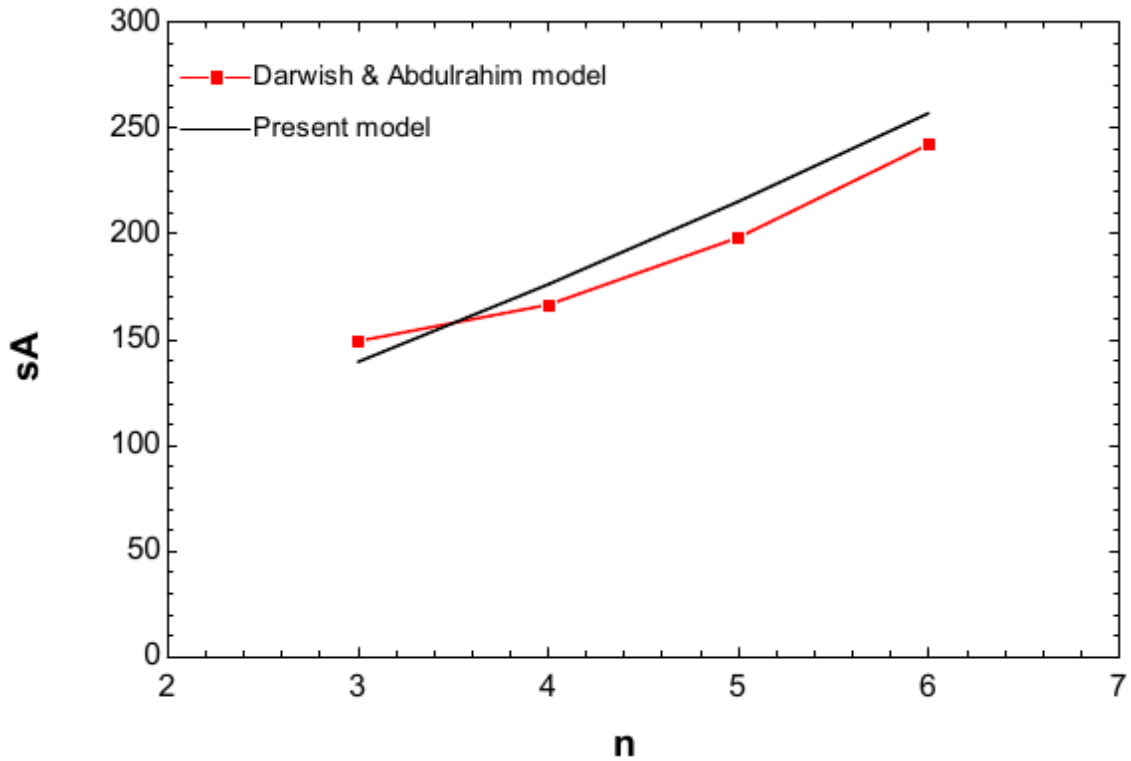


Figure 4.3: Effect of number of effects on the Performance ratio PF/MEE

Figure 4.3 shows the effect of number of effects on the Performance ratio Parallel Feed MED system, the present model has been validated through comparing the results with the model of Darwish & Abdulrahim [7] for the performance ratio and the specific heat transfer surface area. The maximum error has been found to be 6% and that because of different assumption that used in Darwish and Abdulrahim model, it has been assumed that an average temperature to calculate the latent heat in side the effects which is not the case in the present model. Although the results show a good agreement.



**Figure 4.4: Effect of number of effects on the specific heat transfer surface area PF/MEE**

Figure 4.4 shows the effect of number of effects on the specific heat transfer surface area of Parallel Feed MED system, the present model has been validated through comparing the results with the model of Darwish & Abdulrahim [7] for the specific heat transfer surface area, it has been observed that the maximum percentage in error is 4.2%.

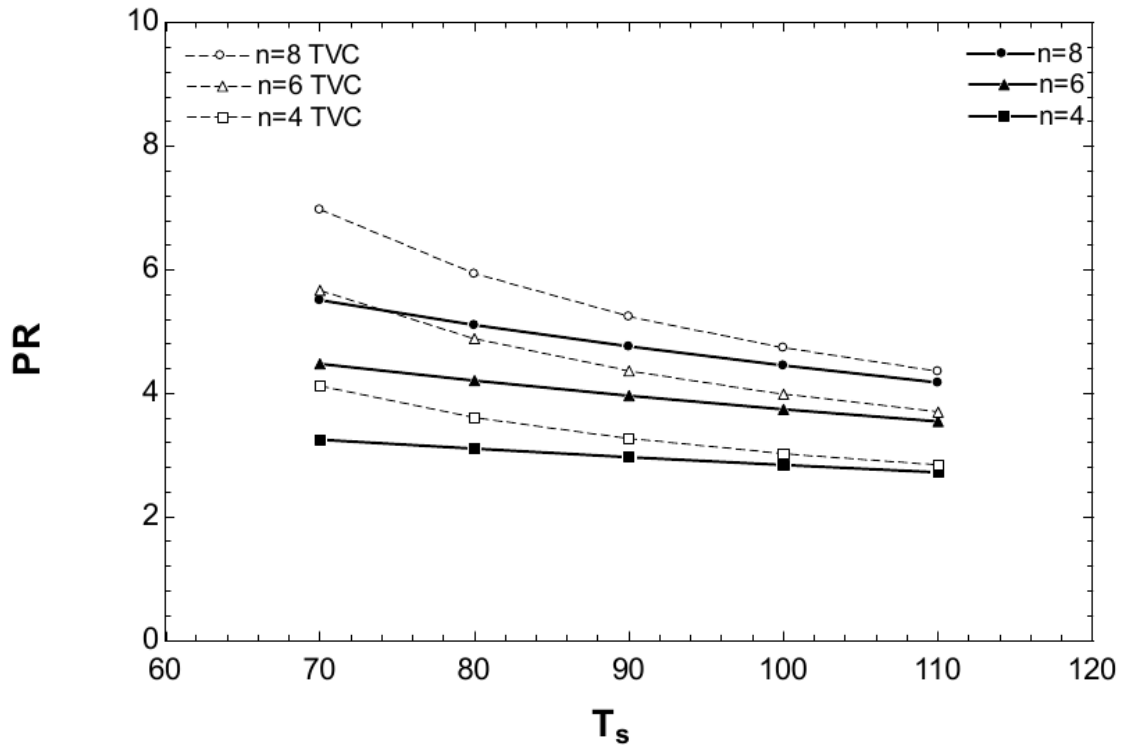


Figure 4.5: Effect of Steam Temperature on Performance Ratio

Figure 4.5 shows the effect of the steam temperature on the thermal performance ratio. It can be clearly seen that as the heating steam temperature increases, the thermal performance ratio decreases because when the steam temperature increases, the heat needed to increase the feed sea water temperature to higher temperature increases so the steam consumption will be higher leading performance ratio to drop. In addition, as the steam temperature increases, the latent heat of the steam decreases, which means that increasing the steam consumption leads to less performance ratio.

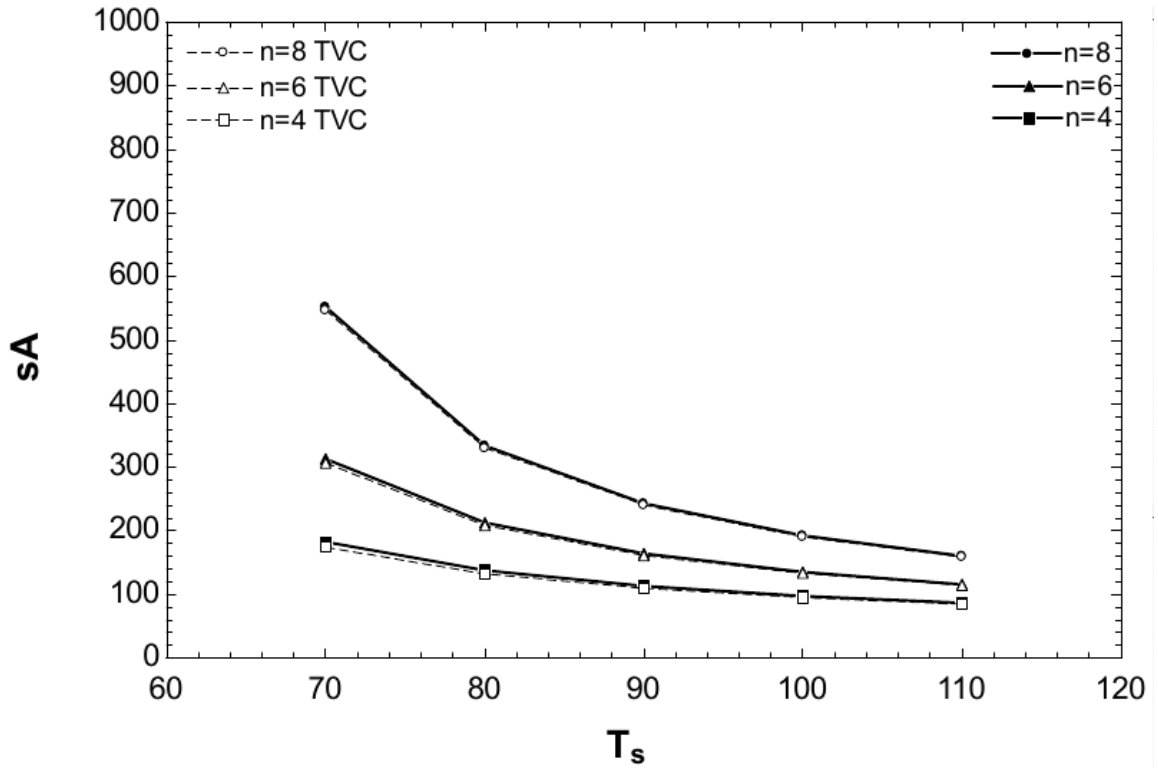
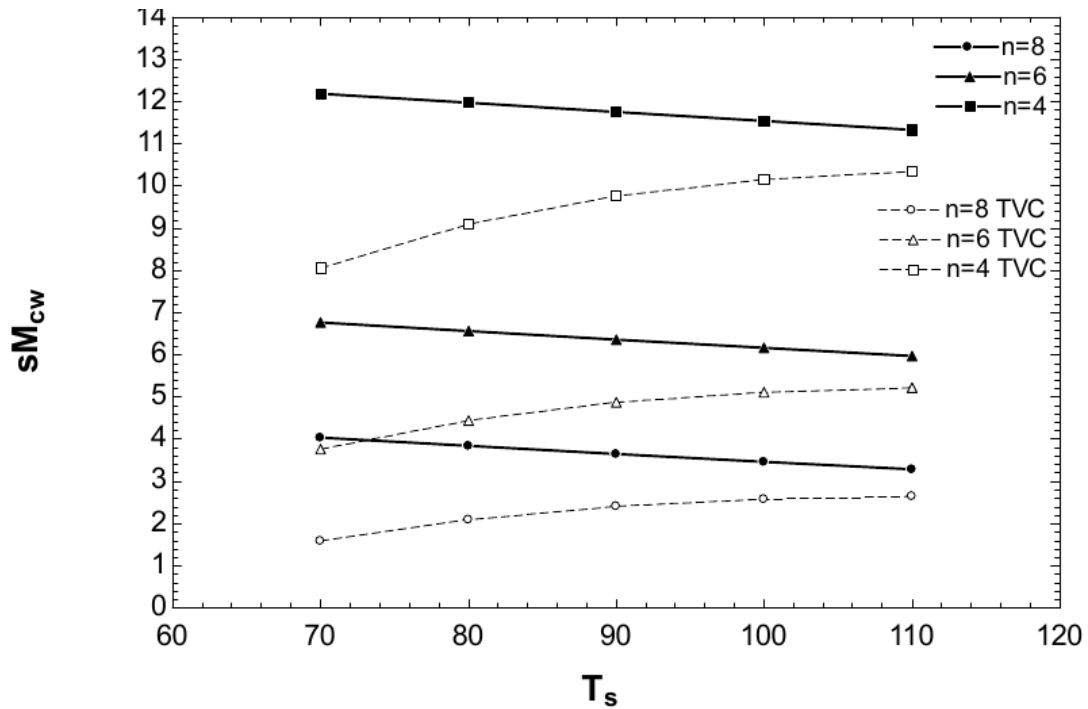


Figure 4.6: Effect of Steam Temperature on Specific heat transfer surface area

TVC: Thermal Vapor Compression

Figure 4.6 shows the relation between the steam temperature and the specific heat transfer surface area. The reason of decreasing the heat transfer surface area with increasing of the heating steam temperature is the temperature difference, when the steam temperature increases, the temperature difference increases. This leads to less heat transfer surface area. Furthermore, increases heating steam temperature increases the overall heat transfer coefficient. This also causes a reduction in the heat transfer surface area.



**Figure 4.7: Effect of Steam Temperature on Specific cooling water flow rate**

Figure 4.7 illustrates the effect of the heating steam temperature on the specific cooling water flow rate, as the heating steam temperature increasing, the vapor generated in the last effect reduces due to reduction in the latent heat and increasing of the sensible heat needed to increase the feed temperature to the saturation temperature, causing a reduction in the cooling water flow rate when the feed sea water and the conversion ratio are constants. Comparing the conventional parallel feed MED system with the parallel feed MED/TVC system, it has been found that in the case of thermal vapor compression there is a dramatic reduction in the specific cooling water flow rate due to reduction in the heat load of the condenser as a result of the entrained vapor to the ejector. In the case of parallel feed thermal vapor compression, as the heating steam temperature increases, the specific cooling water flow rate increases as a result of increasing the thermal load in the last effect and decreasing of the performance ratio.



#### 4.6.2. MEE/PF/TVC different Ejector Positions Model

The following equation is used for MEE/PF/TVC system with 4 effects and the thermal ejector is located after effect number 3. As the position of the ejector is changed the energy balance for the evaporators will change. For instance, in this case the energy balance equation will be as follows:

The energy balance for effect 4

$$(D_3 - m_{ev}) * Lv_3 + df_3 * Lv_3 = D_4 * Lv_4 + F_i * cp * (T_4 - Tf) \quad (4.36)$$

#### 4.7. MEE/PF/TVC different Ejector Positions Model interpretation

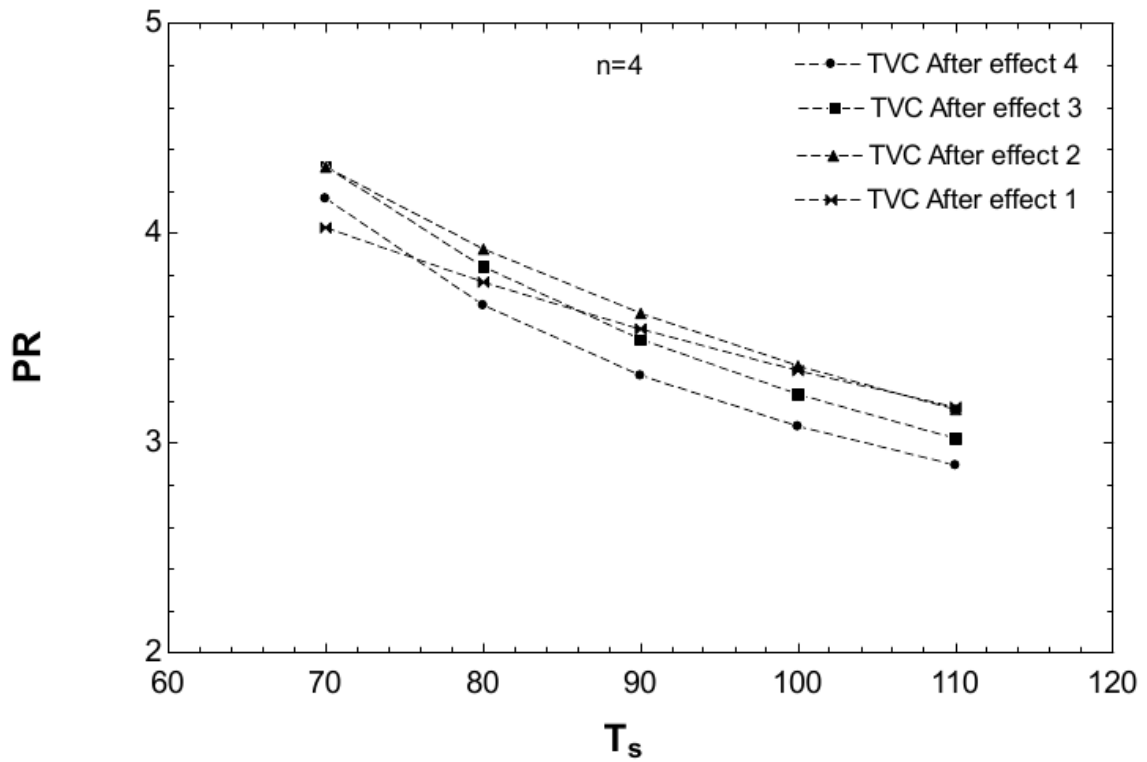


Figure 4.9: Effect of steam temperature on Performance ratio for different ejector positions 4 effects

Figure 4.9 shows the relation between the heating steam temperature and the performance ratio for unit with 4 effects at different ejector positions, the results illustrate that the best position of the ejector that gives highest performance ratio is after the effect that located in the middle. The same trend is obtained for units with 8 and 12 effects as is shown in the figures below.

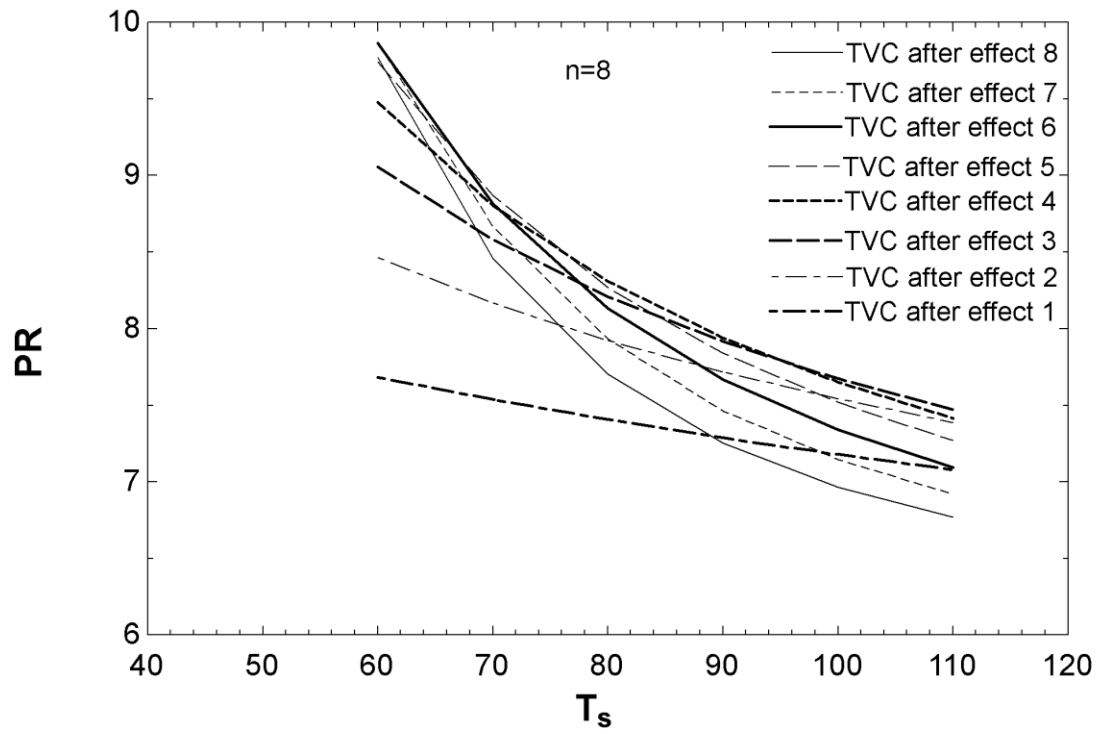


Figure 4.10: Effect of steam temperature on Performance ratio for different ejector positions 8 effects.

Figure 4.10 shows the relation between the heating steam temperature and the performance ratio for unit with 8 effects at different ejector positions

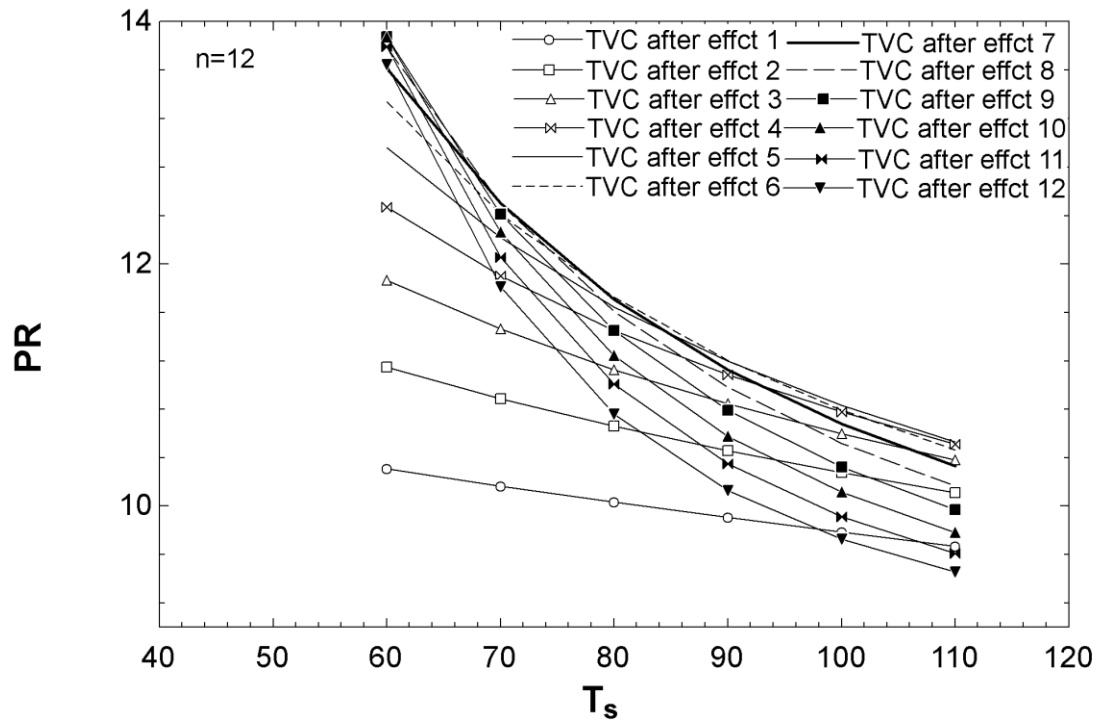


Figure 4.11: Effect of steam temperature on Performance ratio for different ejector positions 12 effects

Figure 4.15 shows the relation between the heating steam temperature and the performance ratio for unit with 12 effects at different ejector positions,

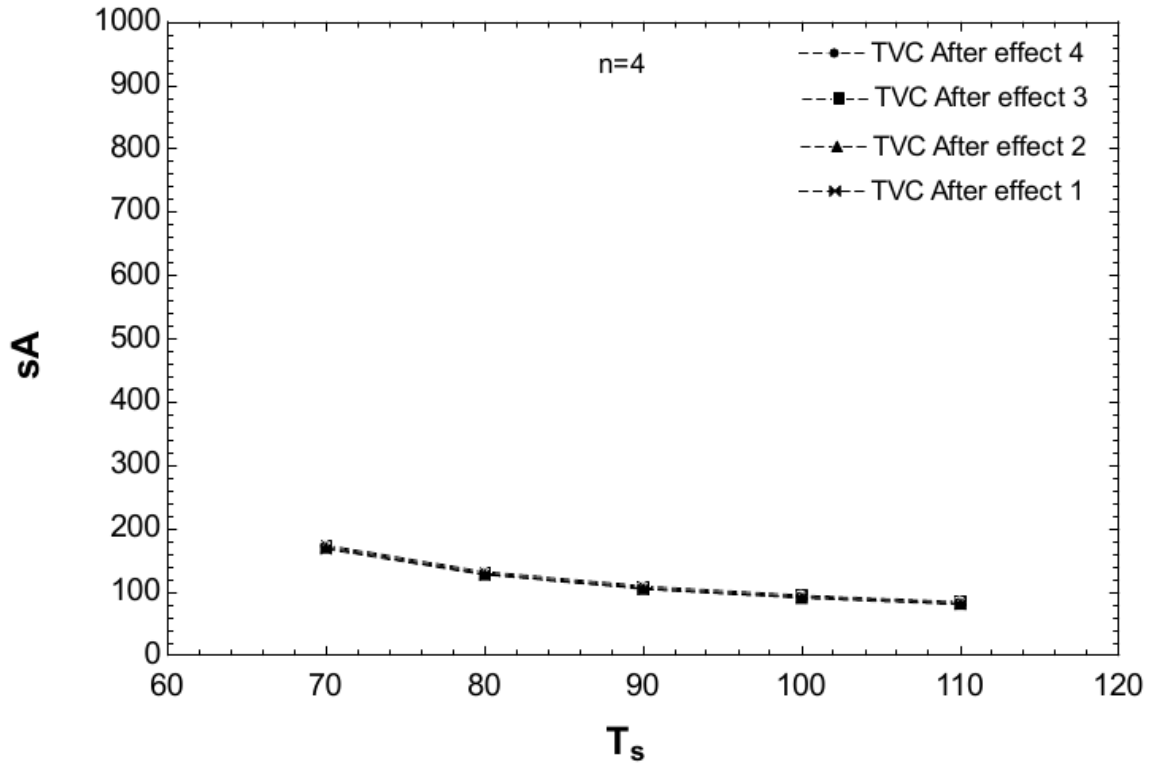


Figure 4.12: Effect of steam temperature on specific heat transfer surface area for different ejector positions 4 effects

Figure 4.12 shows the effect of heating steam temperature and the specific heat transfer surface area for unit with 4 effects, the specific heat transfer surface area decreases as the temperature of heating steam increases and that is because the temperature difference between the effects increasing as the heating steam temperature increases lead to a decrease in the specific heat transfer surface area, changing the thermal vapor compression position does not affect the specific heat transfer surface area. The same trend is obtained for units with 8 and 12 effects as is shown in the figures below.

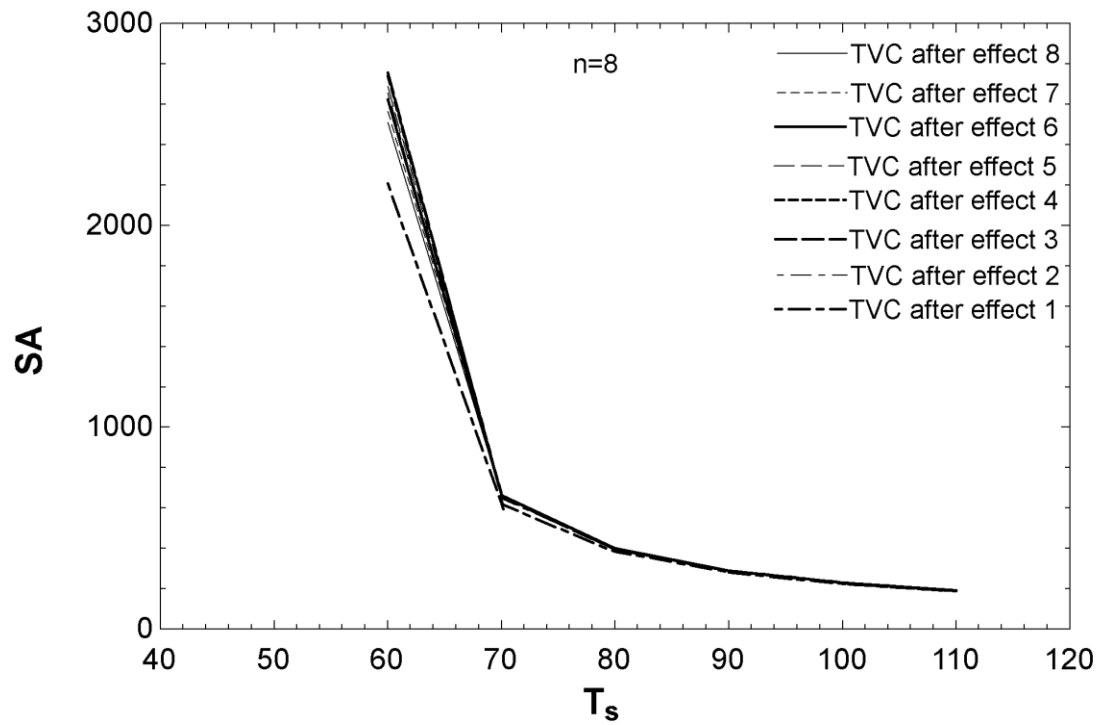
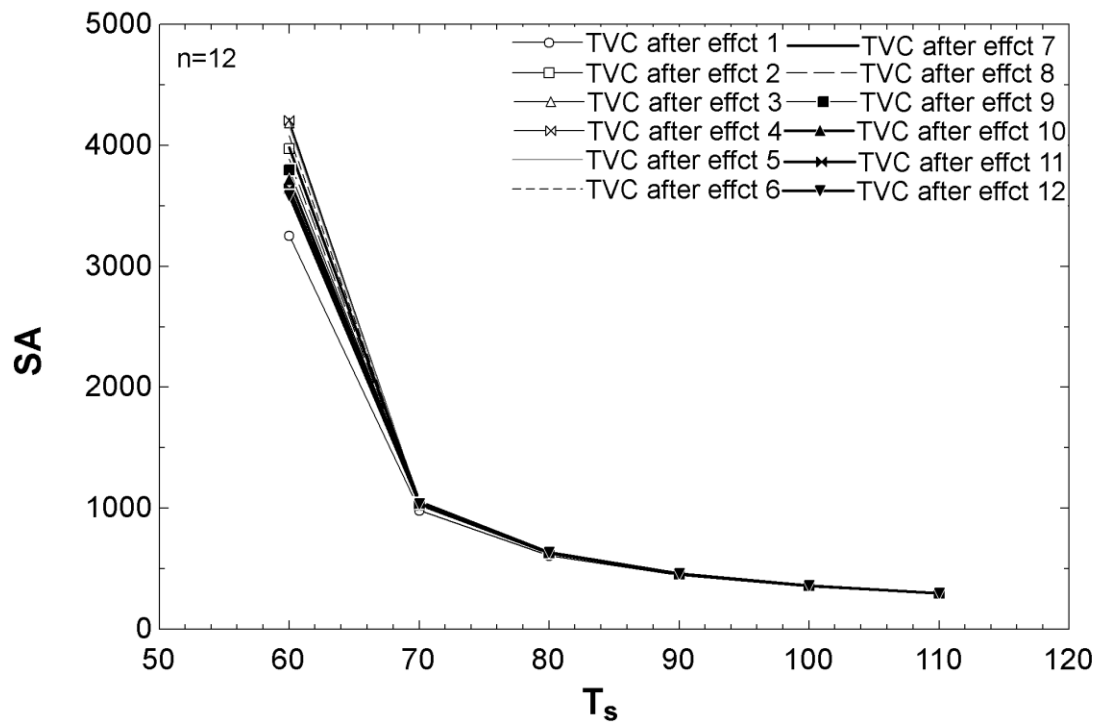


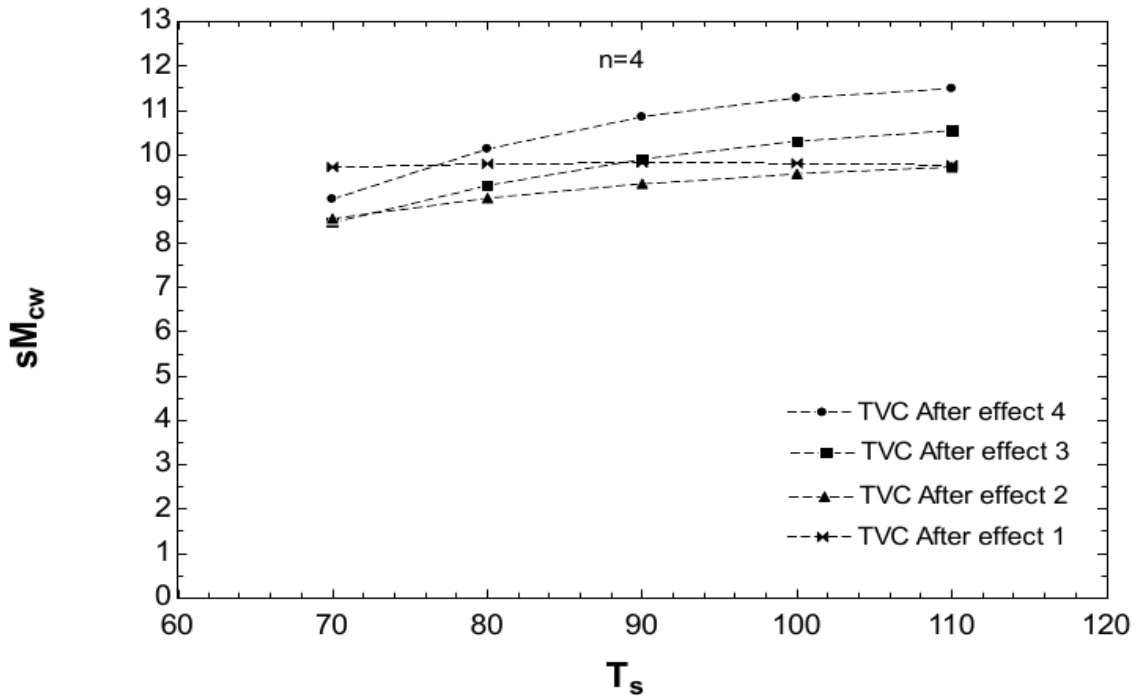
Figure 4.13: Effect of steam temperature on specific heat transfer surface area for different ejector positions 8 effects

Figure 4.13 shows the effect of heating steam temperature and the specific heat transfer surface area for unit with 8 effects at different ejector positions,



**Figure 4.14: Effect of steam temperature on specific heat transfer surface area for different ejector positions 12 effects**

Figure 4.14 shows the effect of heating steam temperature and the specific heat transfer surface area for unit with 12 effects at different ejector positions,



**Figure 4.15: Effect of steam temperature on specific cooling water flow rate for different ejector positions 4 effects**

Figure 4.15 illustrates the effect of the heating steam temperature on the specific cooling water flow rate for unit with 4 effects at different ejector positions, as the heating steam temperature increases the cooling water flow rate increases. This behavior is different from MEE/Parallel system since adding the thermal vapor ejector in which the heat load increase by increasing the heating steam temperature would lead to an increase in the specific cooling water flow rate. However, the lower consumption of the specific cooling water flow rate occurs when the thermal vapor compression ejector is allocated at the middle of the plant, as a result of changing the motive steam flow rate in such a way that reaches the lowest value when the ejector is located in the middle to give maximum performance ration and minimum cooling water flow rate. The same trend is obtained for units with 8 and 12 effects as it is shown in the figures below.

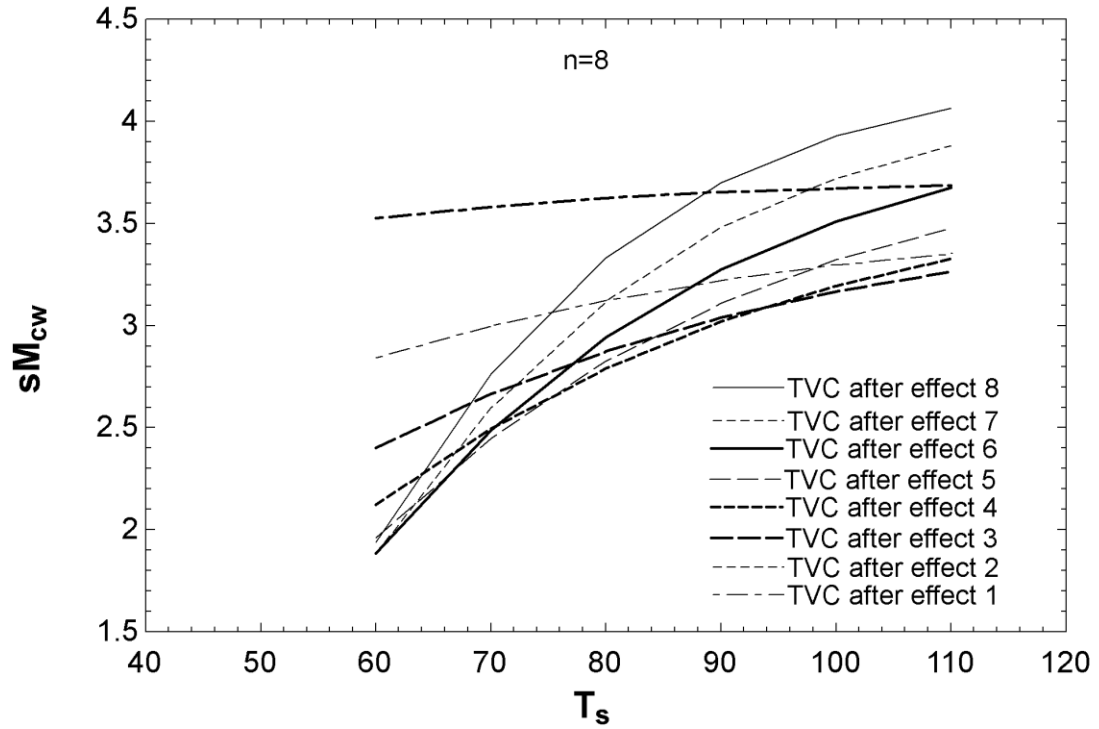


Figure 4.16: Effect of steam temperature on specific cooling water flow rate for different ejector positions 8 effects

Figure 4.16 illustrates the effect of the heating steam temperature on the specific cooling water flow rate for unit with 8 effects at different ejector positions.

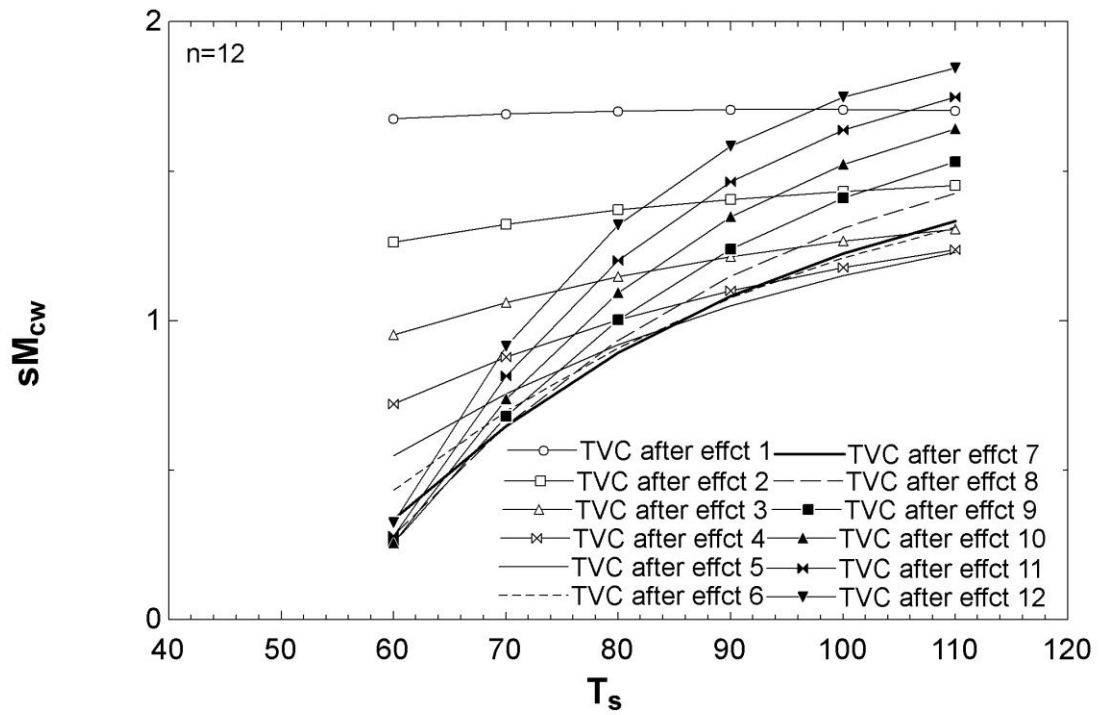


Figure 4.17: Effect of steam temperature on specific cooling water flow rate for different ejector positions 12 effects

Figure 4.17 illustrates the effect of the heating steam temperature on the specific cooling water flow rate for unit with 12 effects at different ejector positions,

## 4.8. MED/PF Exergy Analysis

The exergy of fluid stream is given by the relation:

$$X = \dot{m} (h - h_o - T_o(s - s_o)) \quad (4.37)$$

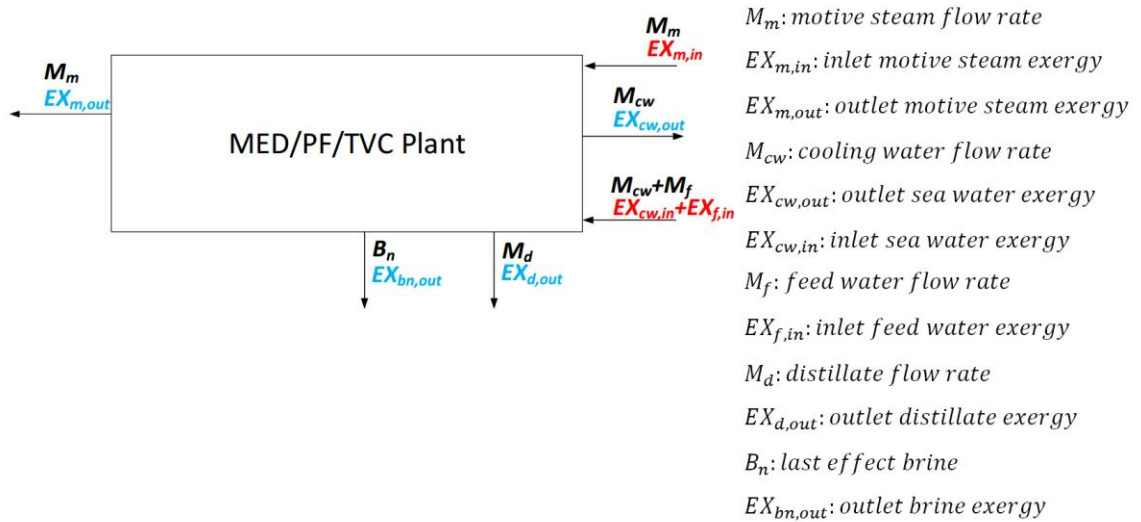


Figure 4.18: Total input and output exergy for parallel feed system

### Exergy Analysis Calculations

First effect

For the hot stream

$$EX_{sin1} = \dot{m}_s * ((hs_{in1} - hs_o) - (T_o) * (ss_{in1} - ss_o)) \quad (4.38)$$

$$EX_{sout1} = \dot{m}_s * ((hs_{out1} - hs_o) - (T_o) * (ss_{out1} - ss_o)) \quad (4.39)$$

$T_o$  is the surrounding temperature in Kelvin

$$\Delta EX_{hot1} = EX_{sin1} - EX_{sout1} \quad (4.40)$$

For the cold stream

(a) Feed Stream

$$EX_{fin1} = F_1 * ((hf_{in1} - hf_o) - (T_o) * (sf_{in1} - sf_o)) \quad (4.41)$$

(b) Brine Stream

$$EX_{bout1} = B_1 * ((hb_{out1} - hf_o) - (T_o) * (sb_{out1} - sf_o)) \quad (4.42)$$

(c) Vapor Stream

$$EX_{vout1} = D_1 * ((hv_{out1} - hs_o) - (T_o) * (sv_{out1} - ss_o)) \quad (4.43)$$

Therefore;

$$\Delta EX_{cold1} = EX_{vout1} + EX_{bout1} - EX_{fin} \quad (4.44)$$

$$\Delta EX_1 = \Delta EX_{hot1} - \Delta EX_{cold1} \quad (4.45)$$

The exergetic efficiency is given by:

$$Efficiency_{EX1} = \frac{\Delta EX_{cold1}}{\Delta EX_{hot1}} \quad (4.46)$$

Total Plant Exergatic Efficiency

$$\eta_T = \frac{EX_D}{EX_S} \quad (4.47)$$

$\eta_T$ =Total Plant Exergatic Efficiency

$EX_D$  = distillate exergy

$EX_s$ = Heating steam exergy

Other effects from  $i=2,n$

For the hot stream (formed vapor inside the previous effect)

$$EX_{sin[i]} = D_{[i-1]} * ((hs_{in[i]} - hs_o) - (T_o + 273) * (ss_{in[i]} - ss_o)) \quad (4.48)$$

$$Delta_{EXhot[i]} = EX_{sin[i]} - EX_{sout[i]} \quad (4.49)$$

For cold stream (seawater stream)

$$EX_{fin[i]} = F_i * ((hf_{in[i]} - hf_o) - (T_o + 273) * (sf_{in[i]} - sf_o)) \quad (4.50)$$

$$EX_{bout[i]} = B_i * ((hb_{out[i]} - hf_o) - (T_o + 273) * (sb_{out[i]} - sf_o)) \quad (4.51)$$

$$Delta_{EXcold[i]} = EX_{vout[i]} + EX_{bout[i]} - EX_{fin[i]} \quad (4.52)$$

$$Delta_{EX[i]} = Delta_{EXhot[i]} - Delta_{EXcold[i]} \quad (4.53)$$

$$Efficiency_{EX[i]} = \frac{\Delta_{EXcold[i]}}{\Delta_{EXhot[i]}} \quad (4.54)$$

**Table 4.1: Exergy Analysis Calculations for PF/TVC system when the ejector is located after effect 4**

Exergy Analysis Calculations FF/TVC after	Last Effect
Blow down Exergy (kw)	10.15
Distillate Exergy (kw)	3.673
Inlet Motive steam Exergy (kw)	123.8
Outlet Motive Exergy (kw)	1.611
Inlet Feed \& Cooling Sea water Exergy (kw)	0
Total Exegetic Efficiency (%)	3.005
Compression Ratio CR (-)	3.006
Entrainment Ratio Ra (-)	2.199
Performance Ratio PR (-)	5.004
Cooling Water Flow Rate (kg/s)	6.638
Entrained Vapor Flow Rate (kg/s)	0.0909
Motive Steam Flow Rate (kg/s)	0.1998
Steam Flow Rate (kg/s)	0.2907
Condenser Exergetic Efficiency (%)	33.52
Ejector Exergetic Efficiency (%)	56
First Effect Exergetic Efficiency (%)	82.85
Second Effect Exergetic Efficiency (%)	85.07
Third Effect Exergetic Efficiency (%)	81.53
Fourth Effect Exergetic Efficiency (%)	75.28

Table 4.1 shows the exergy analysis for PF/TVC system when the ejector is located after effect 4. The results show that the exergy destruction is the highest in the condenser followed by the ejector. However, the total plant second law efficiency is equal to 3.005% which is acceptable comparable with the literature and the values reported in the industry are around 4%.

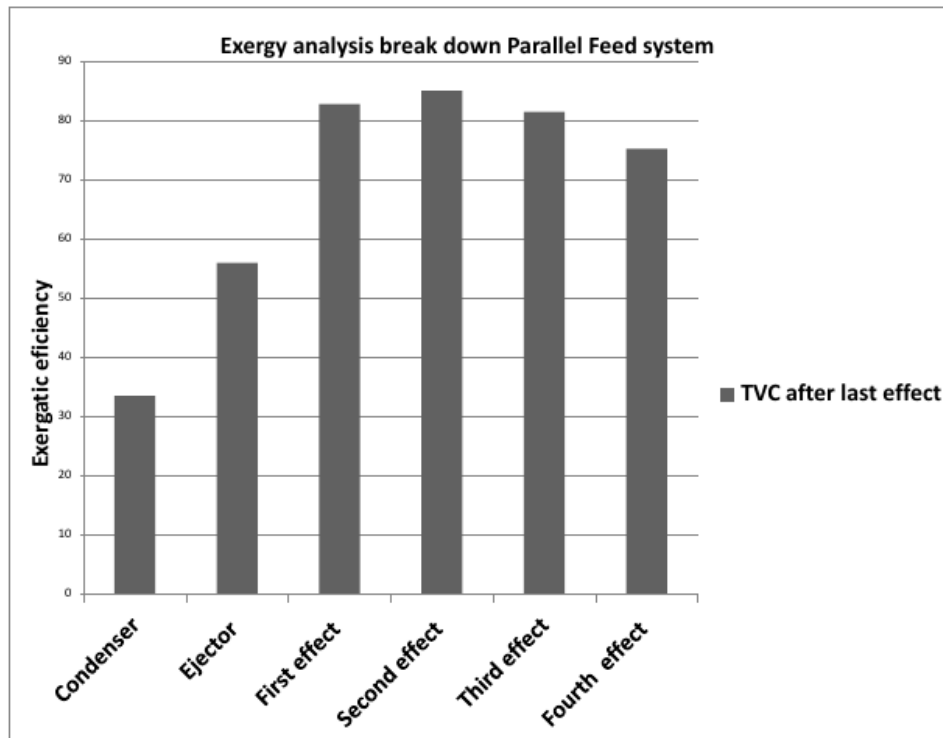


Figure 4.19: Exergy analysis breaks down Parallel Feed System

Figure 4.19 shows the exergy analysis for PF/TVC system when the ejector is located after effect 4. The results show that the exergy destruction is the highest in the condenser followed by the ejector, the reason that makes the condenser is the lower second low efficiency is because of the difference of the temperature between the condensation temperature and the inlet temperature of the intake sea water.

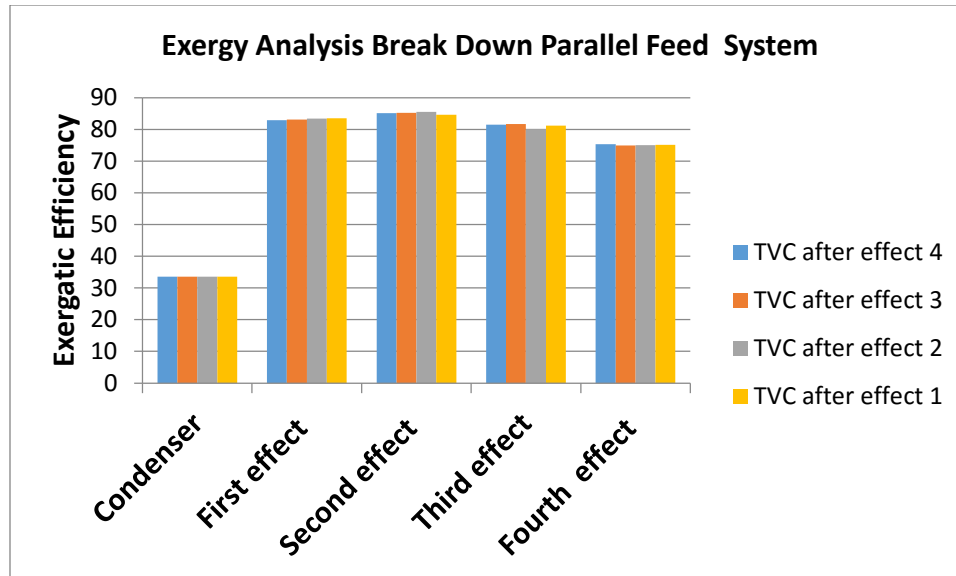
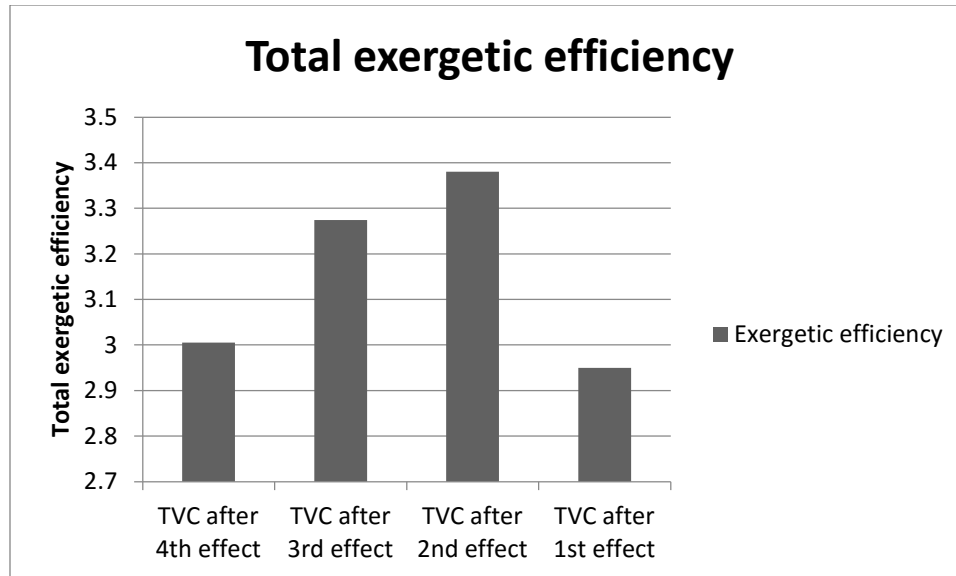


Figure 4.20: Exergy analysis break down for parallel feed system

Figure 4.20 shows the exergy analysis break down for parallel feed system, it can be clearly seen that the condenser exergatic efficiency does not change with changing the ejector position and that because the temperature of the last effect is kept constant. However, the exergy destruction can be decreased by reducing the top brine temperature, increasing the number of stages, and increasing entrainment ratio of the thermo compressor.



**Figure 4.21 Total exergetic efficiency for parallel feed system**

Figure 4.21 shows the total exergetic efficiency for parallel feed flow system, the maximum exergetic efficiency obtained when the ejector is located after the second effect which applies with the performance ratio, However the reason of the exergy losses is the increase of the temperature difference between effects..

# Parallel Cross Multi Effect Evaporation Desalination

## System

Parallel cross multi effect evaporation desalination system has the same configuration like parallel feed multi effect desalination system except that, the brine leaving an effect enters the brine pool of the next effect and that is why it is called parallel cross.

### 5.1. Working Principle

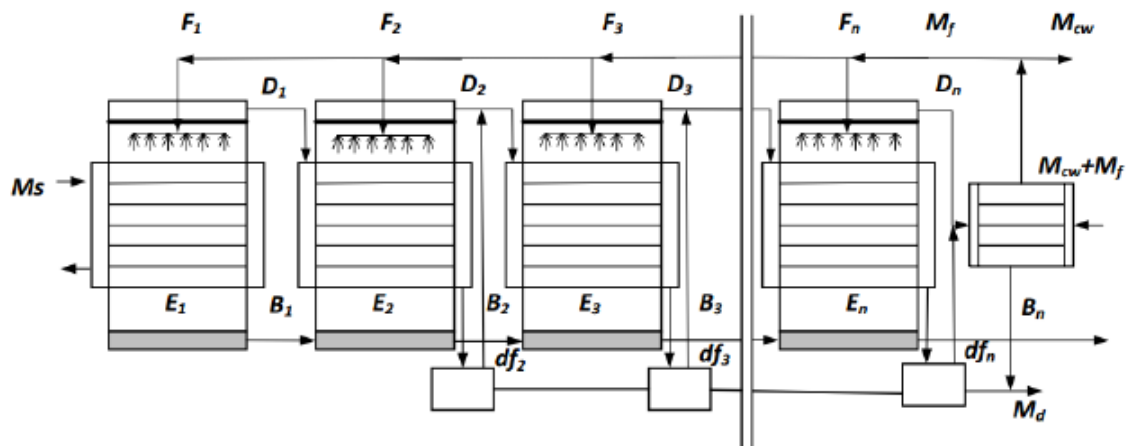


Figure 5.1: Parallel Cross Multi Effect Desalination System

Figure 5.1 shows the parallel cross feed multi effect evaporation system; there are n numbers of effects, the vapor flows from left to right. Each effect has a mist eliminator, brine pool and other constitutes, in this type of desalination systems the vapor flows in the direction of falling pressure and temperature. Whereas feed seawater direction is vertical. The system contains n evaporators and flash boxes and a down condenser. The

number of flash boxes in the parallel crosses feed multi effect evaporation systems are (n-1). In the down condenser, the feed sea water enter to absorb the latent heat of the condensing vapor at the last effect, this causes an increase in the seawater temperature from  $T_{cw}$  to the feed seawater temperature  $T_f$ . Part of this heated seawater will be rejected to the sea as cooling water, the feed seawater is chemically treated and then sprayed inside the evaporators in the form of small droplets. In each evaporator, the feed seawater temperature increases to the saturation temperature, and a portion of it evaporates. The heat required for the preheating and evaporation in the first effect is provided by condensing steam inside tubes. Which may be supplied to the system by an external source for instance turbine, boiler or any other source. The brine leaving the first effect enters the brine pool of the second effect and the brine leaving the second effect enters the third effect and so on. The reason of this brine flow is to make use of the energy associated with brine leaving every effect. since it has higher pressure and temperature than these of the next effect. It flashes. Therefore, an additional amount of vapor is released in the effect. The vapor temperature is less than the boiling temperature of the brine in each effect by the boiling point elevation, BPE, to dismiss the entrained brine droplets the vapor passes through demister or mist eliminator. The amount of the vapor formed in every effect more than the vapor formed in the next effect and that is due to the increase in the specific latent heat of vaporization as temperature decreases.

## 5.2. Multi Effect Evaporation Parallel Cross Feed Desalination System

### Modeling

A mathematical model of Parallel Cross feed multi effect evaporation system presented in this section to provide an effective way to evaluate and design such a system, the mathematical model is solved using Engineering Equation Solver software (EES).

The mathematical model is based on energy balance and mass balance for the system components. The down condenser governing equations are included in the model.

The calculated properties and parameters in the model include:

- Vapor flow rate  $D_i$
- Brine flow rate  $B_i$
- Brine salinity  $X_i$
- Brine temperature  $T_i$
- Heat transfer surface area  $A_i$
- Steam flow rate entering the first effect  $\dot{m}_s$
- Cooling water flow rate  $\dot{m}_{cw}$
- Heat transfer surface area of the condenser  $A_c$

A number of assumptions are made in order to develop the Parallel Cross Feed Multi Effect Desalination System mathematical model:

- Vapor salinity is zero (does not contain salt)
- No energy loss between the effects and the surrounding
- The thermal load is equal for all effects except for the first effect
- The specific heat capacity is constant  $c_p$
- The thermal losses are constants

### 5.2.1. System Configuration

In this part, a mathematical analysis of parallel Cross feed arrangement has been illustrated. The system contains  $n$  evaporators, the flow rate of the feed sea water  $m_f$  with temperature  $T_f$  coming out from the condenser entering the evaporators in parallel. The steam supplied to the first effect  $S$  heats the feed flow,  $F_1$  from temperature of  $T_f$  to  $T_1$  and forms an amount of vapor,  $D_1$  at temperature  $T_{v1}$  which in turn enters to the second effect representing the heat source that rises the temperature of  $F_2$  from  $T_f$  to  $T_2$  and forms an amount of vapor,  $D_2$  that represents the vapor formed in the second effect at temperature  $T_{v2}$  and so on until we reach the last effect, the vapor formed in the last effect enters the down condenser in which the cooling water temperature rises from  $T_{cw}$  to  $T_f$ . As we follow the flow direction, the brine temperature decreases from  $T_1$  to  $T_2$  to  $T_3$  till it reaches  $T_n$ . Vapor flashes in the distilled flash boxes and joins the vapor formed in the same effect. Both streams enter the next effect as a heat source. the brine leaving the first effect enters the second effect and the brine leaving the second effect enters the third effect and so on, as brine leaves effect  $i$  and flows into the brine pool of effect  $(i+1)$ , which is at a lower temperature, a part of it flashes to provide more water vapor in this

effect. this process is occurring in effect 2,3,.....,n. The flashed vapor in effect 2 joins the vapor forms in this effect  $D_2$  to condense in the tubes of the third effect, and so on.

The brine leaving from the first effect is evaluated by:

$$B_1 = F_1 - D_1 \quad (5.1)$$

To generalize, the brine leaving from effect i is calculated from the effect mass balance as follows

$$F_i + B_{i-1} = B_i + D_i \quad (5.2)$$

$$F_i * X_f + B_{i-1} * X_{i-1} = B_i * X_i \quad (5.3)$$

Energy balance equation for the first effect

$$\dot{m}_s * L = F_1 * c_p * (T_1 - T_f) + D_1 * L_1 \quad (5.4)$$

Energy balance equation for the effect i

$$D_{i-1} * L_{i-1} + de_{i-1} * Le_{i-1} + df_{i-1} * Lf_{i-1} = F_i * c_p * (T_i - T_f) + D_i * L_i \quad (5.5)$$

Where,

$de_{i-1}$  is the flashed vapor inside the effect (i-1)

$df_{i-1}$  is the flashed vapor inside the flash box (i-1)

The vapor produced due to brine flashing inside the brine pool

$$de_i = B_{i-1} * c_p * \frac{T_{i-1} - \dot{T}_i}{L_i} \quad (5.6)$$

$$\dot{T}_i = T_i + NEA_i \quad (5.7)$$

The brine leaving from the first and the second effect

Using salt balance equations

$$\frac{\dot{m}_f}{\dot{m}_d} = \frac{X_b}{X_b - X_f} \quad (5.8)$$

Temperature of the vapor formed in each effect is given by:

$$Tv_i = T_i - BPE_i \quad (5.9)$$

The Temperature of the condensate in each effect

$$Tc_i = T_i - BPE_i - \Delta T_{loss} \quad (5.10)$$

The temperature in the flash box differs from the vapor temperature by the non equilibrium allowance

$$\ddot{T}_j = \ddot{T}_{vj} + N\ddot{E}A_j \quad (5.11)$$

The flashed vapor in the second effect flash box

$$df_2 = D_1 * c_p * \frac{(T_{v1} - \ddot{T}_2)}{\dot{L}_{v2}} \quad (5.12)$$

The flashed vapor in the rest of flash boxes

$$df_j = \left( \sum_{i=1}^j D_i \right) * c_p * \frac{(Tv_{j-1} - \ddot{T}_j)}{\dot{L}_{vj}} \quad (5.13)$$

The energy balance in the condenser

$$(D_n + df_n + de_n) * L_{vn} = (\dot{m}_{cw} + \dot{m}_f) * c_p * (T_f - T_{cw}) \quad (5.14)$$

The condenser Log Mean Temperature Difference is needed to calculate the condenser heat transfer surface area

$$LMTD_c = \frac{T_f - T_{cw}}{\text{Ln} \left( \frac{\dot{T}v_n - T_{cw}}{\dot{T}v_n - T_f} \right)} \quad (5.15)$$

The heat transfer surface area of the condenser

$$A_c = \frac{Q_c}{U_c * LMTD_c} \quad (5.16)$$

Area of the first effect

$$A_1 = \frac{m_s * L_s}{U_{e1} * (T_s - T_1)} \quad (5.17)$$

The heat load in the condenser

$$Q_c = (D_n + de_n + df_n) * L_{vn} \quad (5.18)$$

$$Q_c = (\dot{m}_{cw} + \dot{m}_f) * c_p * (T_f - T_{cw}) \quad (5.19)$$

The main output parameters are

- The System Performance Ratio

$$PR = \frac{\dot{m}_d}{\dot{m}_s} \quad (5.20)$$

- The Specific Cooling water flow rate

$$s\dot{m}_{cw} = \frac{\dot{m}_{cw}}{\dot{m}_d} \quad (5.21)$$

- The Specific Heat Transfer Surface Area

$$sA = \frac{\sum_{i=1}^n A_i + A_c}{\dot{m}_d} \quad (5.22)$$

### 5.3. Multi Effect Evaporation Parallel Cross Feed Thermal Vapor Compression (TVC)

#### 5.3.1. System Configuration

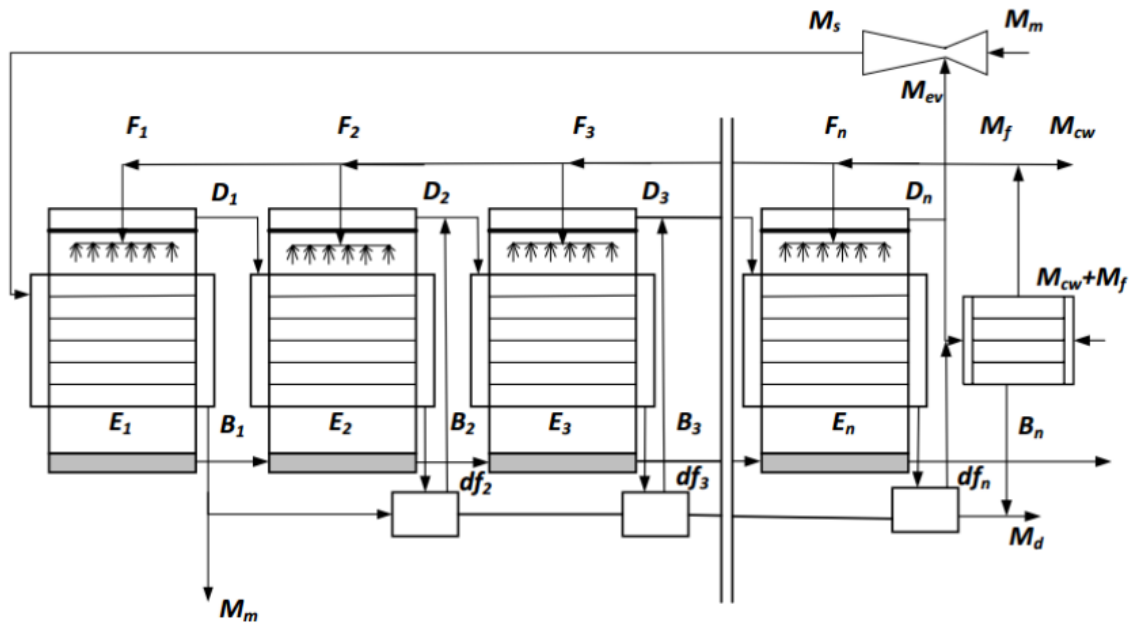


Figure 5.2: MEE/PCF/Thermal Vapor Compression

Figure 5.2 shows the MED/TVC layout for the parallel Cross flow multi effect desalination system

## 5.4. Multi Effect Evaporation Parallel Cross Feed Thermal Vapor

### Compression (TVC) Modeling

Parallel Cross Feed Multi Effect Evaporation Thermal Vapor Compression is similar to parallel Cross Feed Multi Effect Evaporation except for the PCF/TVC there is an additional element which is ejector. Therefore, in the modeling there are two independent loops the Parallel cross feed loop and the thermal ejector loop.

The energy balance in the first effect

$$\dot{m}_s = \frac{D_1 * Lv_1 + \dot{m}_f * c_p * (T_1 - T_f)}{L_s} \quad (5.23)$$

The Motive steam is the difference between the steam and entrained vapor

$$\dot{m}_m = \dot{m}_s - \dot{m}_{ev} \quad (5.24)$$

The heat load in the condenser

$$Q_c = (D_n - \dot{m}_{ev}) * Lv_n \quad (5.25)$$

$$Q_c = (\dot{m}_{cw} + \dot{m}_f) * c_p * (T_f - T_{cw}) \quad (5.26)$$

The condenser Log Mean Temperature Difference is needed to calculate the condenser heat transfer surface area

$$LMTD_c = \frac{T_f - T_{cw}}{\ln\left(\frac{T_v_n - T_{cw}}{T_v_n - T_f}\right)} \quad (5.27)$$

The heat transfer surface area of the condenser

$$A_c = \frac{Q_c}{U_c * LMTD_c} \quad (5.28)$$

The main output parameters are

- The System Performance Ratio

$$PR = \frac{\dot{m}_d}{\dot{m}_s} \quad (5.29)$$

- The Specific Cooling water flow rate

$$s\dot{m}_{CW} = \frac{\dot{m}_{CW}}{\dot{m}_d} \quad (5.30)$$

- The Specific Heat Transfer Surface Area

$$sA = \frac{(\sum_{i=1}^n A_i + A_c)}{\dot{m}_d} \quad (5.31)$$

## 5.5. Multi Effect Evaporation Parallel Cross Feed (with and without TVC) Model interpretation and validation

The model has been validated in terms of the performance ratio and specific heat transfer surface area with El-Dessouky model the results show a very good agreement where the maximum error found to be 6.6%.

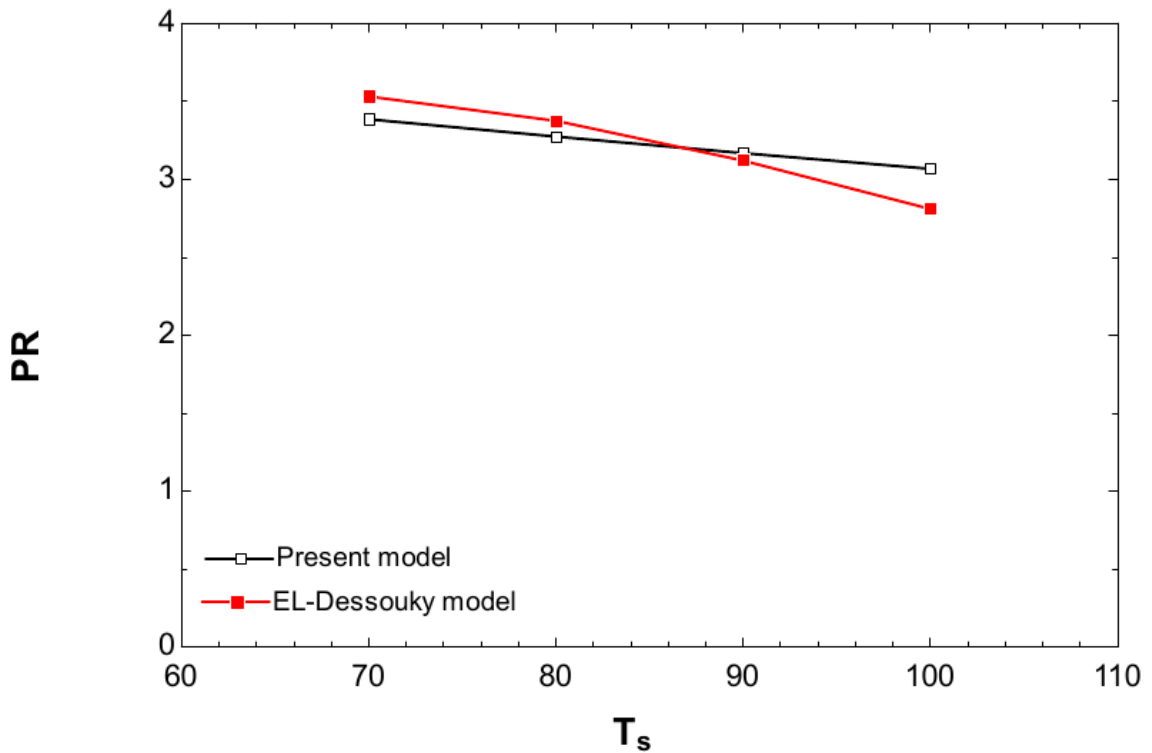


Figure 5.3: Effect of steam temperature on performance ratio

Figure 5.3 shows the PR dependence on  $T_s$  compared with the model of El-Dessouky where a very good agreement is observed.

MED PC is similar in its performance compared with MED PF but it differs in the specific cooling water flow rate

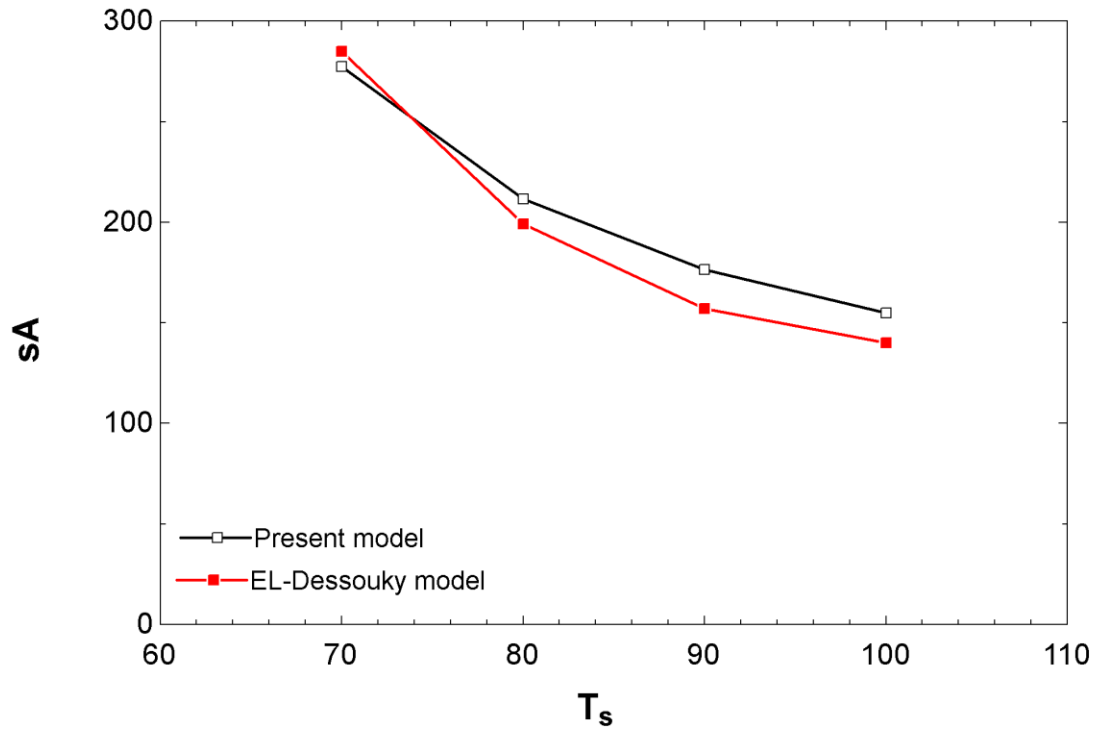


Figure 5.4: Effect of steam temperature on specific heat transfer surface area

Figure 5.4 also shows a very good agreement with the model of El-Dessouky [5] as the specific area is plotted for different values of  $T_s$ .

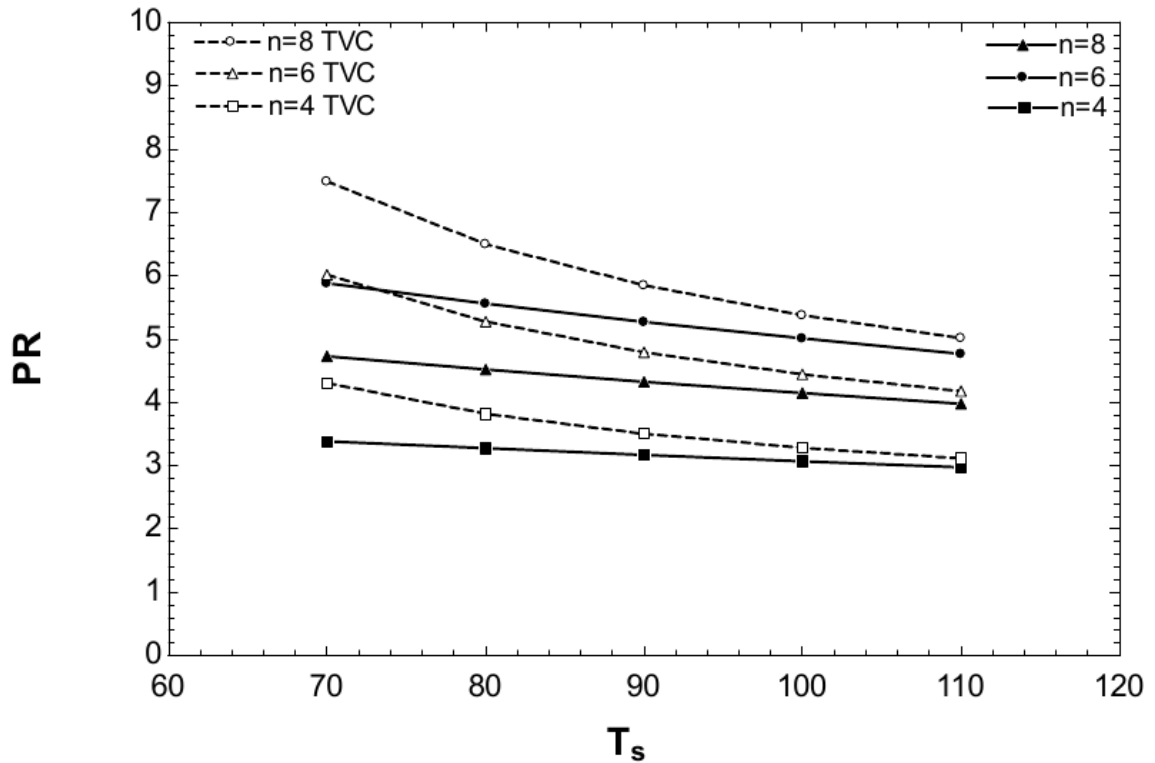


Figure 5.5: Effect of steam temperature on performance ratio

The effect of steam temperature on the performance ratio is depicted in figure 5.5 for plants of different number of effects. It shows that increasing the number of effects has a significant effect in increasing PR. However, increasing the steam temperature reduces the performance ratio because the heat needed to increase the feed seawater temperature to higher temperature increases so the steam consumption will be higher which make the PR less. Also, the latent heat of the steam decrease as temperature increases result in increasing the steam consumption leading to less PR. Moreover, it shows the effect of adding TVC (dashed lines) that also increases PR. This increase is significant at lower  $T_s$  due to the decrease of the motive steam consumption.

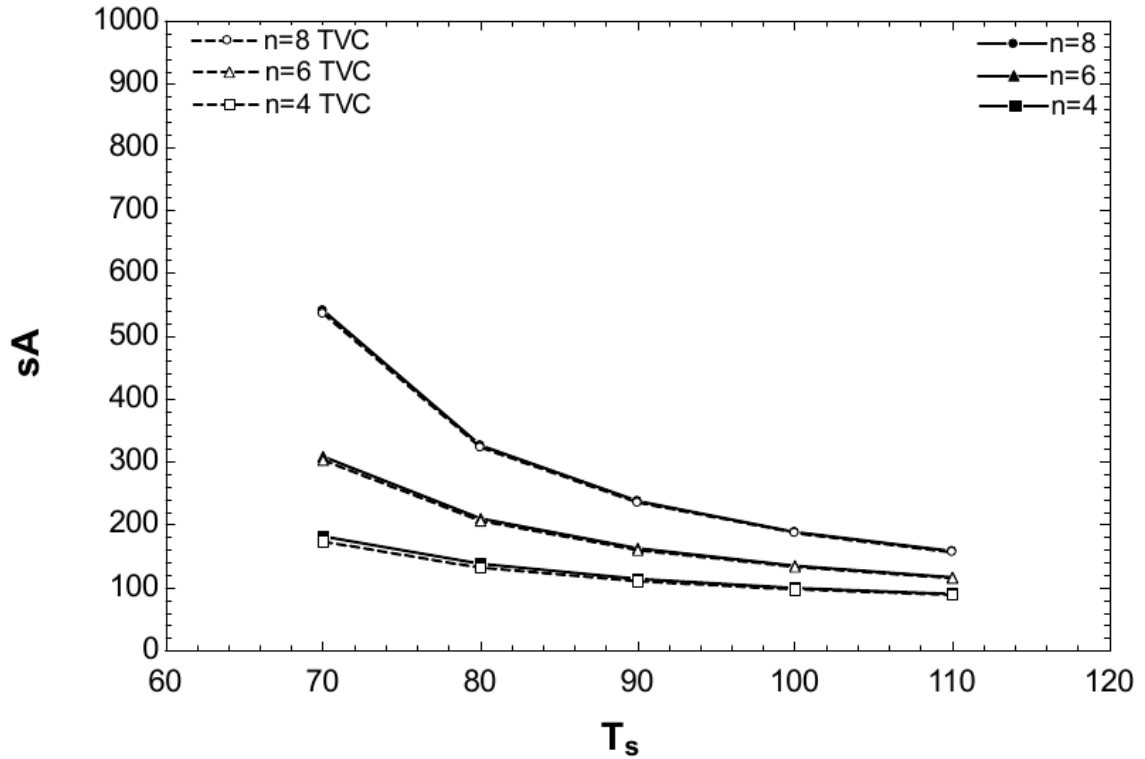


Figure 5.6: Effect of steam temperature on specific heat transfer surface area

Figure 5.6 shows the effect of the steam temperature on the specific heat transfer surface area. The heat transfer surface area decreases with increasing the heating steam temperature. When the steam temperature increases, the temperature difference increases leading to less heat transfer surface area. Furthermore, increasing heating steam temperature increases the overall heat transfer coefficient. This too causes a reduction in the heat transfer surface area. The use of TVC does not affect the specific heat transfer surface area because the difference is only in the condenser area which is lower in the case of TVC, however this difference does not affect the total specific heat transfer surface area significantly.

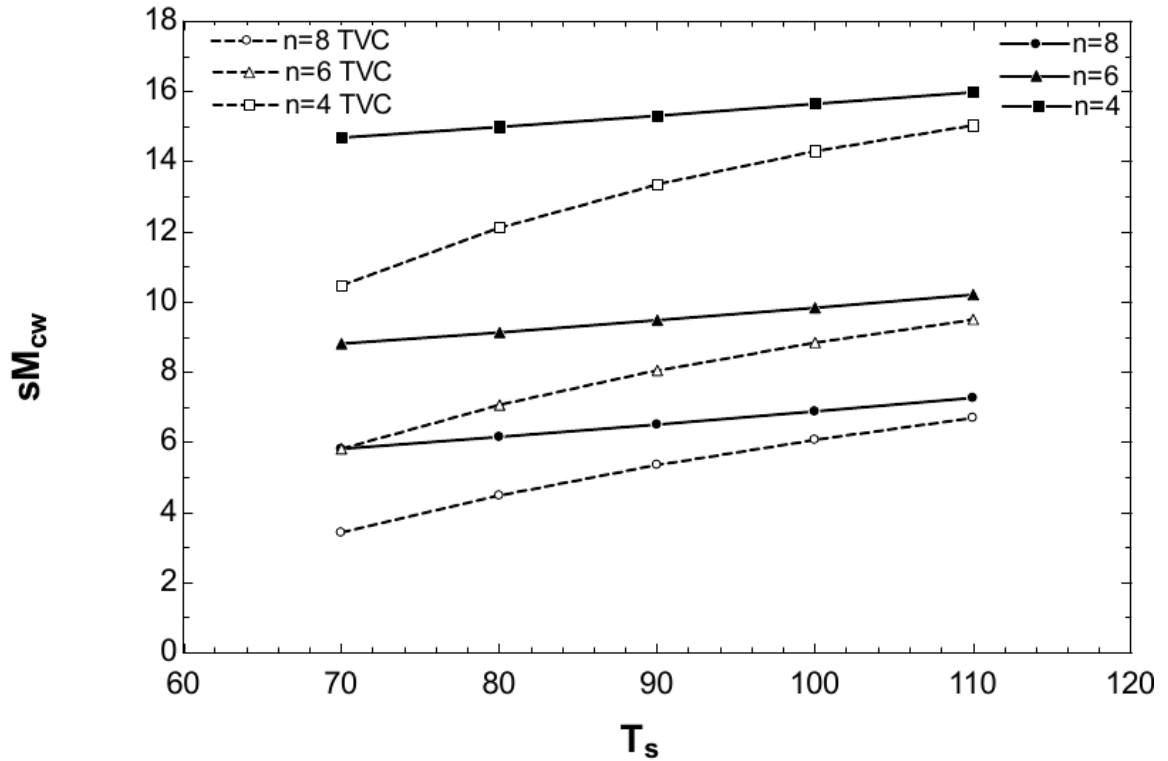


Figure 5.7: Effect of steam temperature on specific cooling water flow rate

Figure 5.7 shows the effect of the heating steam temperature on the specific cooling water flow rate. As the heating steam temperature increases, the specific cooling water flow rate increases as a result of increasing the thermal load in the last effect and decreasing of the performance ratio. In the case of thermal vapor compression, there is a dramatic reduction in the specific cooling water flow rate due to reduction in the heat load of the condenser as a result of the entrained vapor to the ejector.

## 5.6. Multi Effect Evaporation Parallel Cross Thermal Vapor

### Compression different Ejector Positions Model

The model is carried out for MEE/PF/TVC system with 6 effects and the thermal ejector is located after effect number 5. As the position of the ejector is changed the energy balance for the evaporators will change. The energy balance equations are presented blow.

The total distillate produced in the plant

$$\dot{m}_d = \sum_{i=1}^n D_i + \sum_{i=1}^n df_i + \sum_{i=1}^n de_i \quad (5.32)$$

The energy balance of the effects before the entrained vapor effect

$$\begin{aligned} D_{i-1} * Lv_{i-1} + df_{i-1} * Lv_{f_{i-1}} + de_{i-1} * Lve_{i-1} \\ = D_i * Lv_i + F_i * c_p * (T_i - T_f) \end{aligned} \quad (5.33)$$

The energy balance of the effect after the entrained vapor effect

$$\begin{aligned} (D_{i-1} - \dot{m}_{ev}) * Lv_{i-1} + df_{i-1} * Lv_{f_{i-1}} + de_{i-1} * Lve_{i-1} \\ = D_i * Lv_i + F_i * c_p * (T_i - T_f) \end{aligned} \quad (5.34)$$

In this example, the energy balance of the last effect, effect number 4

$$\begin{aligned} (D_3 - \dot{m}_{ev}) * Lv_3 + df_3 * Lv_{f_3} + de_3 * Lve_3 \\ = D_4 * Lv_4 + F_i * c_p * (T_4 - T_f) \end{aligned} \quad (5.35)$$

The heat transfer surface area of the first effect

$$A_1 = \frac{D_1 * Lv_1 + \dot{m}_f * c_p * (T_1 - T_f)}{U_{e1} * (T_s - T_1)} \quad (5.36)$$

The heat transfer surface area of the first effect, for i from 2 to n

$$A_i = \frac{D_i * Lv_i + \dot{m}_f * c_p * (T_i - T_f)}{U_{ei} * (\Delta T_i - \Delta T_{loss})} \quad (5.37)$$

It is important to calculate the steam flow rate in order to determine the system performance ratio

$$\dot{m}_s * L_s = F_1 * c_p * (T_1 - T_f) + D_1 * Lv_1 \quad (5.38)$$

## 5.7. Multi Effect Evaporation Parallel Cross Feed Thermal Vapor

### Compression different Ejector Positions Model interpretation

In this section the effect of placing the ejector in different places is investigated.

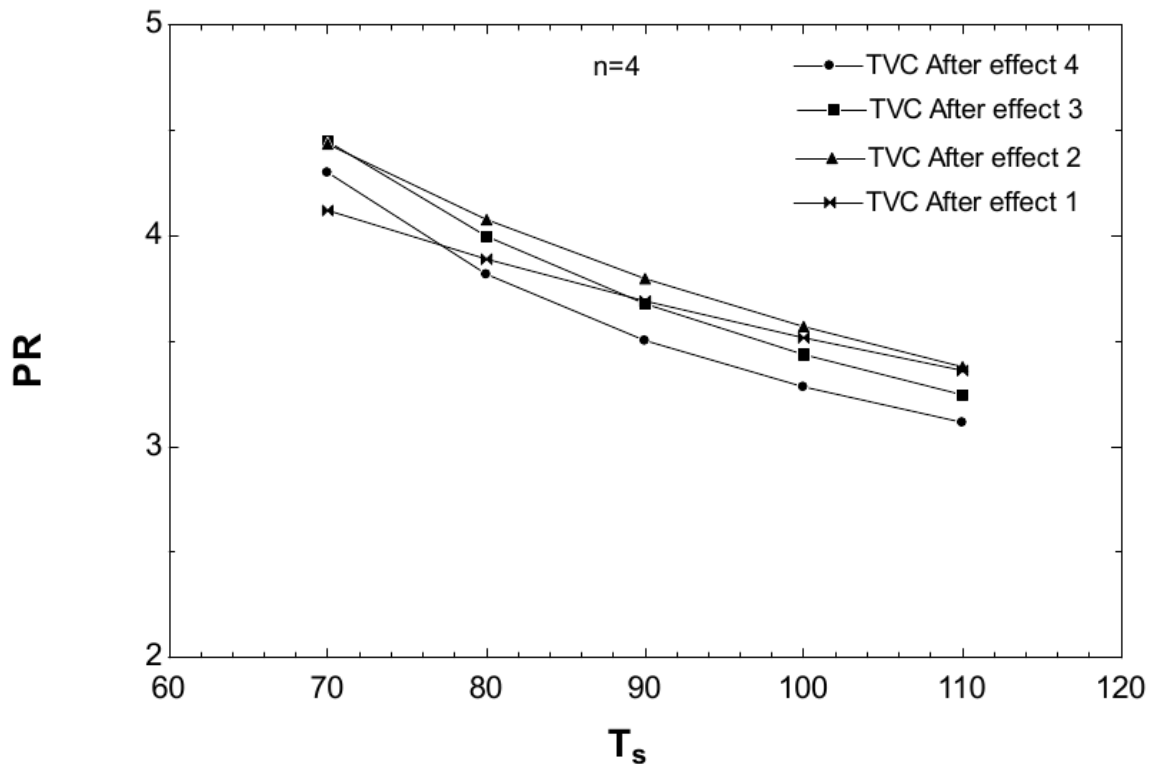


Figure 5.8: Effect of steam temperature on Performance ratio 4 effects

Figure 5.8 shows the effect of the heating steam temperature on the performance ratio for 4 effects different ejector positions for parallel cross multi effect desalination system. The results show that the best position of the ejector for wide range of heating steam temperature that results in the best performance ratio is after the effect that located in the middle, the effect of changing the ejector position is also studied for 6 and 8 effects, the results show the same trend as it is shown in the figures below.

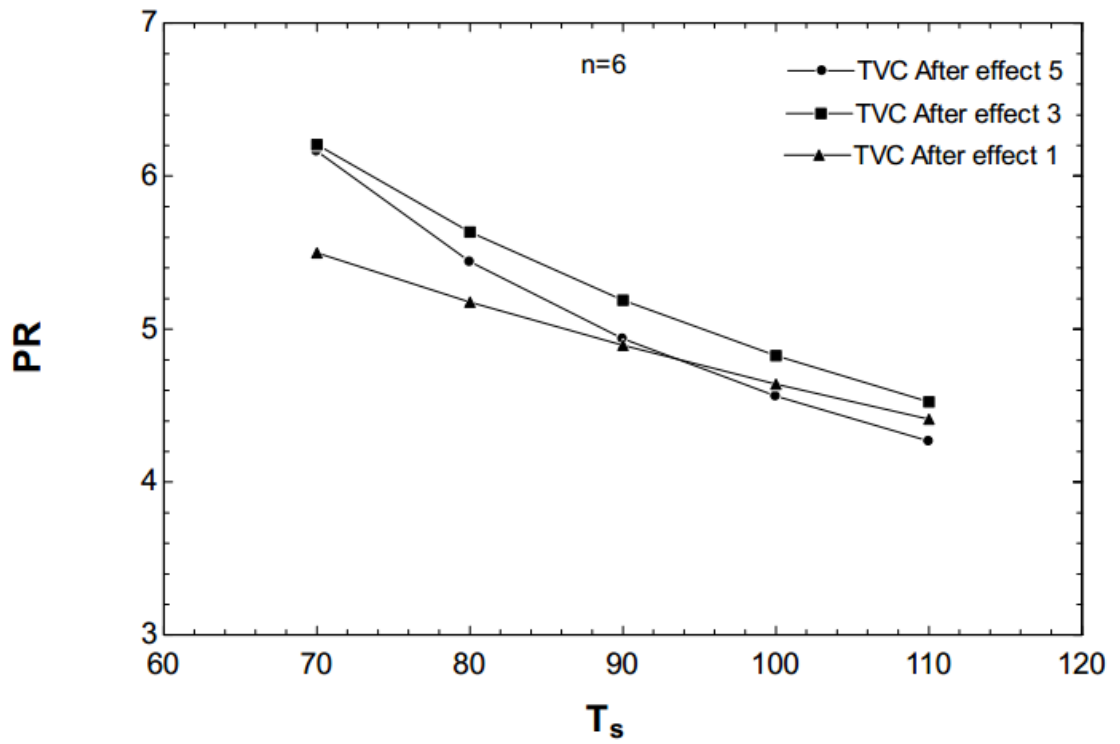


Figure 5.9: Effect of steam temperature on Performance ratio 6 effects

Figure 5.9 shows the effect of the heating steam temperature on the performance ratio for 6 effects different ejector positions for parallel cross multi effect desalination system.

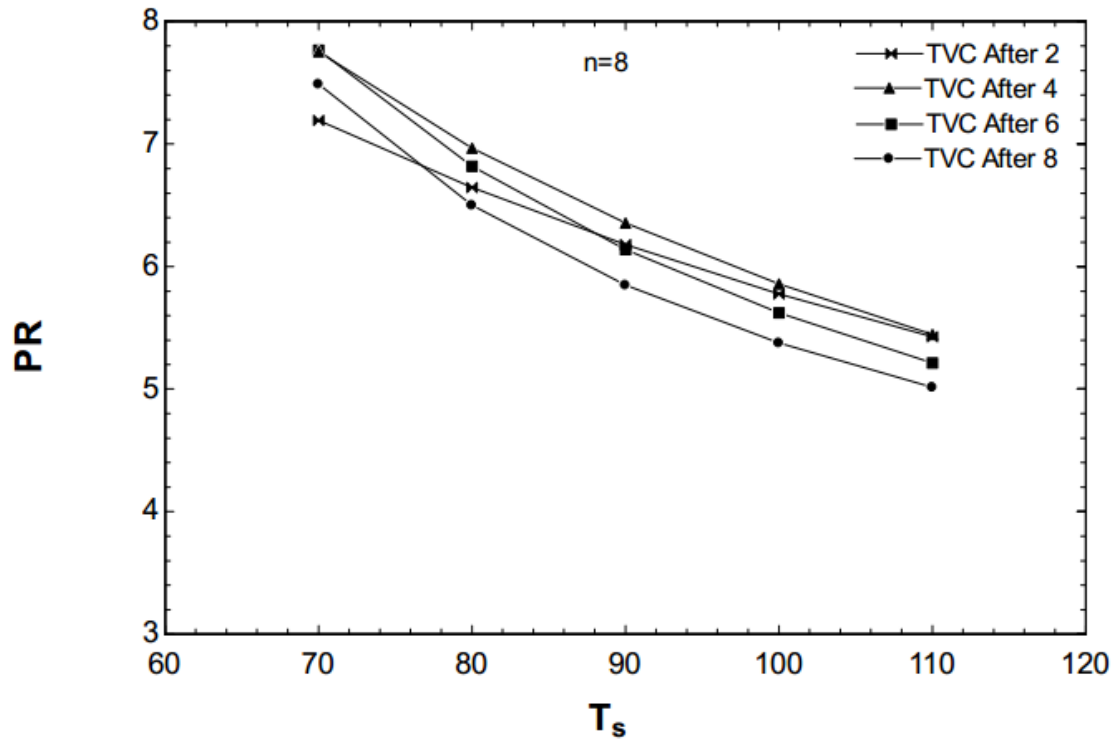


Figure 5.10: Effect of steam temperature on Performance ratio 8 effects

Figure 5.10 shows the effect of the heating steam temperature on the performance ratio for 8 effects different ejector positions for parallel cross multi effect desalination system.

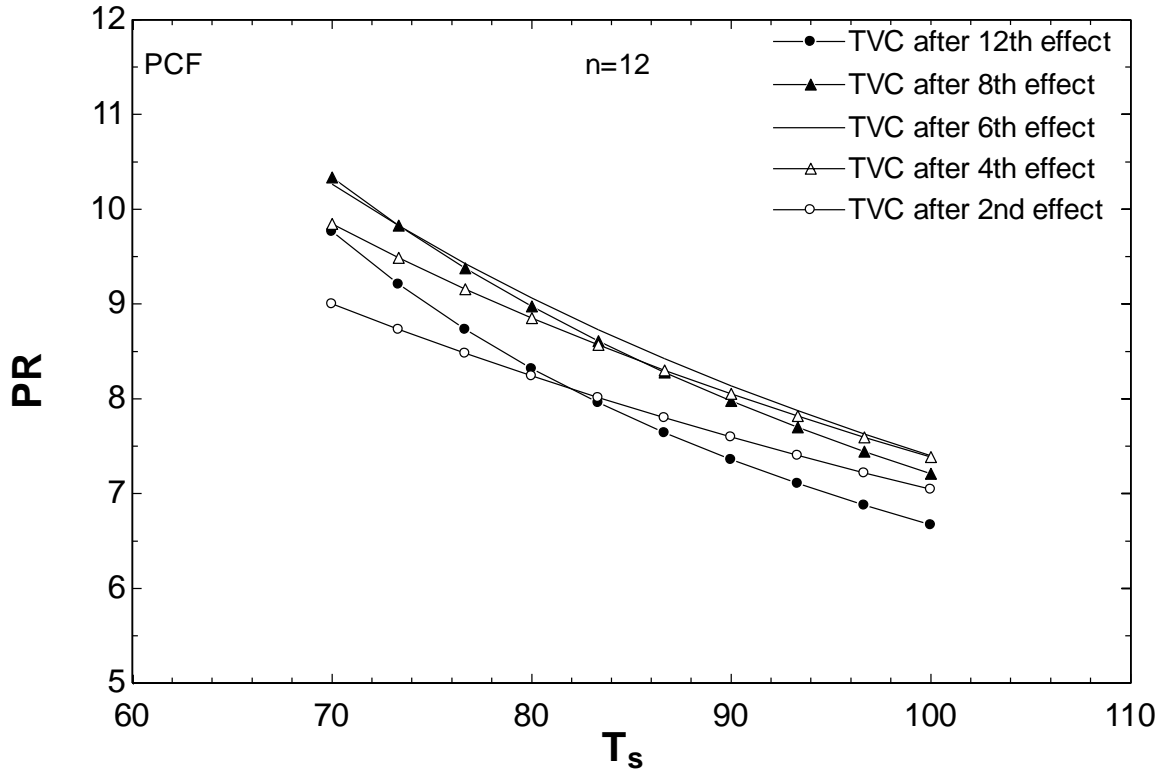
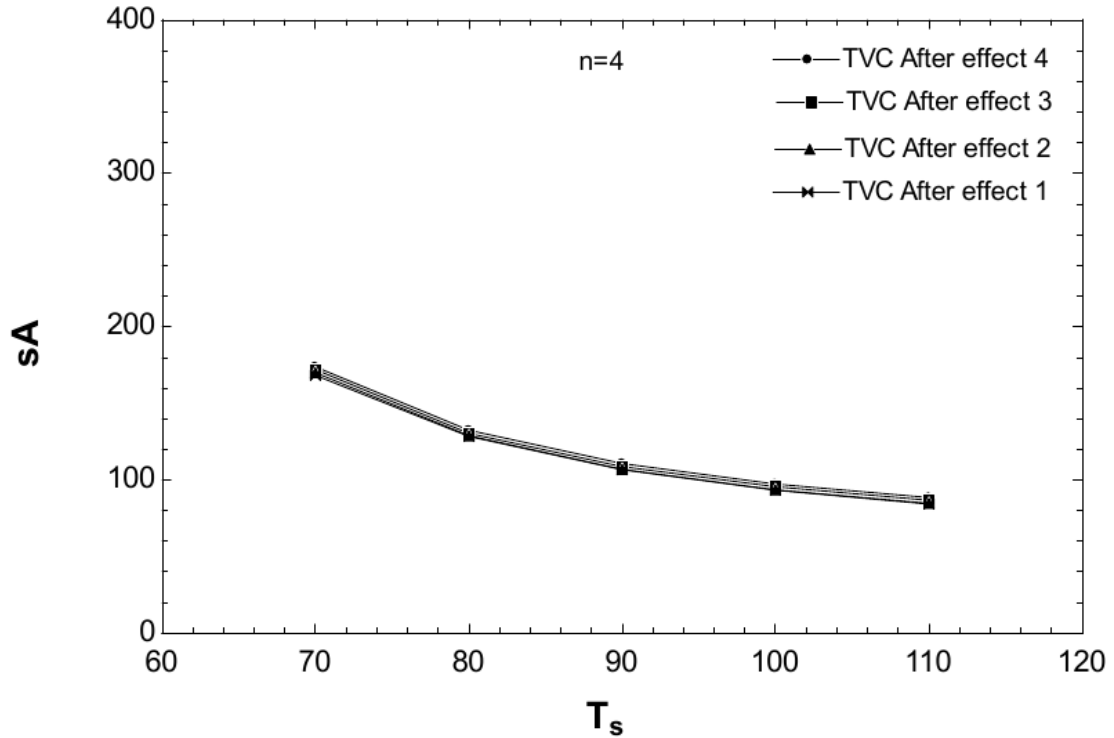


Figure 5.11: Effect of steam temperature on Performance ratio 12 effects

Figure 5.11 shows the effect of the heating steam temperature on the performance ratio for 12 effects different ejector positions for parallel cross multi effect desalination system.



**Figure 5.12: Effect of steam temperature on specific heat transfer surface area 4 effects**

Figure 5.12 shows the effect of heating steam temperature on the specific heat transfer surface area for 4 effects. The specific heat transfer surface area decreases as the temperature of heating steam increases and that because the temperature difference between the effects increasing as the heating steam temperature increases leading to a decrease in the specific heat transfer surface area, changing the thermal vapor compression position does not affect the specific heat transfer surface area in parallel cross multi effect desalination system, because changing ejector position reduces area of the effects after the ejector and increases the area of the effects before the ejector which in turn balance each other's so that the total area remains constant. The effect of changing the ejector position is also studied for 6 and 8 effects, the results show the same trend as it is shown in the figures below.

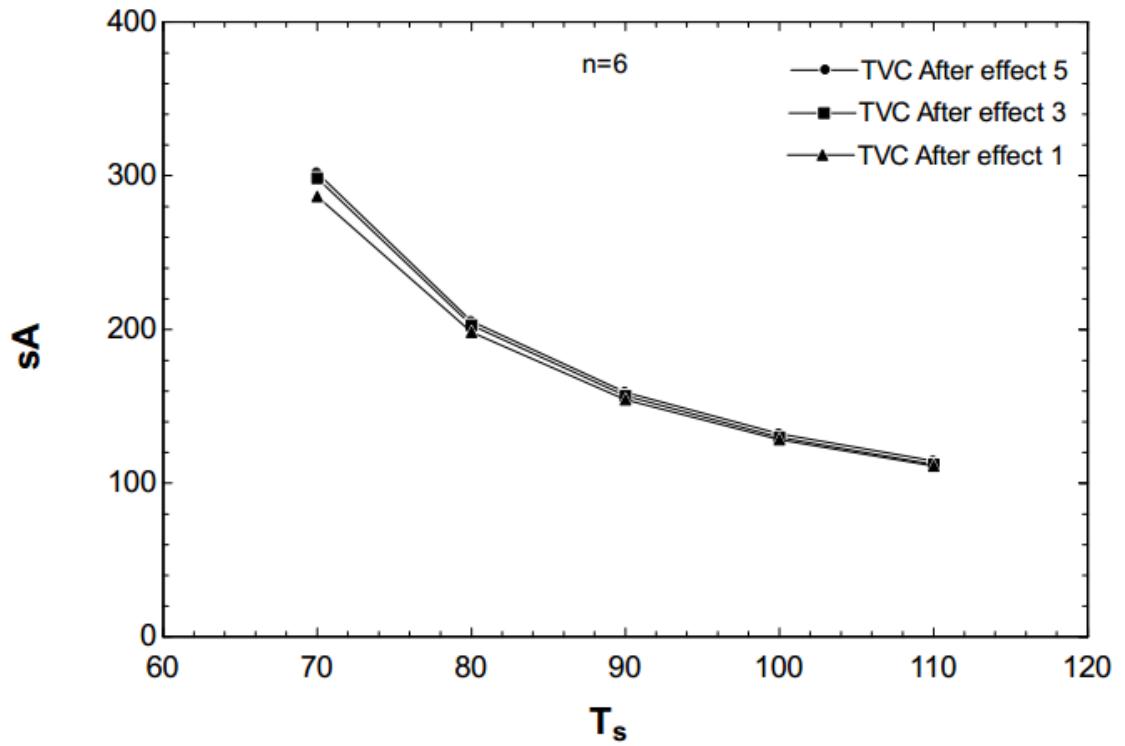


Figure 5.13: Effect of steam temperature on specific heat transfer surface area 6 effects

Figure 5.13 shows the effect of heating steam temperature on the specific heat transfer surface area for 6 effects different ejector positions parallel cross multi effect desalination system.

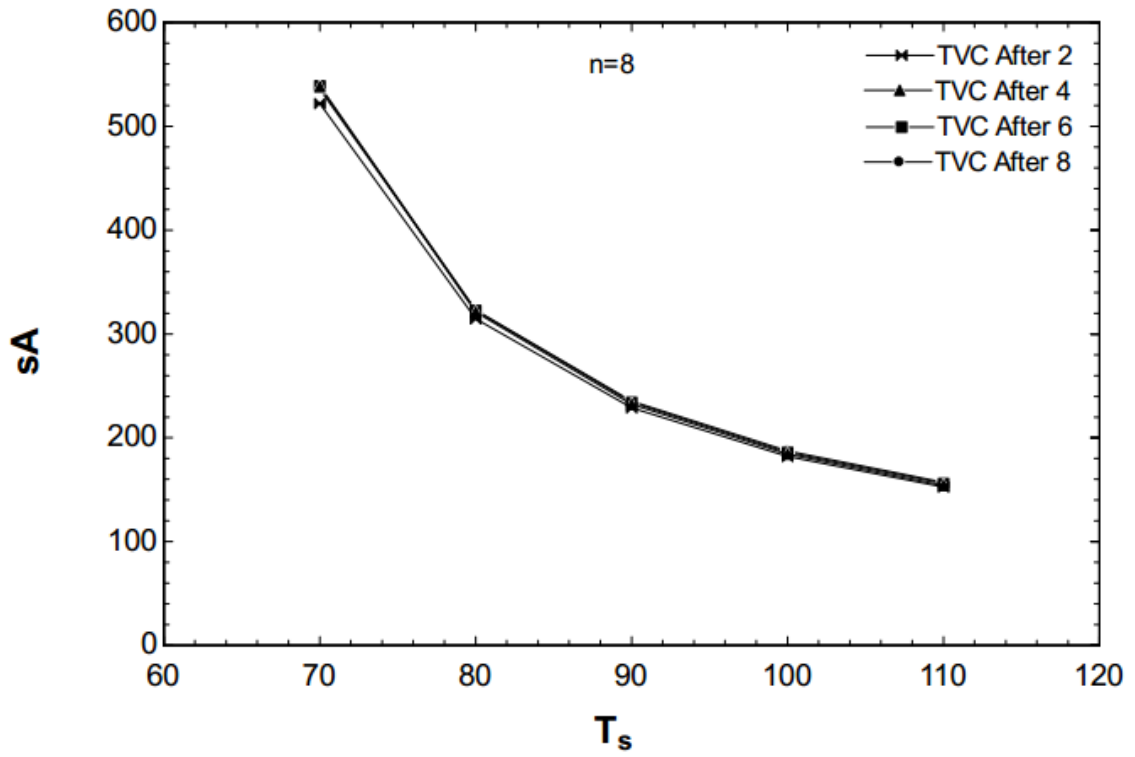
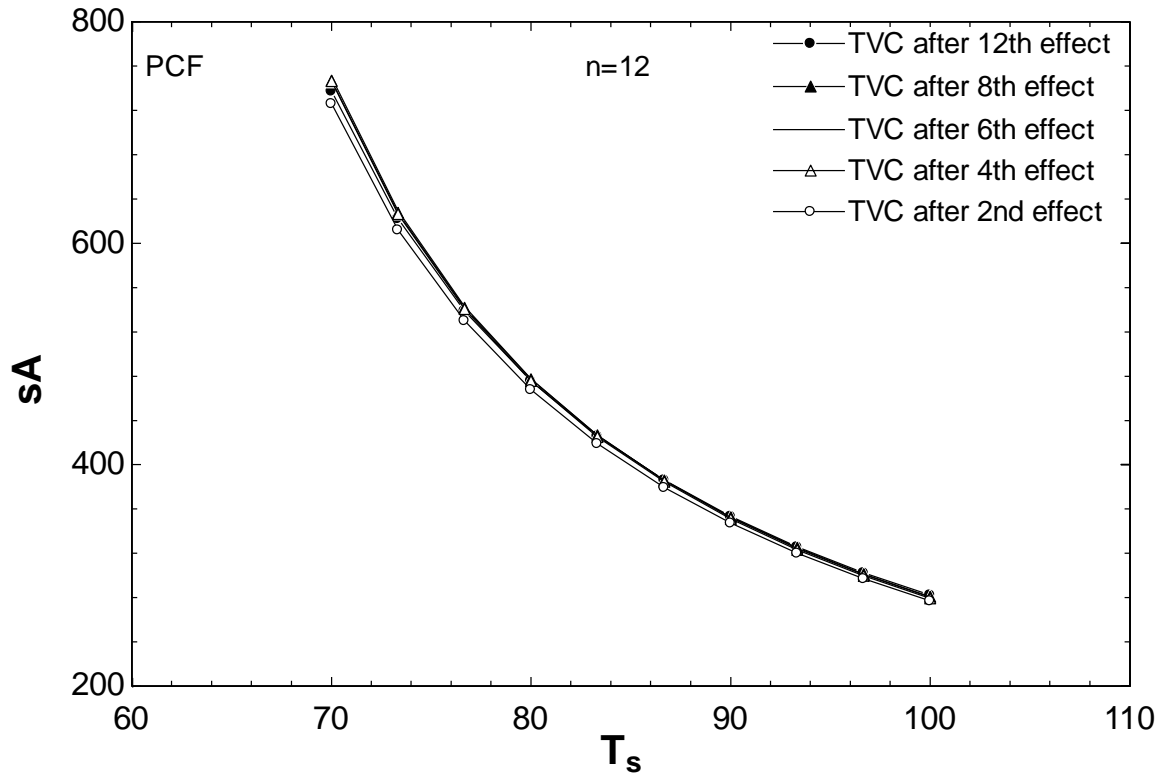


Figure 5.14: Effect of steam temperature on specific heat transfer surface area 8 effects

Figure 5.14 shows the effect of heating steam temperature on the specific heat transfer surface area for 8 effects different ejector positions parallel cross multi effect desalination system.



**Figure 5.15: Effect of steam temperature on specific heat transfer surface area 12 effects**

Figure 5.15 shows the effect of heating steam temperature on the specific heat transfer surface area for 12 effects different ejector positions parallel cross multi effect desalination system.

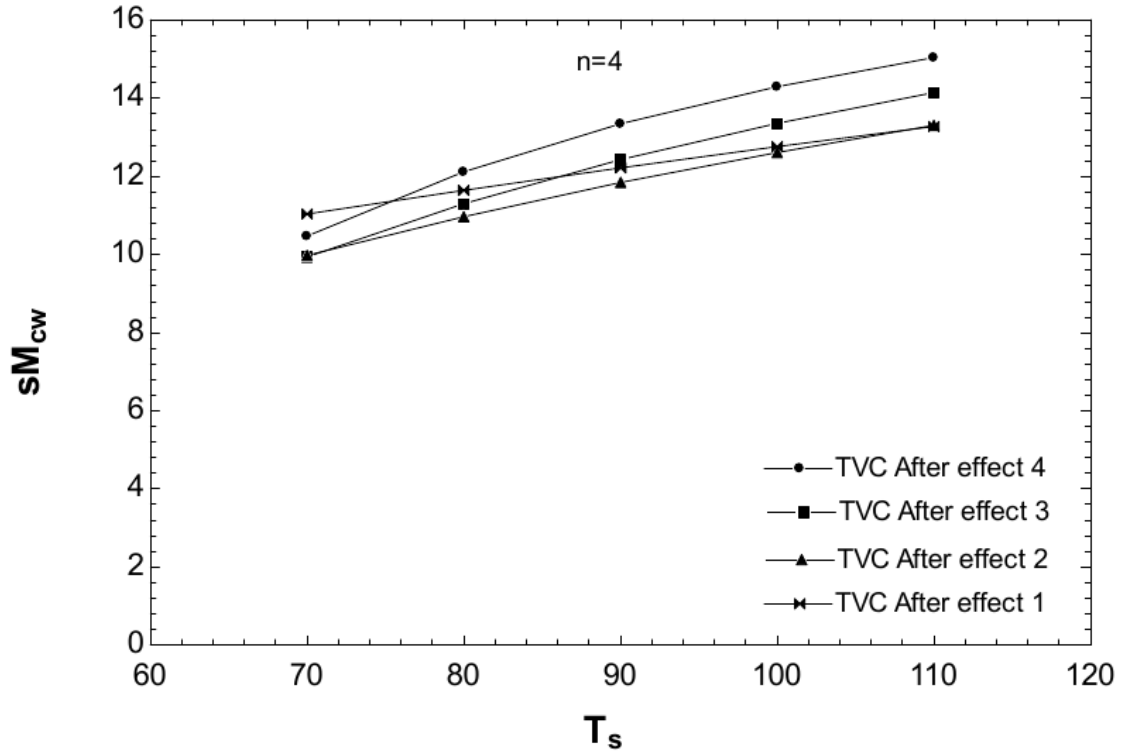


Figure 5.16: Effect of steam temperature on specific cooling water flow rate 4 effects

Figure 5.16 illustrates the effect of the heating steam temperature on the specific cooling water flow rate for 4 effects at different positions of the ejector. As the heating steam temperature increasing the cooling water flow rate increases. It happens by adding the thermal vapor ejector in which the heat load increases by increasing the heating steam temperature, which leads to an increase in specific cooling water flow rate. However, the lower consumption of the specific cooling water flow rate occurs when the thermal vapor compression ejector is located at the middle of the plant. The effect of changing the ejector position is also studied for 6 and 8 effects, the results show the same trend as it is shown in the figures below.

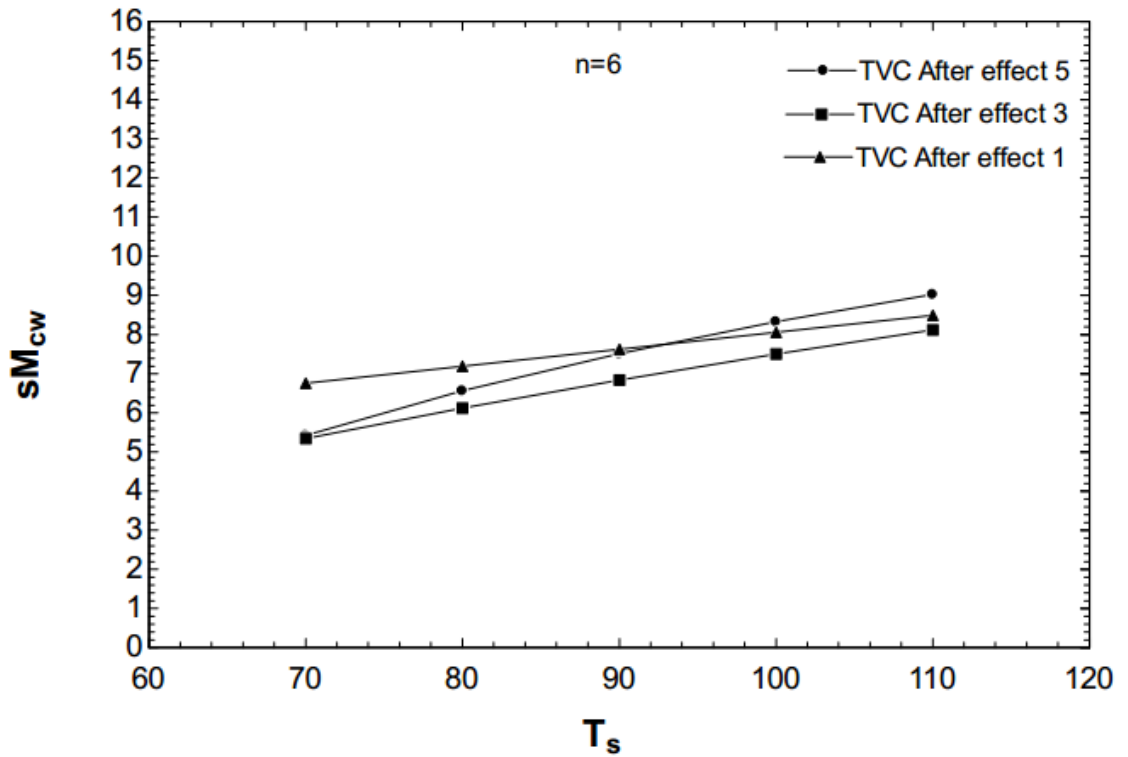


Figure 5.17: Effect of steam temperature on specific cooling water flow rate 6 effects

Figure 5.17 illustrates the effect of the heating steam temperature on the specific cooling water flow rate for 6 effects at different ejector positions parallel cross multi effect desalination system.

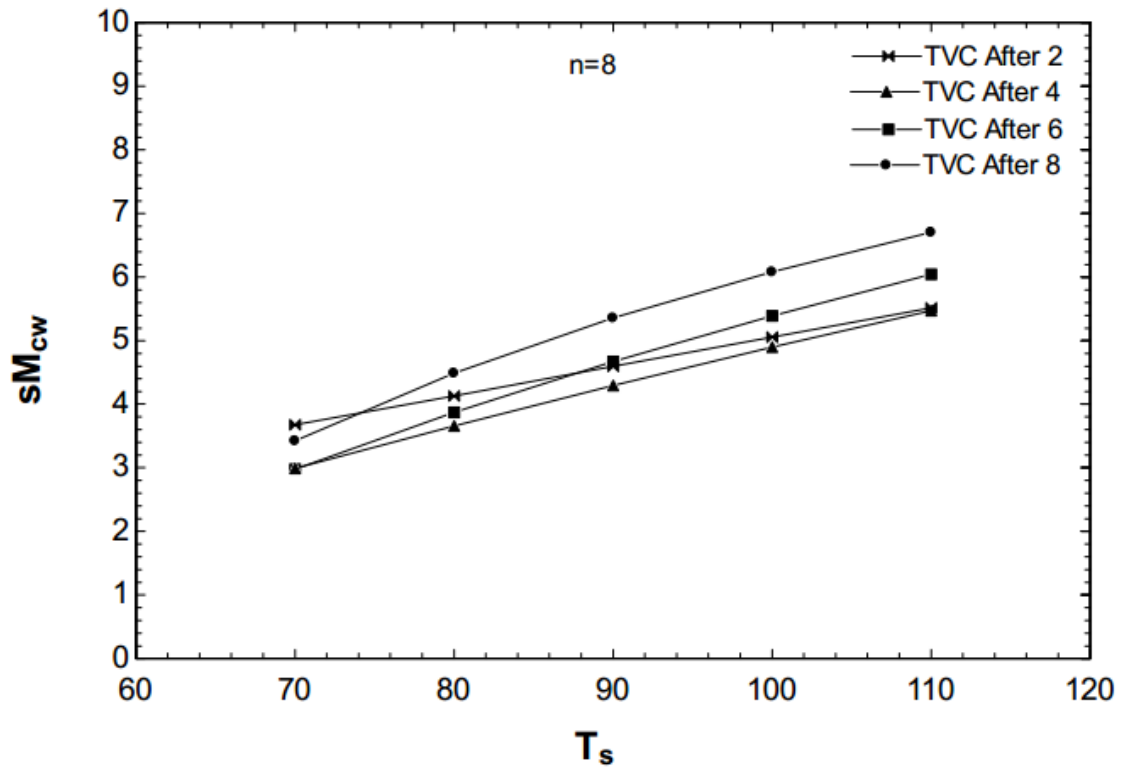


Figure 5.18: Effect of steam temperature on specific cooling water flow rate 8 effects

Figure 5.18 illustrates the effect of the heating steam temperature on the specific cooling water flow rate for 8 effects at different ejector positions parallel cross multi effect desalination system.

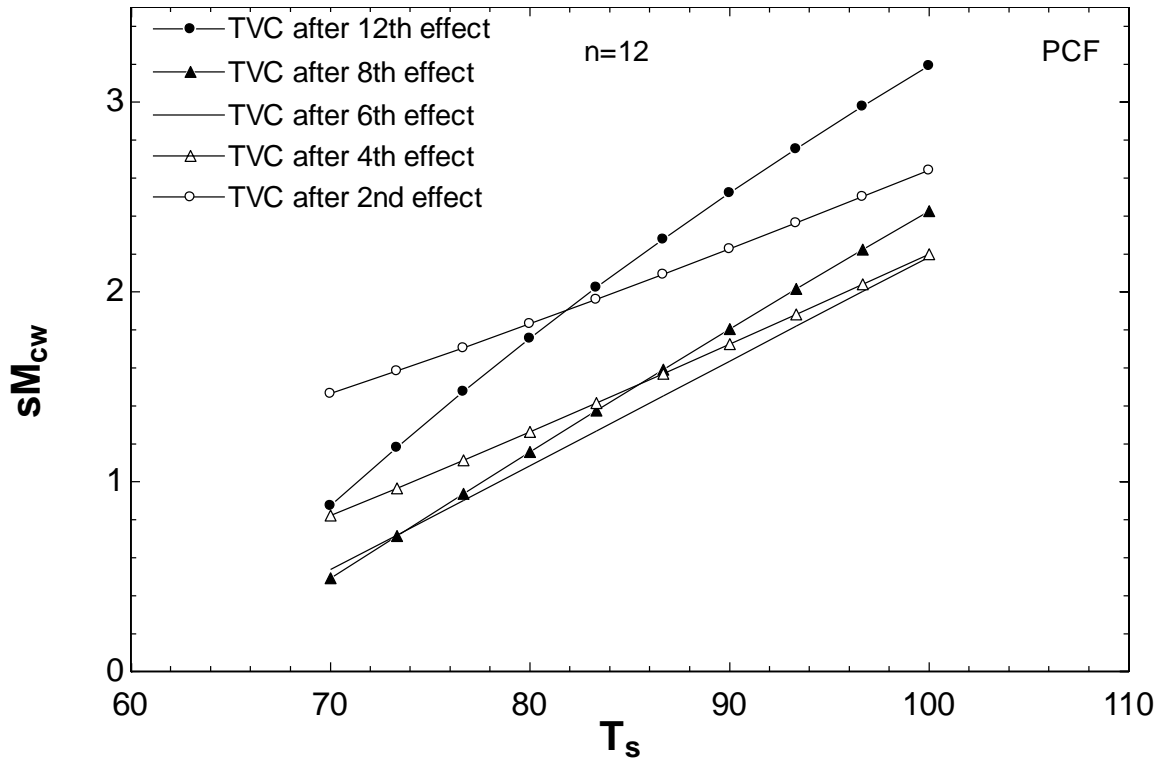


Figure 5.19 Effect of steam temperature on specific cooling water flow rate 12 effects

Figure 5.19 illustrates the effect of the heating steam temperature on the specific cooling water flow rate for 12 effects at different ejector positions parallel cross multi effect desalination system.

## 5.8. Exergy Analysis

The exergy of fluid stream is

$$X = \dot{m} (h - h_o - T_o(s - s_o)) \quad (5.39)$$

### 5.8.1. Exergy Analysis Calculations

First Effect

For the hot stream

$$EX_{sin1} = \dot{m}_s * ((hs_{in1} - hs_o) - (T_o) * (ss_{in1} - ss_o)) \quad (5.40)$$

$$EX_{sout1} = \dot{m}_s * ((hs_{out1} - hs_o) - (T_o) * (ss_{out1} - ss_o)) \quad (5.41)$$

$$\Delta EX_{hot1} = EX_{sin1} - EX_{sout1} \quad (5.42)$$

$T_o$  is the ambient temperature in *kelvin*

For the cold stream

(a) Feed Stream

$$EX_{fin1} = F_1 * ((hf_{in1} - hf_o) - (T_o) * (sf_{in1} - sf_o)) \quad (5.43)$$

(b) Brine Stream

$$EX_{bout1} = B_1 * ((hb_{out1} - hf_o) - (T_o) * (sb_{out1} - sf_o)) \quad (5.44)$$

(c) Vapor Stream

$$EX_{vout1} = D_1 * ((hv_{out1} - hs_o) - (T_o) * (sv_{out1} - ss_o)) \quad (5.45)$$

Therefore;

$$\Delta EX_{cold1} = EX_{vout1} + EX_{bout1} - EX_{fin} \quad (5.46)$$

$$\Delta EX_1 = \Delta EX_{hot1} - \Delta EX_{cold1} \quad (5.47)$$

The exergetic efficiency is given by:

$$\eta_{EX1} = \frac{\Delta EX_{cold1}}{\Delta EX_{hot1}} \quad (5.48)$$

Other Effects from i=2,n

For the hot stream (formed vapor inside the previous effect)

$$EX_{sin1} = (D_{[i-1]} + df_{[i-1]}) * ((hs_{ini} - hs_o) - (T_o) * (ss_{ini} - ss_o)) \quad (5.49)$$

$$EX_{sout1} = (D_{[i-1]} + df_{[i-1]}) * ((hs_{outi} - hs_o) - (T_o) * (ss_{outi} - ss_o)) \quad (5.50)$$

$$\Delta EX_{hot1} = EX_{sin1} - EX_{sout1} \quad (5.51)$$

For cold stream (sea water stream)

$$EX_{fin[i]} = F_i * ((hf_{in[i]} - hf_o) - (T_o) * (sf_{in[i]} - sf_o)) \quad (5.52)$$

This equation is only applied for parallel cross multi effect desalination system

$$EX_{\{b\ in\}[i]} = EX_{\{b\ out\}[i-1]} \quad (5.53)$$

$$EX_{\{b\ in\}[i]} = B_{\{i-1\}} * ((hb_{\{out\}[i-1]} - hf_o) - (T_o) * (sb_{\{out\}[i-1]} - sf_o)) \quad (5.54)$$

$$EX_{bout[i]} = B_i * ((hb_{out[i]} - hf_o) - (T_o) * (sb_{out[i]} - sf_o)) \quad (5.55)$$

$$EX_{vout[i]} = D_i * ((hv_{out[i]} - hf_o) - (T_o) * (sv_{out[i]} - sf_o)) \quad (5.56)$$

$$\Delta EX_{cold[i]} = EX_{vout[i]} + EX_{bout[i]} - EX_{fin[i]} - EX_{bin[i]} \quad (5.57)$$

$$\Delta EX_{[i]} = \Delta EX_{hot[i]} - \Delta EX_{cold[i]} \quad (5.58)$$

$$\eta_{EX[i]} = \frac{\Delta EX_{cold[i]}}{\Delta EX_{hot[i]}} \quad (5.59)$$

**Table 5.1: Exergy analysis for PCF/TVC system when the ejector is located after effect 4**

Exergy Analysis Calculations PCF/TVC after	Last Effect
Blow down Exergy (kw)	7.029
Distillate Exergy (kw)	3.606
Inlet Motive steam Exergy (kw)	121.6
Outlet Motive Exergy (kw)	1.582
Inlet Feed \& Cooling Sea water Exergy (kw)	0
Total Exegetic Efficiency (%)	3.003
Compression Ratio CR (-)	3.006
Entrainment Ratio Ra (-)	2.199
Performance Ratio PR (-)	5.094
Cooling Water Flow Rate (kg/s)	8.262
Entrained Vapor Flow Rate (kg/s)	0.08926
Motive Steam Flow Rate (kg/s)	0.1963
Steam Flow Rate (kg/s)	0.2856
Condenser Exergetic Efficiency (%)	39.66
Ejector Exergetic Efficiency (%)	56.05
First Effect Exergetic Efficiency (%)	82.81
Second Effect Exergetic Efficiency (%)	83.91
Third Effect Exergetic Efficiency (%)	79.62
Fourth Effect Exergetic Efficiency (%)	72.46

Table 5.1 shows the exergy analysis for PCF/TVC system when the ejector is located after effect 4. The results show that the exergy destruction is the highest in the condenser followed by the ejector. However, the total plant second law efficiency is equal to 3.003%.

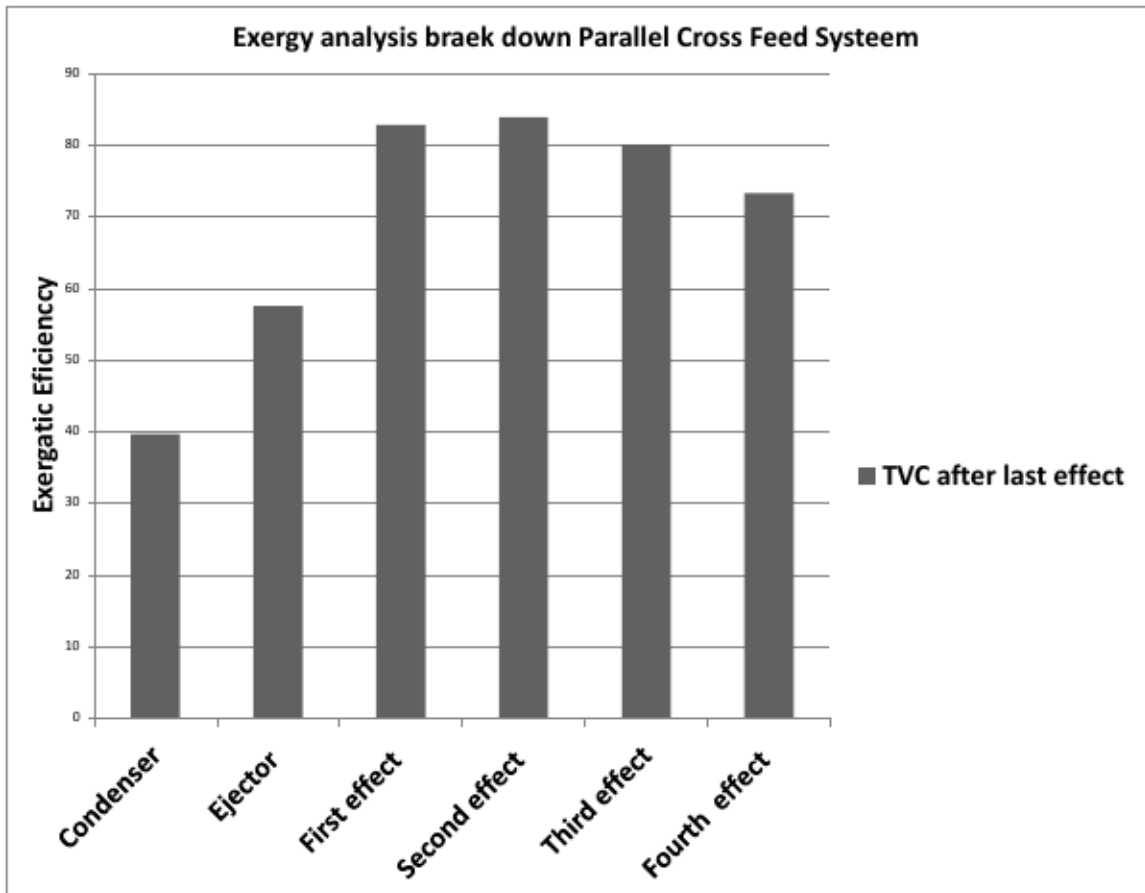


Figure 5.20: Exergy analysis for PCF/TVC system 4 effects

Figure 5.20 shows the exergy analysis for PCF/TVC system when the ejector is located after effect 4. The results show that the exergy destruction is the highest in the condenser followed by the ejector. However, increases the number of effects increases the second law efficiency due to better use of energy. The same trend is applied for 6,8,10 and 12 effects as shown in following figures.

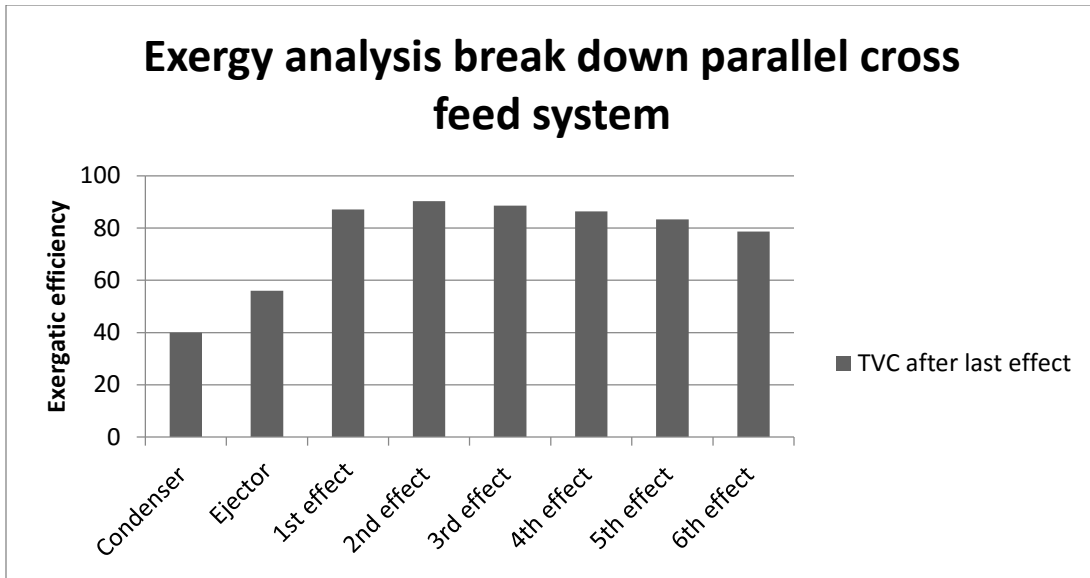


Figure 5.21: Exergy analysis for PCF/TVC system 6 effects

Figure 5.21 shows the exergy analysis for parallel cross feed multi effect desalination system thermal vapor compression with 6 effects.

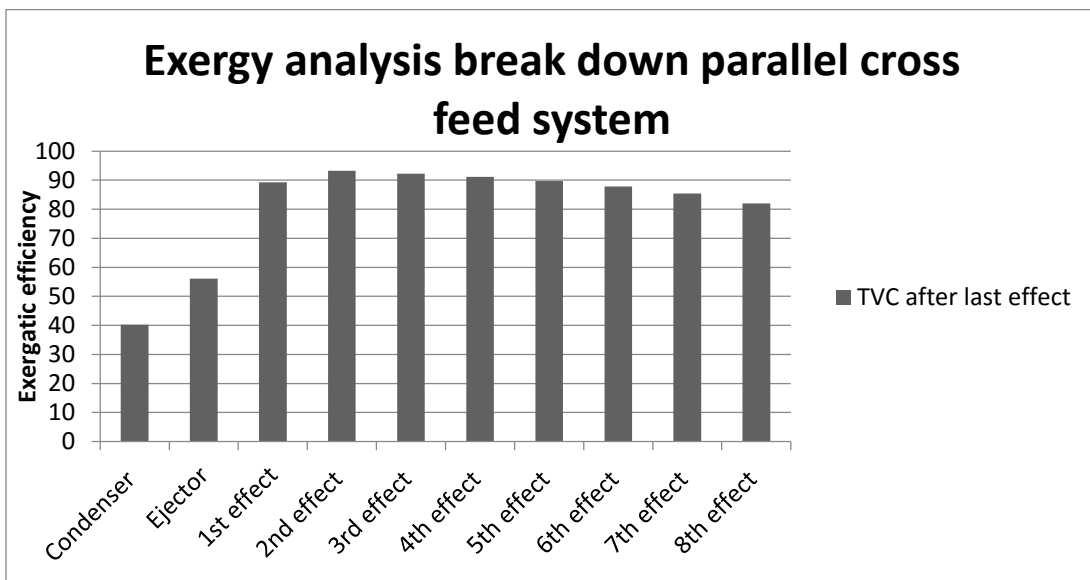


Figure 5.22: Exergy analysis for PCF/TVC system 8 effects

Figure 5.22 shows the exergy analysis for parallel cross feed multi effect desalination system thermal vapor compression with 8 effects.

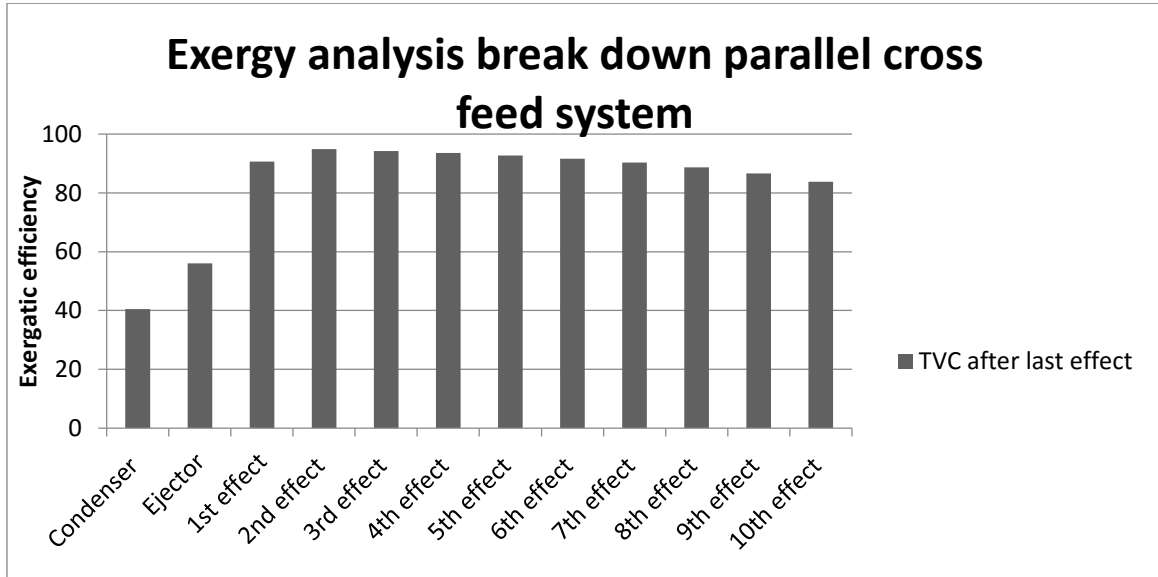


Figure 5.23: Exergy analysis for PCF/TVC system 10 effects

Figure 5.23 shows the exergy analysis for parallel cross feed multi effect desalination system thermal vapor compression with 10 effects.

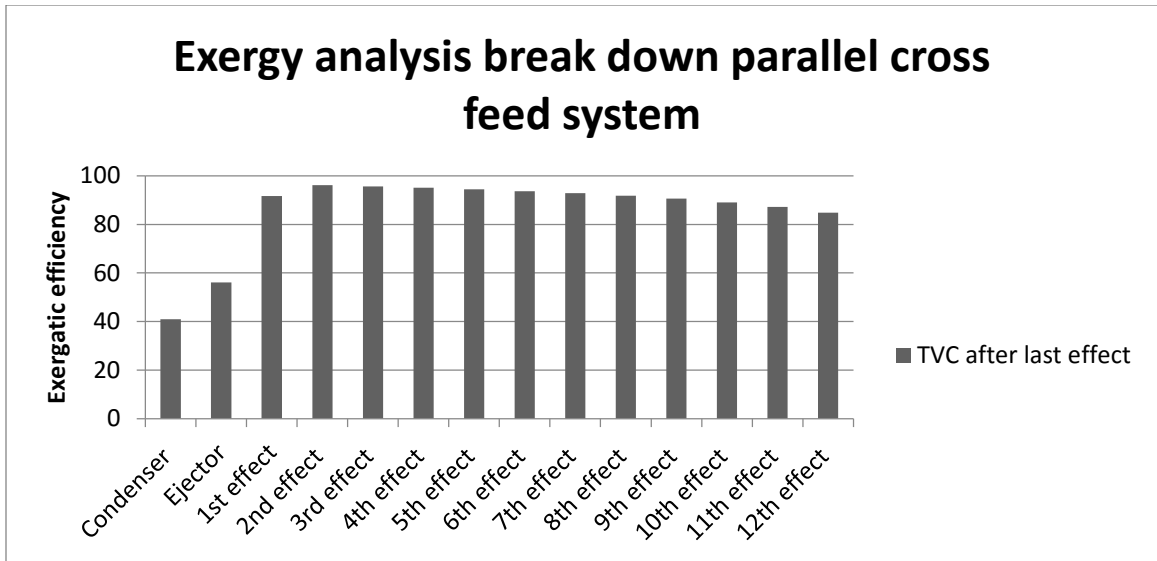


Figure 5.24: Exergy analysis for PCF/TVC system 12 effects

Figure 5.24 shows the exergy analysis for parallel cross feed multi effect desalination system thermal vapor compression with 12 effects.

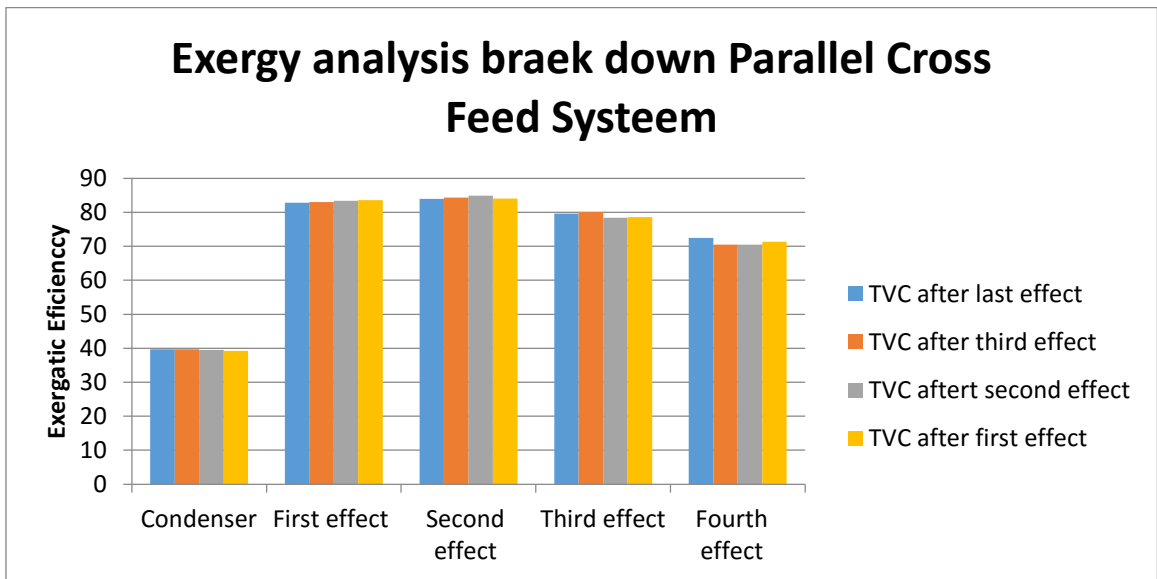


Figure 5.25: Exergy analysis breaks down for parallel cross feed system

Figure 5.25 shows the exergy analysis break down for parallel cross feed system, it can be clearly seen that the condenser exergatic efficiency does not changed with changing the ejector position and that because the temperature of the last effect is kept constant. However, the exergy destruction can be decreased by reducing the top brine temperature, increasing the number of stages, and increasing entrainment ratio of the thermo compressor.

## 5.9. Economic Analysis

The unit cost of the product depend on the arrangement of the MED-PCF plant, and if it is a stand alone or combined with power plant. In addition, the plant capacity and performance ratio affect the unit cost of product. In this study the plant is treated as a standalone.

The main factors that affect the unit cost of the product:

- Plant capital cost
  - Annual desalination plant depreciation.
- Annual operation and maintenance costs
  - Heat and power energy
  - Chemicals
  - Maintenance and spare parts
  - Labor cost

### 5.9.1. Unit cost of water calculations

- Annual capital cost

There are two ways to calculate the annual capital cost

1. Annual amortized capital

$$\begin{aligned} \text{Water annual amortized capital cost} \\ = (\text{Total capital cost } \$ * f) \end{aligned} \quad (5.60)$$

Where,

$f$  is the capital recovery ratio

$$f = \frac{i * (1 + i)^n}{(1 + i)^n - 1} \quad (5.61)$$

$i$  is the interest rate

$n$  is the plant life in years

2. Straight line depreciation cost

$$\text{Annual capital cost} = \frac{\text{Total capital cost}}{\text{The plant life}} \quad (5.62)$$

- **Capital unit cost**  $\left(\frac{\$}{m^3}\right)$

$$\begin{aligned} \text{capital unit cost} \left(\frac{\$}{m^3}\right) \\ = \frac{\text{Total capital cost}}{\text{Total annual water production (m}^3\text{)}} \end{aligned} \quad (5.63)$$

$$\begin{aligned} \text{Total annual water production (m}^3\text{)} \\ = \text{plant design capacity} * 365 * \text{load factor} \end{aligned} \quad (5.64)$$

- **Annual operating cost energy unit cost**  $\left(\frac{\$}{m^3}\right)$

- **Heat cost**  $\left(\frac{\$}{m^3}\right)$

$$\text{Boiler fuel requirements} = \frac{2326}{PR * \text{boiler efficiency}} \left(\frac{kJ}{kg}\right) \quad (5.65)$$

$$\begin{aligned} \text{Unit heat cost} \left(\frac{\$}{m^3}\right) \\ = \frac{\text{Boiler fuel requirements} \left(\frac{kJ}{kg}\right) * \text{Fuel cost} \left(\frac{\$}{GJ}\right)}{1000} \end{aligned} \quad (5.66)$$

- **Power unit cost**  $\left(\frac{\$}{m^3}\right)$

$$\begin{aligned}
 \text{Power unit cost } \left( \frac{\$}{m^3} \right) & \\
 &= \text{power consumption} \left( \frac{kWh}{m^3} \right) * \text{unit power cost} \left( \frac{\$}{kWh} \right) \quad (5.67)
 \end{aligned}$$

**Unit water production cost**  $\left( \frac{\$}{m^3} \right)$  is a summation of:

Unit capital cost  $\left( \frac{\$}{m^3} \right)$

Unit heat cost  $\left( \frac{\$}{m^3} \right)$

Unit power cost  $\left( \frac{\$}{m^3} \right)$

Unit operation & maintenance cost  $\left( \frac{\$}{m^3} \right)$

### **Case Study:**

The desalination plant is assumed to be a stand alone and the steam supplied to the system by boiler. The unit cost of the product depends on the arrangement of the MED plant. The following data is industrial data of saline water conversion corporation (SWCC) plant.

Evaluate of unit water production cost of a standalone (single purpose) MED plant

### **Operation Data:**

Total water production= 2 MIGD

Plant load factor = 95%

MED PR = 8, 9, 10, 11

MED power consumption =  $1.8 \frac{kWh}{m^3}$

Boiler Efficiency = 90%

### **Cost Factors**

Plant life = 25 years

Discount rate = 6%

MED plant capital cost =  $9 \frac{\$}{IGD}$

Where, IGD : imperial gallons per day

Fuel energy cost = 2.5, 4, 7, 9 ( $\frac{\$}{GJ}$ )

Power cost =  $0.05 \frac{\$}{kwh}$

Sea water intake and outlet cost = 11.7% of desalter capital cost

Foundation and building = 20% of desalter capital cost

Erection & commissioning = 15% of desalter capital cost

Spare cost = 15% of desalter capital cost

Engineering & contingency = 10% of desalter capital cost

$$\text{Chemicals cost} = 0.025 \left( \frac{\$}{m^3} \right)$$

$$\text{Operation \& maintenance cost} = 0.12 \left( \frac{\$}{m^3} \right)$$

Cost parametric analysis MED system using amortized capital approach

Changing the performance ratio for constant fuel energy cost of  $4 \frac{\$}{Gj}$

**Table 5.2: Cost Parametric analysis for MED PCF system for fuel energy cost of  $4 \frac{\$}{Gj}$**

<i>n</i>	25	Seawater cost (%)	0.117	Plant load factor	0.95
Discount rate	0.06	Foundation & building (%)	0.2	MED PR (-)	8
MED Capital cost (\$/IGD)	9	Erection & commission (%)	0.15	MED power consumption( $kw/m^3$ )	1.8
Fuel energy cost (\$/Gj)	4	Spare cost (%)	0.15	Boiler Efficiency	0.9
Power cost (\$/kwh)	0.05	Total water production(IGD)	2000000	Capital recovery factor (-)	0.0728
Fuel energy cost (\$/Gj)	4				
PR	8	9	10	11	
Unit capital cost ( $\$/m^3$ )	0.722	0.7222	0.7222	0.7222	
Heat unit cost ( $\$/m^3$ )	1.2922	1.1486	1.0338	0.9398	
Power unit cost ( $\$/m^3$ )	0.09	0.09	0.09	0.09	
Chemicals cost ( $\$/m^3$ )	0.025	0.025	0.025	0.025	
O & M cost ( $\$/m^3$ )	0.12	0.12	0.12	0.12	
Unit product cost ( $\$/m^3$ )	2.2494	2.1058	1.991	1.897	

Table 5.2 shows cost analysis for different performance ratios, as the performance ratio increases the unit product cost decreases as a result of heat unit cost decreases.

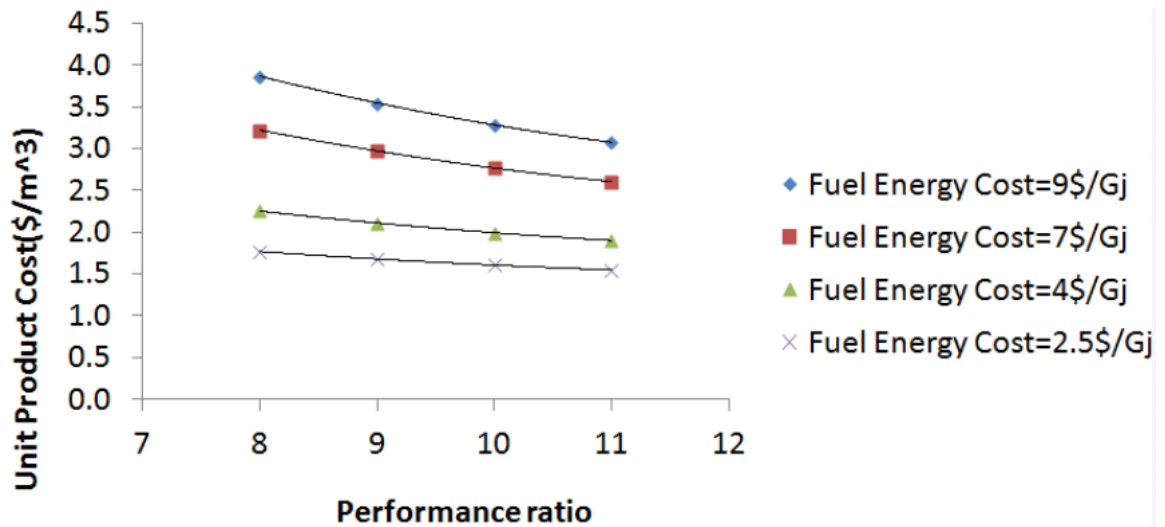


Figure 5.26: Cost Parametric analysis for MED system for different fuel energy costs

Figure 5.26 shows parametric study for different values of fuel energy costs. The results show that increasing fuel energy cost increase the unit product cost. However for standalone MED plant increasing the performance ratio from 8 to 11 reduces the unit cost of the product from 2.25 to 1.9 ( $\$/m^3$ ) for fuel energy cost of 4( $\$/GJ$ ).

# Conclusions

This chapter presents the conclusions of the results of this work.

## 6.1. Conclusion

As a result of this work the following points can be made

- A mathematical model based on mass and energy balances have been developed and validated with models available in the literature for three types of Multi Effect Desalination systems: Forward Feed, Parallel Feed and Parallel Cross Feed type of systems, thermal vapor compression has been added to the system and different positions of the ejector have been studied. In addition, exergetic and economic analysis have been performed.
- Increasing the number of effects increases the second law efficiency due to better use of energy.
- Performance of Multi Effect Evaporation systems have been evaluated by evaluating the performance ratio, specific heat transfer surface area and specific cooling water flow rate as a function of steam and top brine temperatures.
- More effects lead to better performance ratio and higher specific heat transfer surface area however, increasing the number of effects has a limitation due to the total temperature difference between evaporators.
- MED system has an advantage of utilizing steam with low temperature. Therefore, low grade energy can be used, for example waste heat or steam from power plant. Thermal vapor compression increases the performance ratio of the system by 30% and reduces the specific cooling water flow rate by 34% for a

system with 4 effects. While changing the position of the ejector affects the Performance ratio and the specific cooling water flow rate.

- However, for wide range of specific heating steam temperature the best Performance Ratio occurs when the ejector is situated in the middle.
- For a four effect thermal vapor compression system, the highest second law efficiency and performance ratio is gained in the middle. However, the exergy destruction can be decreased by reducing the top brine temperature, increasing the number of stages, and increasing entrainment ratio of the thermo compressor.
- For a four effect forward feed thermal vapor compression system, the performance ratio, specific heat transfer surface area and specific cooling water flow rate are 5.275,  $357.2(m^2/(kg/s))$  and 6.794 respectively, while in the case of four effect forward feed system, the performance ratio, specific heat transfer surface area and specific cooling water flow rate 3.626,  $363.9(m^2/(kg/s))$  and 11.74 respectively.
- The performance ratio, specific heat transfer surface area and the specific cooling water flow rate for four effect parallel feed with thermal vapor compression system are 4.1,  $174.1(m^2/(kg/s))$  and 8.05 respectively while, the performance ratio, specific heat transfer surface area and the specific cooling water flow rate for four effect parallel cross feed with thermal vapor compression system are 4.2,  $168.1(m^2/(kg/s))$  and 11.03. Similar observations apply to plants with six, 8, 10 and 12 effects.

## References

- [1] H. T. El-Dessouky and H. M. Ettouney, *Fundamentals of Salt Water Desalination*. Amsterdam, The Netherlands: *ELSEVIER SCIENCE B.V.*, 2002.
- [2] H. T. El-Dessouky, H. M. Ettouney, and Y. Al-Roumi, "Multi-stage flash desalination: present and future outlook," *Chem. Eng. J.*, vol. 73, no. 2, pp. 173–190, May 1999.
- [3] a. Ophir and F. Lokiec, "Advanced MED process for most economical sea water desalination," *Desalination*, vol. 182, no. 1–3, pp. 187–198, Nov. 2005.
- [4] Karan Mistry and J. Lienhard, "An Economics-Based Second Law Efficiency," *Entropy*, vol. 15, no. 7, pp. 2736–2765.
- [5] H. T. El-dessouky, H. M. Ettouney, and F. Mandani, "Performance of parallel feed multiple effect evaporation system for seawater desalination," vol. 20, pp. 1679–1706, 2000.
- [6] M. a. Darwish, F. Al-Juwayhel, and H. K. Abdulaheim, "Multi-effect boiling systems from an energy viewpoint," *Desalination*, vol. 194, no. 1–3, pp. 22–39, Jun. 2006.
- [7] M. a. Darwish and H. K. Abdulrahim, "Feed water arrangements in a multi-effect desalting system," *Desalination*, vol. 228, no. 1–3, pp. 30–54, Aug. 2008.
- [8] N. H. Aly and A. K. El-fiqi, "Thermal performance of seawater desalination systems," *ELSEVIER*, vol. 158, no. May, pp. 127–142, 2003.
- [9] F. Tahir, M. Atif, and M. A. Antar, Recent Progress in Desalination, Environmental and Marine Outfall Systems "The Effect of Fouling on Performance and Design Aspects of Multiple Systems" *Springer International Publishing Switzerland*, chapter 4, 2015.
- [10] K. H. Mistry, M. a. Antar, and J. H. Lienhard V, "An improved model for multiple effect distillation," *Desalin. Water Treat.*, vol. 51, no. 4–6, pp. 807–821, Jan. 2013.
- [11] M. Ameri, S. S. Mohammadi, M. Hosseini, and M. Seifi, "Effect of design parameters on multi-effect desalinationsystem specifications," *Desalination*, vol. 245, no. 1–3, pp. 266–283, Sep. 2009.
- [12] M. A. Darwish and H. El-Dessouky, "The heat recovery thermal vapour-compression desalting system: A comparison with other thermal desalination processes," *Appl. Therm. Eng.*, vol. 16, no. 6, pp. 523–537, Jun. 1996.

- [13] F. N. Alasfour, M. a. Darwish, and a. O. Bin Amer, "Thermal analysis of ME—TVC+MEE desalination systems," *Desalination*, vol. 174, no. 1, pp. 39–61, Apr. 2005.
- [14] H. T. El-Dessouky and H. M. Ettouney, "Multiple-effect evaporation desalination systems. thermal analysis," *Desalination*, vol. 125, no. 1–3, pp. 259–276, Nov. 1999.
- [15] M. a. Darwish and A. Alsairafi, "Technical comparison between TVC/MEB and MSF," *Desalination*, vol. 170, no. 3, pp. 223–239, Nov. 2004.
- [16] H. El-Dessouky, I. Alatiqi, S. Bingulac, and H. Ettouney, "Steady-State Analysis of the Multiple Effect Evaporation Desalination Process," *Chem. Eng. Technol.*, vol. 21, no. 5, p. 437, May 1998.
- [17] R. K. Kamali and S. Mohebinia, "Experience of design and optimization of multi-effects desalination systems in Iran," *Desalination*, vol. 222, no. 1–3, pp. 639–645, Mar. 2008.
- [18] a. O. Bin Amer, "Development and optimization of ME-TVC desalination system," *Desalination*, vol. 249, no. 3, pp. 1315–1331, Dec. 2009.
- [19] I. S. Al-Mutaz and I. Wazeer, "Development of a steady-state mathematical model for MEE-TVC desalination plants," *Desalination*, vol. 351, pp. 9–18, Oct. 2014.
- [20] M. Al-Sahali and H. Ettouney, "Developments in thermal desalination processes: Design, energy, and costing aspects," *Desalination*, vol. 214, no. 1–3, pp. 227–240, Aug. 2007.
- [21] R. Kouhikamali and N. Sharifi, "Experience of modification of thermo-compressors in multiple effects desalination plants in Assaluyeh in IRAN," *Appl. Therm. Eng.*, vol. 40, pp. 174–180, Jul. 2012.
- [22] I. Janghorban Esfahani, Y. T. Kang, and C. Yoo, "A high efficient combined multi-effect evaporation–absorption heat pump and vapor-compression refrigeration part 1: Energy and economic modeling and analysis," *Energy*, vol. 75, pp. 312–326, Oct. 2014.
- [23] D.-C. Alarcón-Padilla and L. García-Rodríguez, "Application of absorption heat pumps to multi-effect distillation: a case study of solar desalination," *Desalination*, vol. 212, no. 1–3, pp. 294–302, Jun. 2007.
- [24] M. Safar and M. Al-Shammari, "Multi-effect distillation plants- state of the art.pdf." *ELSEVIER* " vol. 126 pp. 45–59, 1999.

- [25] İ. H. Yılmaz and M. S. Söylemez, "Design and computer simulation on multi-effect evaporation seawater desalination system using hybrid renewable energy sources in Turkey," *Desalination*, vol. 291, pp. 23–40, Apr. 2012.
- [26] P. Druetta, P. Aguirre, and S. Mussati, "Minimizing the total cost of multi effect evaporation systems for seawater desalination," *Desalination*, vol. 344, pp. 431–445, Jul. 2014.
- [27] D. C. Alarcón-Padilla, L. García-Rodríguez, and J. Blanco-Gálvez, "Design recommendations for a multi-effect distillation plant connected to a double-effect absorption heat pump: A solar desalination case study," *Desalination*, vol. 262, no. 1–3, pp. 11–14, Nov. 2010.
- [28] H.-J. Joo and H.-Y. Kwak, "Performance evaluation of multi-effect distiller for optimized solar thermal desalination," *Appl. Therm. Eng.*, vol. 61, no. 2, pp. 491–499, Nov. 2013.
- [29] K. Zhao and Y. Liu, "Theoretical study on multi-effect solar distillation system driven by tidal energy," *Desalination*, vol. 249, no. 2, pp. 566–570, Dec. 2009.
- [30] H. S. Aybar, "Desalination system using waste heat of power plant," *ELSEVIER*, vol. 166, pp. 167–170, 2004.
- [31] O. a. Hamed, a. M. Zamamiri, S. Aly, and N. Lior, "Thermal performance and exergy analysis of a thermal vapor compression desalination system," *Energy Convers. Manag.*, vol. 37, no. 4, pp. 379–387, Apr. 1996.
- [32] H.-S. Choi, T.-J. Lee, Y.-G. Kim, and S.-L. Song, "Performance improvement of multiple-effect distiller with thermal vapor compression system by exergy analysis," *Desalination*, vol. 182, no. 1–3, pp. 239–249, Nov. 2005.
- [33] a. Piacentino and E. Cardona, "Advanced energetics of a Multiple-Effects-Evaporation (MEE) desalination plant. Part II: Potential of the cost formation process and prospects for energy saving by process integration," *Desalination*, vol. 259, no. 1–3, pp. 44–52, Sep. 2010.
- [34] O. J. Morin, "Design and operating comparison of MSF and MED systems," *Desalination*, vol. 93, no. 1–3, pp. 69–109, Aug. 1993.
- [35] A.Ophir and F.Lokiec IDE TEchnologies Ltd., "Review-of-MED-Fundamentals-and-Costing. pdf.
- [36] A. S. Nafey, H. E. S. Fath, A. A. Mabrouk, and M. A. Elzzeky, "Exergy and thermo-economics investigation of multi effect evaporation (MEE) and hybrid multi effect evaporation - multi stage flash (MEE-MSF) systems," *Ninth International Water Technology Conference*, 2005.

- [37] A. S. Nafey, H. E. S. Fath, and A. a. Mabrouk, "Exergy and thermoeconomic evaluation of MSF process using a new visual package," *Desalination*, vol. 201, no. 1–3, pp. 224–240, Nov. 2006.
- [38] A. A. Mabrouk, A. S. Nafey, and H. E. S. Fath, "Thermoeconomic analysis of some existing desalination processes," *ELSEVIER*, vol. 205, no. May 2006, pp. 354–373, 2007.

## Vitae

Name : Khalid Abdelbasit Khalid

Nationality : Sudanese

Date of Birth : 14/04/1991

Email :Khalidabdelbasit91@gmail.com

Address : Sudan – Khartoum

### Academic Background:

M.Sc. Mechanical Engineering: King Fahd University of Petroleum and Minerals  
(KFUPM), Dhahran, Saudi Arabia 2015

B.S Mechanical Engineering: University of Khartoum  
Khartoum, Sudan 2011

### Research interest:

Thermal sciences, fluid mechanics, and Heat transfer.

### Publications:

Experimental investigations on the performance of a cross flow air heated humidifier. ASME 2015 International Mechanical Engineering Congress & Exposition IMECE-2015, November 13-19, 2015, Houston, Texas, USA

### Short courses:

Theory and application of microcontroller. International Islamic University of Malaysia (IIUM). {20<sup>th</sup> to 22<sup>nd</sup> September 2010}

Cac service course IG dem air conditioning academy, teaching by Mr. Kim.

Experience:

Teaching Assistant 2013-2014

King Fahd University of petroleum & Minerals

Dhahran, Saudi Arabia

Teaching Assistant May 2012 - Aug 2012

International University of Africa

Khartoum, Sudan

Teaching Assistant Sep 2011 –Nov 2012

University of Khartoum

Khartoum, Sudan

|